1-1-2002

Studies of PPI Dendrimers: Structures, Properties, and Potential Applications

Dian He

STUDIES OF PPI DENDRIMERS — STRUCTURES, PROPERTIES, AND POTENTIAL APPLICATIONS

Thesis submitted to
The Graduate College of
Marshall University

In partial fulfillment of the
Requirements for the degree of
Master of Science
Chemistry

by

Dian He

Marshall University

August 15th, 2002

This thesis was accepted on _____
Month Day Year

as meeting the research requirements for the master's degree.

Advisor_____

Department of

_____

_____
Dean of the Graduate College

ABSTRACT

**STUDIES OF PPI DENDRIMERS —
STRUCTURES, PROPERTIES, AND POTENTIAL APPLICATIONS**

by Dian He

The research reported in this thesis focused on **p**oly(**p**ropylene **i**mine) (PPI) dendrimers, in terms of their structures, properties and potential applications. Different analytical techniques, including our main research tool, NMR spectroscopy, as well as AFM imaging and UV-vis spectroscopy, were used for the elucidation of structural information. The study showed (1) PPI dendrimers tend to have the extended chain conformation in polar solvents because of the strong interaction between solvent and dendrimer molecules, while in nonpolar solvents the dendrimers are inclined to have the back-folded chain conformation as a result of the weaker interaction between solvent and dendrimer molecules; (2) Inverse micelles between PPI dendrimers and long chain aliphatic acids can be formed successfully and spontaneously through self-assembling in both polar and nonpolar solvents, and the self-assembled inverse micelles have different morphologies in different solvents; (3) PPI dendrimers have shown to have catalytic properties in the hydrolysis of esters under quite mild conditions, *e.g.*, slightly basic solution and room temperature. The role of dendrimers in this catalysis may be as a template to orient the reactants in optimized positions for the hydrolysis reactions. The mechanism of this catalysis is still under investigation.

DEDICATION

To my wife and my parents, for their support throughout the entire period of my study in Marshall University for pursuing this degree.

ACKNOWLEDGMENTS

I would like to express my sincere appreciation to Prof. Minghui Chai, my advisor for my graduate study at Marshall University, for her dedication to the accomplishment of my Master's research project and her guidance and inspiration throughout my entire graduate study in the Department of Chemistry. I also would like to show my appreciation to Prof. Robert J. Morgan, Prof. Lawrence R. Schmitz, Prof. Michael L. Norton, and Prof. John W. Larson, for their advice on the problems that I encountered during my study for this degree. My gratitude also goes to the other faculty members and staff in the department.

I would like to thank the graduate student, Ms. Fan Zhang, for her great help on obtaining all the AFM images; and thank the other students in Dr. Chai's group, especially Mr. Aaron K. Holley, for his help and cordial friendship.

I wish to acknowledge the Marshall University Science Faculty NASA Research Enhancement Award(s) (REA) and Marshall University Pilot Research Award for financial support of this research, and NSF-WV EPSCOR for purchasing the 500 MHz NMR spectrometer used for this work.

TABLE OF CONTENTS

LIST OF FIGURES

LIST OF TABLES

LIST OF SYMBOLS / NOMENCLATURE

AFM	***A***tomic ***F***orce ***M***icroscopy
$DABF_4$	dipyrido[1,2-c:2',1'-e] imidazol-5-ium, 6(dimethylamino)-2,10-bis (hydroxycarbonyl), tetrafluoroborate
$DEBF_4$	dipyrido[1,2-c:2',1'-e] imidazol-5-ium, 6(dimethylamino)-2,10-bis (methoxycarbonyl), tetrafluoroborate
HETCOR	***Het***eronuclear ***Cor***relation Spectroscopy
NMR	***N***uclear ***M***agnetic ***R***esonance
NOE	***N***uclear ***O***verhauser ***E***ffect
NOESY	***N***uclear ***O***verhauser ***E***ffect ***S***pectroscop***y***
PPI	***P***oly(***p***ropylene ***i***mine)
PPI-*n*	***n***th Generation ***P***oly(***p***ropylene ***i***mine) Dendrimer
T_1	Spin-Lattice Relaxation Time
UV-vis	***U***ltra***v***iolet ***Vis***ible Light Absorbance Spectroscopy

CHAPTER I – A BRIEF REVIEW ON POLY(PROPYLENE IMINE) DENDRIMER

The first cascade structure of oligo(propylene imine) was synthesized by Vögtle *et al.* in 1978, based on a repetitive reaction sequence of double Michael additions of an amine to acrylonitrile, followed by the reduction of the nitriles to primary amines (Figure 1).[1] However, it was not until fifteen years later that large scale synthesis of PPI – **p**oly(**p**ropylene **i**mine) dendrimers was developed, using a modified Vögtle route by Wörner and Mülhaupt[2] and de Brabander-van den Berg and Meijer[3] in 1993, respectively. Vögtle's synthesis utilized the homogeneous reducing reagent – Co(II) / $NaBH_4$, which caused several difficulties in product separation and purification, presumably because of the highly effective coordination of the synthesized products with metal ions. In the modified synthesis, the cyano groups were reduced using H_2 on Raney cobalt, allowing the product to be easily separated from the reaction mixture (Figure 1).

The resulting three-dimensional propagation in this synthesis can generate a highly symmetrical, spherically shaped macromolecule with a multitude of unique properties and functions. Currently, large amounts of pure PPI dendrimers are commercially available from Aldrich Chemical Co. and DSM, The Netherlands. Since the addition of each layer of propylene imine branches to PPI dendrimer framework doubles the amino substituents on the surface, the steric hindrance will be enhanced drastically. Consequently, the reaction will stop at a certain generation for the dendrimer synthesis. So far, the highest generation of PPI dendrimer that has been synthesized is PPI-5, the 5^{th} generation of PPI dendrimer.

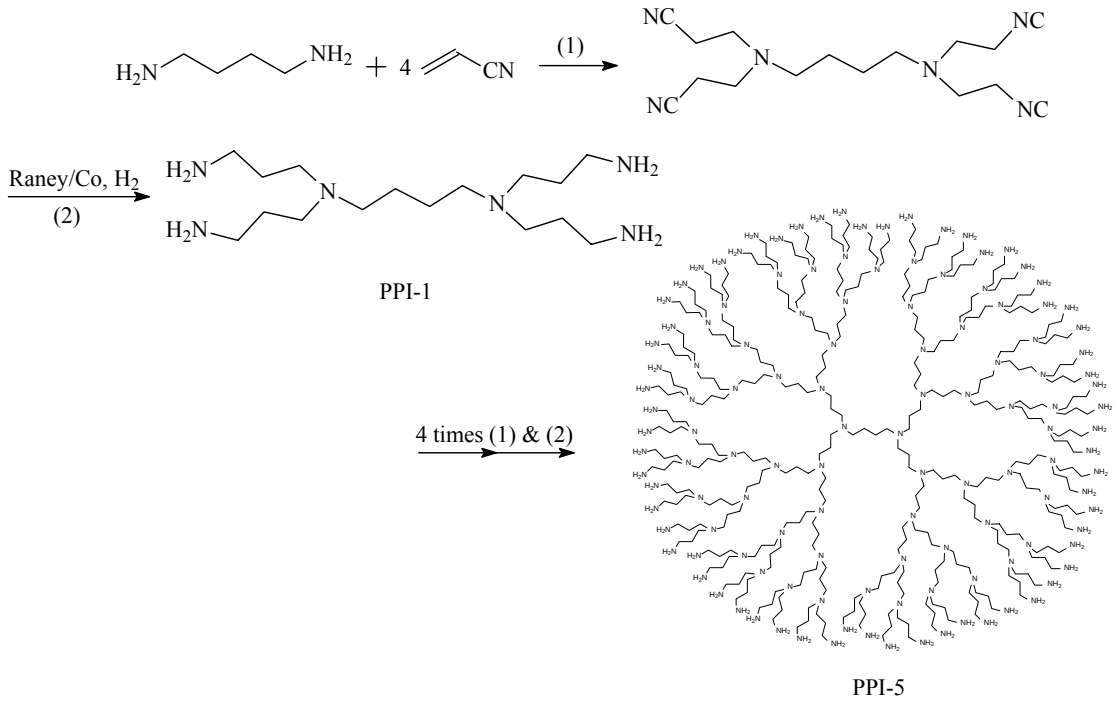

Figure 1. Synthetic scheme of poly(propylene imine) dendrimer

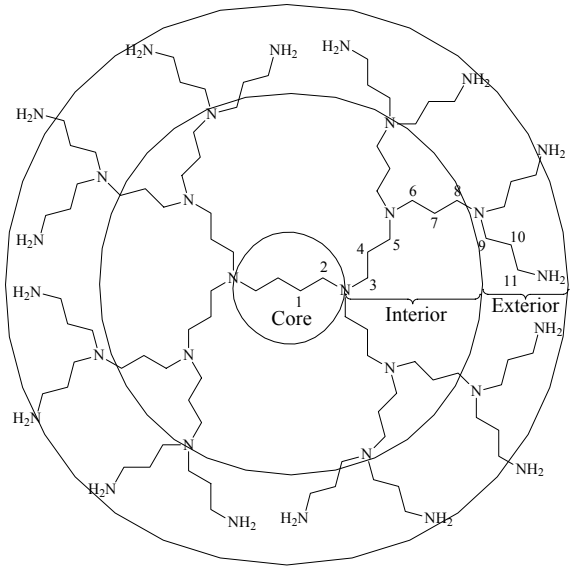

Figure 2. Different components of the dendrimer structure in labeled PPI-3 dendrimer

In general, structural components of a dendrimer can be classified into three different components – a core, an interior and an exterior. For PPI dendrimers, the core is composed of diaminobutane functionalities, the exterior contains the outmost propylene

imine chain, and the interior is specified as the intermediate portion between the core and the exterior. These distinctive areas are depicted in Figure 2. The core of PPI-3 is comprised of methylenes 1 and 2, the exterior are made of methylenes 9, 10 and 11, and all the rest methylenes, from 3 to 8, belong to the interior part (Figure 2).

Dendrimers are monodispersed macromolecules. Because of dendrimer's special molecular architecture, they show some significantly improved physical and chemical properties compared with conventional linear polymers. In solution and in the molten state, linear polymers exist as flexible coils; in contrast, dendrimers generally form tightly packed spheres. This has a great impact on their rheological properties; dendrimer solutions have significantly lower intrinsic viscosity than linear polymers.[4] Besides, the presence of many functional chain-ends is also responsible for the high solubility and miscibility, and the high functionality of dendrimers.[4] Lower generation dendrimers, which are large enough to be spherical but do not form a tightly packed surface, have enormous surface areas in relation to volume (up to 1000 m^2/g).[5]

Many potential applications for dendrimers are based on their molecular uniformity, multifunctional surface and the presence of internal cavities (or dendritic voids). These specific properties make dendrimers suitable for a variety of biomedical and industrial applications.[6] For example, dendrimers have been tested in preclinical studies as contrast agents for magnetic resonance imaging (MRI), which is a diagnostic method producing images of organs and blood vessels. The gadolinium salts of diethylenetriaminepentaacetic acid (DTPA) are used clinically as contrast agents for enhancing sensitivity and specificity of MRI, but these salts diffuse into the extravenous area because of their low molecular mass.[7] Preliminary tests showed dendrimers containing surface chelated gadolinium ions

are more effective contrast agents than the conventional ones (the gadolinium DTPA salts).[8] Dendrimers have been used in the targeted delivery of drugs and other therapeutic agents. Drug molecules can be loaded both in the interior of the dendrimers as well as attached to the surface groups. For example, the therapeutic effectiveness of a drug is strongly related to its solubility in the aqueous environment of the body. There are many substances which have a strong therapeutic activity but because of their lack of solubility in aqueous solution, they are not practical for use in the therapeutic applications. Water soluble dendrimers, such as PPI dendrimers, are capable of binding and solubilizing small acidic hydrophobic molecules with antifungal or antibacterial properties. The bound substrates can be released upon contacting with the target organism.[9] In gene therapy, dendrimers can act as carriers, or vectors. These vectors transfer genes through the cell membrane into the nucleus. Currently the main types of vectors are liposomes and genetically engineered viruses. Another commonly studied dendrimer, the poly(amidoamine) (PAMAM) dendrimer, has been tested as genetic material carrier. PAMAM dendrimers can interact with the phosphate groups of the nucleic acids through their terminal amine groups; this ensures consistent formation of transfection complexes.[10] Besides biomedical applications, dendrimers are used to improve many industrial processes. The combination of high surface area and high solubility make dendrimers useful as nanoscale catalysts.[11] They combine the advantages of homogenous and heterogeneous catalysts, namely, the good accessibility of active sites and ease of separation from the reaction mixture.

CHAPTER II – PROBING SOLVENT EFFECT ON THE CHAIN CONFORMATION OF PPI-2 DENDRIMER VIA NMR

Introduction

The pioneering studies of dendrimer structure were done using theoretical calculations and computer simulations. However, they led to two controversial models for these compounds: a dense core model and a dense shell model. De Genes and Hervet presented a model with a low density region near the core and a high density on the surface (dense shell), suggesting the presence of cavities (dendritic voids) inside dendrimers.[12] The model of Lescanec and Muthukumar, on the other hand, showed a decrease in density going from the core to the periphery of the dendrimer (dense core).[13] Mansfield and Klushin obtained similar dense core results based on Monte Carlo simulations.[14] Wallace *et al.* added detailed balance, a necessary but not sufficient condition for a simulation to achieve thermal equilibrium, to the original Monte Carlo simulation scheme proposed by Mansfield and Klushin. This new model showed much better agreement with another simulation model, *Exact Analytical Method*, in which so-called "exact structure factors" of an ideal dendrimer could be obtained.[15] Murat and Grest also showed an increase of back-folding with increasing generation and a strong effect of solvent polarity on the mean radius of each generation dendrimer.[16] Boris and Rubinstein also predicted that density should decrease radiating from the center using a self-consistent mean field model.[17] Tande *et al.* suggested it was important to consider the thermodynamic interactions of dendrimers and solvents when comparing the simulation and experimental results.[18] Lee *et al.* found that poly(amidoamine) (PAMAM)

dendrimers had significant back-folding at neutral pH but they tended to have a highly ordered extended conformation at lower pH (≤4) based on molecular dynamics simulations. These structural differences undoubtedly contribute to the capability of PAMAM as the gene carrier.[19]

For PPI dendrimers, Welch and Muthukumar reported the conformational changes of PPI dendrimers as a function of ionic strength based on Monte Carlo simulations.[20] Scherrenberg *et al.* studied PPI dendrimers using viscometry and small angle neutron scattering (SANS) and observed a linear relationship between the dendritic radii and the generation number.[21] The results from their study are consistent with the molecular simulations by Murat and Grest. Zacharopoulos and Economou also proposed a dense-core model based on computer simulations of PPI dendrimers in molten state (400 K). The overall density profiles exhibit a gradual decrease from the center toward the surface of the molecule.[22] Adhiya and Wesdemiotis used tandem mass spectrometry to show that in the gas phase, PPI dendrimers prepared from different solvents had different conformations.[23] NMR (**n**uclear **m**agnetic **r**esonance spectroscopy) studies on PPI-3 dendrimers were performed in both polar (chloroform) and nonpolar (benzene) solvents by Chai *et al.* The results from this study clearly demonstrated solvent affects the structures of these dendrimers. However, the study was only undertaken in two solvent systems.[24]

In this study, we used NMR spectroscopy to investigate thoroughly the solvent effect on the dendritic chain conformations of PPI-2 using a more diverse selection of solvents. The study was performed with both low (0.043 *M*, 0.017 *M*, 0.0086 *M*) and high (0.35 *M*, 0.086 *M*) concentrations of dendrimer using ^{1}H, ^{13}C 1D NMR and ^{1}H-^{13}C HETCOR

(**het**eronuclear **cor**relation spectroscopy) 2D NMR techniques. ^{13}C T_1 relaxation (spin-lattice relaxation) measurements in different solvents were also used for the examination of the chain dynamics of the dendrimer.

Experimental

Chemicals and Sample Preparations. Various masses of PPI-2 (from 5 mg to 200 mg) were dissolved in 0.7 ml of various deuterated solvents in 5 mm NMR tubes for NMR studies. The sample concentrations in this study are listed in Table 1. PPI-2 dendrimer and deuterium oxide were obtained from Aldrich Chemical Co. Dioxane-d_8 and carbon tetrachloride were purchased from Norell Inc. and Fisher Scientific Company, respectively. All other deuterated solvents were purchased from Cambridge Isotope Labs.

Table 1. Different Concentrations of PPI-2 Dendrimer in Variant Solvent

Solvent	Concentration (*M*)			
carbon tetrachloride	0.086	0.043	0.017	0.0086
deuterium oxide	0.35	0.043	0.017	0.0086
methanol-d_4	0.35	0.043	0.017	0.0086
benzene-d_6	0.35	0.043	0.017	0.0086
acetonitrile-d_3	0.35	0.043	0.017	0.0086
chloroform-*d*	0.35	0.043	0.017	0.0086
1,4-dioxane-d_8	0.35	0.043	0.017	0.0086

NMR Measurements. NMR spectra were obtained on a Varian XL 200 MHz spectrometer equipped with a Varian switchable probe, and on a Varian Unity 500 MHz spectrometer equipped with a Varian broadband probe. Solvents were also used as internal references for both ^1H and ^{13}C chemical shifts, except in the case of carbon tetrachloride (^1H) and deuterium oxide (^{13}C) solutions, where a small amount of benzene-d_6 was put in a concentric NMR tube and used as the external reference. The chemical shifts of different solvents are listed in Table 2. All NMR experiments were performed at

ambient temperature. All data were processed with Varian VNMR software on a SUN Ultra-60 workstation.

Table 2. Solvent Chemical Shifts (Referenced to TMS)

Solvent	Chemical Shift (multiplicity) (ppm)*	
	^{1}H	^{13}C
acetonitrile-d_3	1.94 (5)	1.39 (7), 118.69 (1)
benzene-d_6	7.16 (1)	128.39 (3)
chloroform-*d*	7.27 (1)	77.23 (3)
1,4-dioxane-d_8	3.53 (m)	66.66 (5)
methanol-d_4	4.87 (1), 3.31 (5)	49.15 (7)
deuterium oxide	4.80 (DSS)	—

* Data from Cambridge Isotope Labs NMR Solvent Data Chart.

One-dimensional NMR on the Varian XL 200 MHz spectrometer. The ^{1}H spectra of all solutions were acquired at 200.057 MHz, using 1.5 s acquisition time, 2093.8 Hz spectral width, 7 μs pulse width and 64 transients for concentrated samples and 256 transients for diluted samples. All ^{13}C spectra were acquired at 50.309 MHz, using 1.25 s acquisition time, 12004.8 Hz spectral width, 20 μs pulse width, 2 s relaxation delay and 10240 transients with swept-square wave modulated ^{1}H decoupling. ^{13}C T_1 measurements (inverse recovery pulse sequence) were performed at 50.309 MHz, using 1.25 s acquisition time, 6882.3 Hz spectral width, 28.0 μs (90°) pulse width, 20 s relaxation delay and 128 transients per spectrum with 10 different d_2 delays (range: 0.039 ~ 20 s) with swept-square wave modulated ^{1}H decoupling.

One-dimensional NMR on the Varian Unity 500 MHz spectrometer. The ^{1}H spectra of all solutions were acquired at 499.209 MHz, using 3.0 s acquisition time, 4000.0 Hz spectral width, 5 μs pulse width and 16 transients for concentrated samples and 64 transients for diluted samples. All ^{13}C spectra were acquired at 125.538 MHz, using 1.2 s acquisition time, 29996.3 Hz spectral width, 7.8 μs pulse width, 5 s relaxation delay and

16 transients for concentrated samples and 1024 transients for diluted samples, with WALTZ-16 modulated ^{1}H decoupling. ^{13}C T_1 measurements were performed at 125.538 MHz, using 1.2 s acquisition time, 29996.3 Hz spectral width, 7.8 μs (90°) pulse width, 6 s relaxation delay and 256 transients per spectrum with 10 different d_2 delays (range: 0.013 ~ 6.4 s) with WALTZ-16 modulated ^{1}H decoupling.

Two-dimensional NMR. The 2D ^{13}C-^{1}H HETCOR spectra were acquired at 125.538 MHz, using 0.05 s acquisition time. ^{1}H and ^{13}C 90° pulse widths were 22 μs and 7.8 μs, respectively. 5500.0 Hz ^{1}H (f_1) and 2000.0 Hz ^{13}C (f_2) spectral widths were used. 128 transients were averaged for each of 256 real t_1 increments. A combination of Sinebell and Gaussian weighting is applied to both dimensions, zero filling used for performing 2D Fourier transform on a 1024 × 1024 matrix.

Results and Discussion

Chemical Shift Assignments. Figure 3 is the ^{1}H NMR spectra of 0.043 *M* PPI-2 in benzene-d_6 obtained on the 200 MHz [Figure 3(a)] and the 500 MHz [Figure 3(b)] spectrometers. The spectra show that the higher magnetic field gives much better resolution in the NMR spectra for the same sample. The ^{13}C NMR spectrum of PPI-2 in benzene-d_6 is shown in Figure 4, which exhibits well-resolved resonances for nearly all methylene carbons. Figure 5 is the 2D HETCOR spectrum of PPI-2 in benzene-d_6. The ^{1}H-^{13}C cross peaks from all methylenes of PPI-2 are clearly resolved in the 2D spectrum for chemical shift assignments of both ^{1}H and ^{13}C resonances. The resonance assignments are marked in all figures, based on the labeling in the structure shown in Figure 3. Based on the 2D ^{1}H-^{13}C HETCOR spectra, it is possible to assign all the overlapped ^{1}H

resonances because of the structural similarity of the different parts in the dendrimers. The chemical shift assignments are labeled in the spectra shown in Figure 3, 4, 5, according to the same labeling in Figure 3.

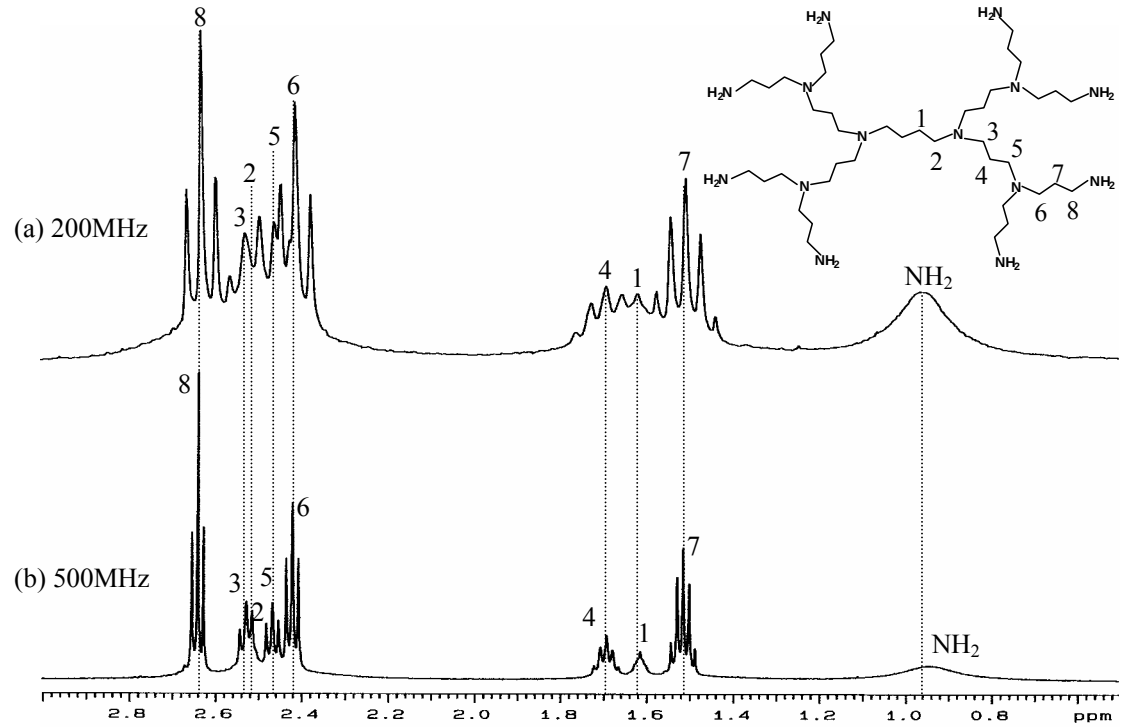

Figure 3. One-dimensional ^{1}H NMR spectra acquired (a) on 200 MHz (b) on 500 MHz spectrometers of 0.043 *M* PPI-2 in benzene-d_6 solution with labeled PPI-2 structure

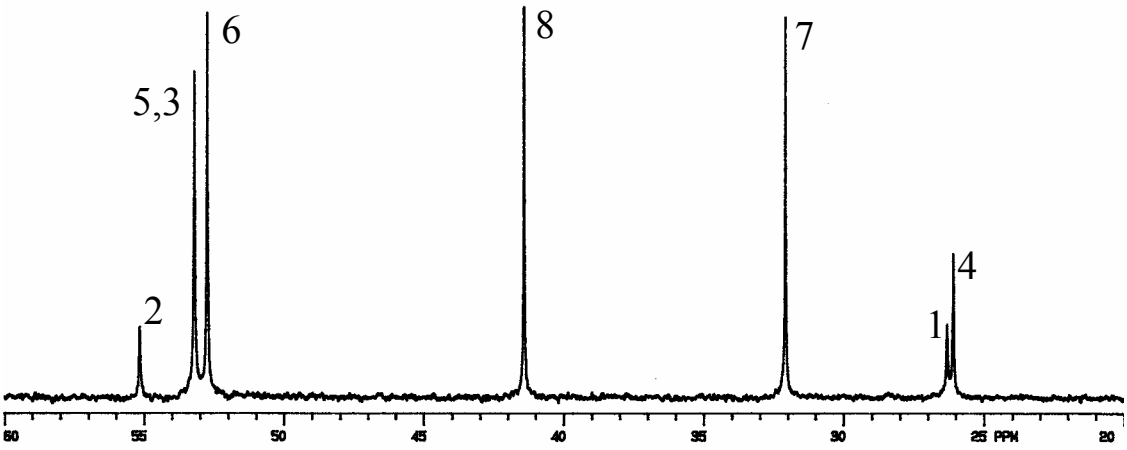

Figure 4. One-dimensional ^{13}C chemical shift assignments on 0.043 *M* PPI-2 in benzene-d_6 solution

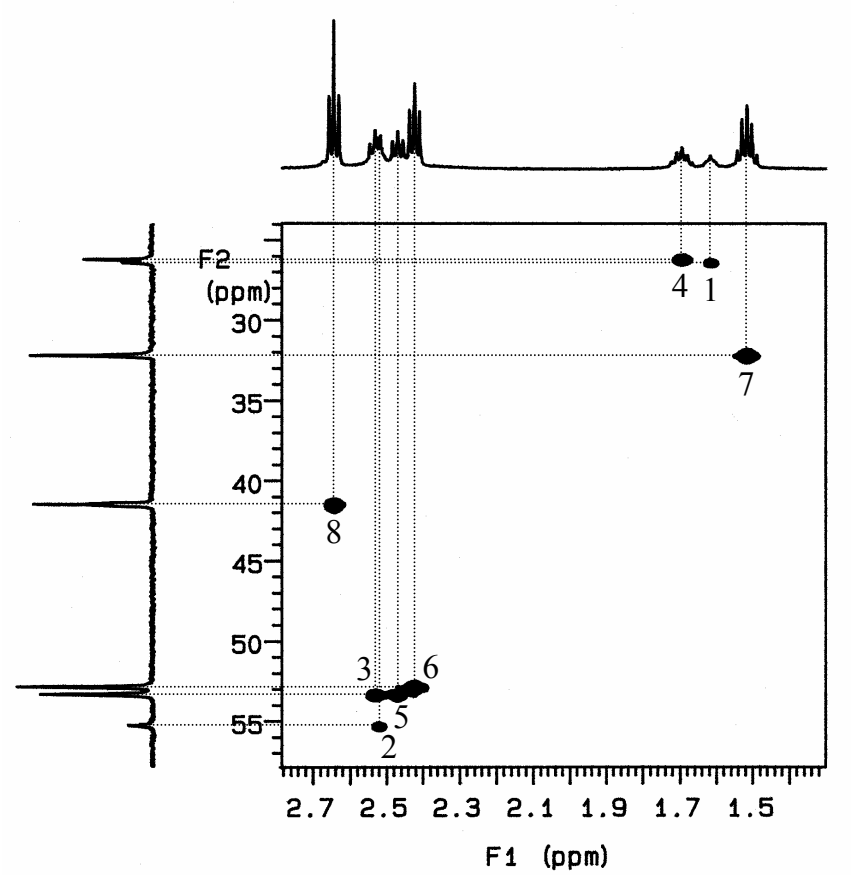

Figure 5. Two-dimensional ^{13}C-^{1}H HETCOR spectrum chemical shift assignments on 0.043 *M* PPI-2 in benzene-d_6 solution

Solvent Effect on Chemical Shifts. Based on the chemical shift assignments shown above, we can assign the ^{1}H and ^{13}C chemical shifts of PPI-2 at different concentrations in different solvents. All the chemical shift assignments have been summarized in Tables 3 and 4, on which we will rely upon for the studies of PPI-2 conformational changes in different solutions.

In Tables 3 and 4, we can see a general trend for any particular solvent case, the chemical shifts of three relatively dilute solutions are similar to each other, but the chemical shifts of the more concentrated (0.35 *M*) solutions behave differently. In the dilute solutions, the molecular interactions happen mainly between PPI-2 and the solvent molecules. However, in the high concentration (0.35 *M*) solutions, the interactions

between PPI-2 molecules themselves become dominant; PPI-2 molecules can gather together. This increases the induced dipole interactions between PPI-2 molecules, thus the dendrimer molecule cannot maintain a perfect spherical shape due to this aggregation. So it is almost common that at a high concentration (0.35 *M*), all the chemical shifts, for both ^{1}H and ^{13}C, are shifted to the higher field direction as compared to the corresponding low concentration solutions (0.0086 *M* ~ 0.043 *M*).

Table 3. The ^{1}H Chemical Shifts of Different Concentrations in Various Solvents

Different PPI-2 Solutions			Chemical Shift (ppm)								
Solvent		Concentration (*M*)	H1	H2	H3	H4	H5	H6	H7	H8	NH_2
Nonpolar	Dioxane-d_8	0.35	1.387	2.348	2.362	1.511	2.362	2.390	1.485	2.605	1.626
		0.043	1.398	2.352	2.373	1.517	2.373	2.400	1.488	2.614	—
		0.017	1.400	2.359	2.375	1.516	2.375	2.401	1.488	2.616	1.646
		0.0086	1.402	2.363	2.377	1.524	2.377	2.403	1.496	2.617	—
	Benzene-d_5	0.35	1.516	2.435	2.449	1.615	2.408	2.394	1.507	2.631	1.592
		0.043	1.615	2.520	2.528	1.694	2.464	2.417	1.514	2.635	1.100
		0.017	1.615	2.516	2.530	1.694	2.469	2.422	1.516	2.642	0.950
		0.0086	1.618	2.522	2.530	1.695	2.463	2.414	1.510	2.630	0.932
Protic	Methanol-d_4	0.35	1.470	2.470	2.466	1.632	2.466	2.498	1.634	2.668	—
		0.043	1.465	2.477	2.457	1.632	2.457	2.484	1.632	2.654	—
		0.017	1.466	2.481	2.458	1.635	2.458	2.502	1.635	2.659	—
		0.0086	1.466	2.483	2.469	1.640	2.469	2.506	1.640	2.671	—
	D_2O	0.35	1.413	2.453	2.420	1.603	2.420	2.446	1.575	2.574	—
		0.043	1.468	2.514	2.486	1.655	2.486	2.532	1.639	2.646	—
		0.017	1.470	2.509	2.484	1.664	2.484	2.529	1.640	2.636	—
		0.0086	1.473	2.520	2.490	1.661	2.490	2.536	1.642	2.646	—
Polar Aprotic	$CDCl_3$	0.35	0.954	1.950	1.956	1.115	1.956	2.010	1.142	2.260	1.423
		0.043	1.355	2.362	2.358	1.533	2.358	2.415	1.547	2.668	1.700
		0.017	1.384	2.390	2.390	1.559	2.390	2.448	1.579	2.713	1.505
		0.0086	1.397	2.399	2.399	1.574	2.399	2.455	1.588	2.719	—
	CD_3CN	0.35	1.372	2.334	2.353	1.487	2.353	2.375	1.473	2.586	1.428
		0.043	1.395	2.350	2.374	1.512	2.374	2.395	1.498	2.603	—
		0.017	1.397	2.350	2.364	1.507	2.364	2.396	1.493	2.605	1.802
		0.0086	1.398	2.352	2.366	1.510	2.366	2.398	1.495	2.606	—

It has been observed that chemical shifts of PPI-2 in polar solvents showed little change with the change of concentration because the polar solvent molecules can penetrate inside the interior part of a dendrimer to solvate the dendrimer molecule. This causes an averaging of the chemical environments of different methylene groups in different layers of a dendrimer, and makes the chemical shifts of these methylenes quite similar to each other. The averaging effect is similar at different concentrations. However,

in the solutions of nonpolar solvents, the solvent molecules cannot penetrate to the inside of PPI-2 dendrimers and just enclose the dendrimer molecules. Therefore, within a certain concentration range, the chemical shifts of the same methylene groups almost remain the same at different concentrations.

Table 4. The ^{13}C Chemical Shifts of Different Concentrations in Various Solvents

Different PPI-2 Solutions			Chemical Shift (ppm)							
Solvent		Concentration (*M*)	C1	C2	C3	C4	C5	C6	C7	C8
Nonpolar	Dioxane-d_8	0.35	26.034	54.972	53.106	25.766	53.185	52.729	32.167	41.333
		0.043	26.073	55.011	53.139	25.848	53.230	52.744	32.302	41.381
		0.017	26.094	55.016	53.150	25.882	53.241	52.749	32.342	41.385
		0.0086	26.079	55.023	53.157	25.83	53.236	52.756	32.217	41.356
	Benzene-d_5	0.35	26.244	55.149	53.238	25.978	53.238	52.801	32.053	41.402
		0.043	26.345	55.231	53.221	26.133	53.279	52.823	32.072	41.406
		0.017	26.401	55.258	53.311	26.211	53.311	52.841	32.202	41.472
		0.0086	26.412	55.266	53.253	26.190	53.315	52.855	32.108	41.439
Protic	Methanol-d_4	0.35	26.071	55.379	53.498	25.215	53.541	53.147	31.215	41.462
		0.043	25.959	55.365	53.415	24.952	53.473	53.026	31.016	41.330
		0.017	25.964	55.375	53.420	24.976	53.483	53.035	30.948	41.311
		0.0086	25.949	55.365	53.400	24.952	53.454	53.016	30.734	41.257
	D_2O	0.35	24.509	54.012	52.116	22.759	52.116	51.624	29.293	40.045
		0.043	24.453	53.947	51.994	22.639	52.021	51.527	28.946	39.889
		0.017	24.467	53.939	52.007	22.637	52.007	51.520	29.068	39.893
		0.0086	24.460	53.945	52.013	22.649	52.013	51.526	29.001	39.881
Polar Aprotic	$CDCl_3$	0.35	24.420	53.478	51.560	23.931	51.618	51.217	30.068	39.785
		0.043	25.274	54.410	52.450	24.789	52.528	52.087	30.941	40.691
		0.017	25.362	54.483	52.518	24.891	52.591	52.155	31.067	40.953
		0.0086	25.337	54.507	52.552	24.877	52.635	52.159	31.125	40.958
	CD_3CN	0.35	26.050	54.999	53.157	25.715	53.194	52.778	32.169	41.438
		0.043	26.069	55.010	53.197	25.697	53.227	52.814	32.070	41.452
		0.017	26.134	55.035	53.227	25.821	53.256	52.836	32.267	41.504
		0.0086	26.152	55.057	53.256	25.842	53.281	52.866	32.260	41.511

Solvent effects upon ^{13}C chemical shifts can also be derived from the spectra in Figures 6 and 7. In nonpolar solvents the chemical shifts of PPI-2 in each different solvent are similar. This indicates that in nonpolar solvents, the dendritic arms of PPI-2 are in a back-folded conformation, and solvent molecules only enclose the dendrimer. Thus, the interactions between dendrimer and solvent occur primarily on the outside of PPI-2. Under these conditions, the chemical environment of PPI-2 is determined by its own intrinsic structure. Therefore, the chemical shifts of PPI-2 are similar in different concentrations for dilute solutions (0.0086 ~ 0.043 *M*) regardless of the type of solvent.

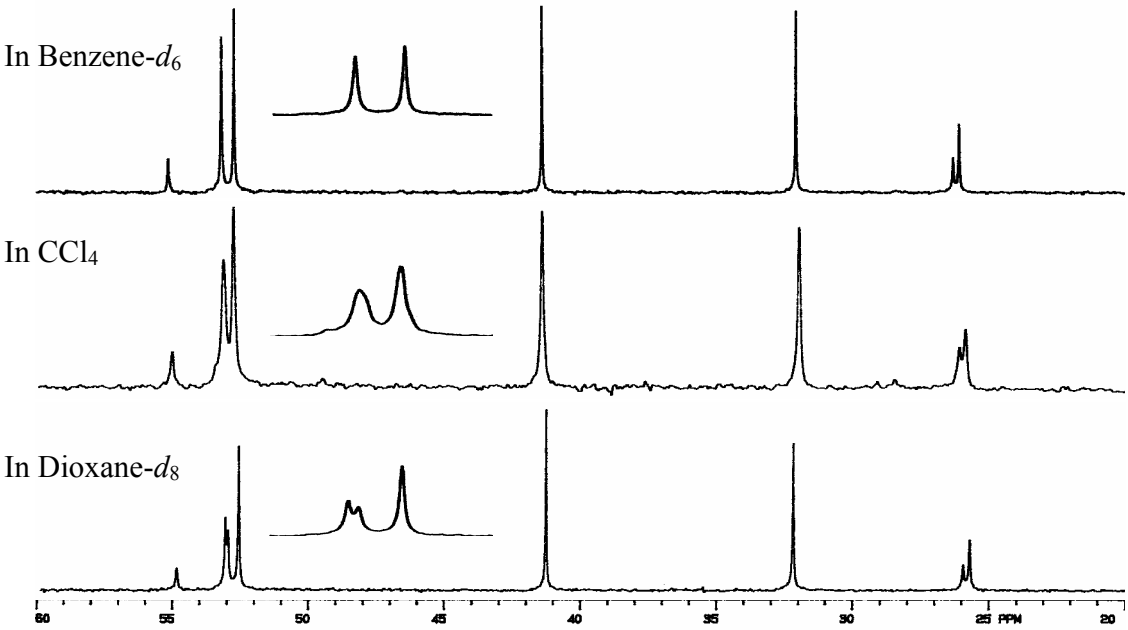

Figure 6. The ^{13}C spectra of 0.043 *M* PPI-2 in different nonpolar solvents, the smaller inserted spectra show the expansion of 52~54 ppm.

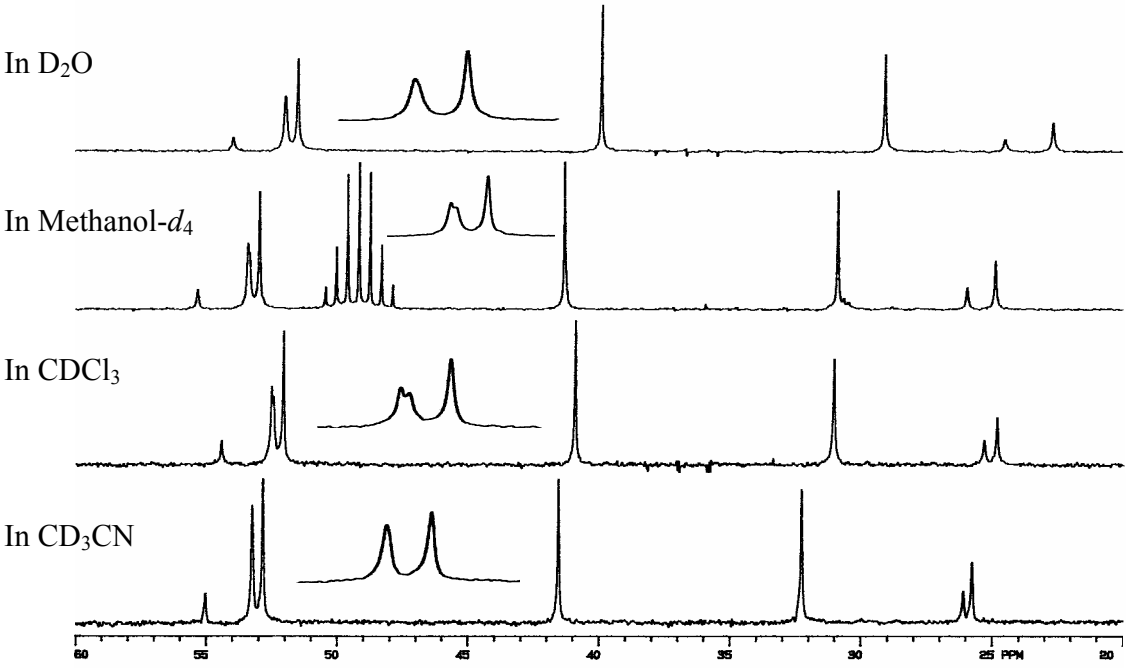

Figure 7. The ^{13}C spectra of 0.043 *M* PPI-2 in different polar solvents, the smaller inserted spectra show the expansion of 52~54 ppm.

In polar solvents, either protic or aprotic, PPI-2 dendrimer's behavior is rather different when compared with that in nonpolar solvents since polar solvent molecules can

penetrate to the inside of dendrimer molecule and change the chemical environment of the dendrimer to some extent. From acetonitrile to deuterium oxide, as the polarity increases, the ^{13}C chemical shift difference between methylene groups 1 and 4 also increases. With increasing polarity, the interaction between solvent molecules and the dendrimer becomes more dominant. Because methylene group 1 is in the core, it does not interact with the solvent as much as methylene group 4 does. The higher polarity of the solvent causes a larger differentiation of the resonances of these methylene groups. Also, the chemical shifts of methylene groups 6, 7 and 8 change in the same way. Because they are all located at the exterior part of the dendrimer, these groups are almost completely solvated by solvent molecules. Therefore, the trends in chemical shift are similar. Methylene groups 3, 4 and 5 are solvated differently in different polar solvents, so their chemical shifts are solvent dependent. However, methylene groups 1 and 2 are in the core part and are solvated least by the solvent, so they behave similarly in different solvents.

Solvent Effects on ^{13}C T_1 values. ^{13}C T_1 values of PPI-2 in different solvents are listed in Table 5. We can see the ^{13}C T_1 values of PPI-2 dendrimer at lower concentration are all longer than those at higher concentration. This is because at lower concentration, the PPI-2 molecules can tumble faster than those at higher concentration. Theoretically, at a certain magnetic field strength, the spin-lattice relaxation time T_1 is inversely proportional to correlation time τ_c as shown in the following equation:[25]

$$\frac{1}{T_1\left(^{13}C\right)} = \left(\frac{\mu_0}{4\pi}\right)^2 \frac{N\gamma_H^2\gamma_C^2\hbar^2\tau_c}{r_{CH}^6}$$

where N is the number of attached hydrogens, γ_H, γ_C is the gyromagnetic ratio for ^{1}H and ^{13}C respectively, $\hbar$ is the Planck constant divided by 2π, r_{CH} is the distance between ^{1}H and ^{13}C, and μ_0 is magnetic permeability of a vacuum.

Table 5. Comparison of ^{13}C T_1 Values in Different Solvents

Different PPI-2 Solutions					^{13}C T_1 Values (s)							
Solvent	Dielectric Constant	Viscosity (20°C) (mPa·s)	Spectrometer Frequency	Concentration (*M*)	C1	C2	C3	C4	C5	C6	C7	C8
dioxane-d_8	2.2	1.21	500 MHz	0.35	0.1870	0.1678	0.1938	0.2064	0.2064	0.2681	0.4694	0.8166
				0.017	0.2357	0.1944	0.2651	0.3028	0.3062	0.4015	0.7037	1.247
			200 MHz	0.35	0.171	0.0996	0.121	0.134	0.133	0.189	0.335	0.685
benzene-d_6	2.3	0.69	500 MHz	0.35	0.2106	0.1971	0.2225	0.2361	0.2377	0.3208	0.5233	0.8794
				0.017	0.3194	0.3461	0.4020	0.4015	0.4020	0.5822	0.9883	1.550
			200 MHz	0.35	0.160	0.130	0.201	0.160	0.201	0.201	0.419	0.776
methanol-d_4	32.7	0.52	500 MHz	0.35	0.1849	0.1790	0.1980	0.2143	0.2033	0.2557	0.4156	0.6834
				0.017	0.3536	0.2478	0.2525	0.2619	0.2745	0.3496	0.5482	0.9218
			200 MHz	0.35	0.122	0.111	0.155	0.122	0.155	0.155	0.267	0.494
D_2O	78.5	1.24	500 MHz	0.35	0.1660	0.1530	0.1668	0.1868	0.1668	0.2220	0.3471	0.5756
				0.017	0.1793	0.1972	0.1934	0.1972	0.1934	0.2562	0.4302	0.7404
			200 MHz	0.35	0.0764	0.0698	0.0777	0.0862	0.0777	0.103	0.189	0.353
$CDCl_3$	4.8	0.57	500 MHz	0.35	0.2190	0.1860	0.2033	0.2241	0.2258	0.2883	0.4529	0.7213
				0.017	0.3283	0.2552	0.2932	0.3651	0.3619	0.4526	0.6691	1.079
			200 MHz	0.35	0.154	0.109	0.197	0.154	0.197	0.197	0.364	0.645
CD_3CN	37.5	0.39	500 MHz	0.35	0.2776	0.2386	0.2847	0.3013	0.3103	0.4315	0.7504	1.266
				0.017	0.5158	0.4206	0.4966	0.5052	0.5479	0.7964	1.291	2.207
			200 MHz	0.35	0.158	0.121	0.202	0.158	0.202	0.202	0.419	0.777

τ_c is the time taken for the molecule to rotate by roughly 1 radian about any axis, and τ_c is approximately equal to the rotational relaxation time τ_r. Debye gives τ_r as: $\tau_r = 4\pi\eta a^3 / 3kT$, where η is the viscosity of the solvent, and a is the radius of the molecule.

The Debye equation shown above indicates that τ_c is directly proportional to viscosity. Thus, if all the other conditions remained the same there should be an inversely proportional relationship between T_1 and viscosity (η). However, this is not the case for the data listed in Table 5, which indicates the T_1 values are not only affected by viscosity, but by additional factors as well. In more polar solvents (larger dielectric constants), the interaction between dendrimer and solvent molecules is stronger, which impedes the

motion of the dendrimer molecules. Therefore, the values of T_1 become shorter. The inverse correlation of T_1 and viscosity can be observed, but the relationship is not linear.

Polar solvent molecules can penetrate inside dendrimer molecules. This can cause averaging of the local motions for different layers of the dendrimer. Thus, the overall T_1 values are closer in polar solvents. However, in nonpolar solutions, the local motions of different layers are mainly determined by the intramolecular interactions between the dendrimer molecules themselves. Consequently, the difference in T_1 values of the methylenes at different layers of the dendrimer will be larger than those in polar solutions. Some oxygen-containing solvents, such as methanol-d_4, dioxane-d_8 and deuterium oxide, have oxygen atoms that can form hydrogen bonds with the amine groups of the PPI-2 dendrimer. Thus, the solvent molecules can actually attach to the dendrimer surface and make the motion of the molecule even more restricted. Therefore, in these solutions the methylene groups on the surface (the exterior) have the smallest ^{13}C T_1 values.

We observed the general trend that the T_1 values for carbon atoms are proportional to their distance from the core; the carbons with the shortest T_1 values are closest to the core. This can be explained as follows. The exterior methylene groups have relatively more freedom (shorter τ_c), in which the nuclear relaxation is the least efficient (longer T_1). So they have the largest T_1 values. Additionally, the carbons attached to the nitrogen atom (C2 and C3, C5 and C6) show shorter T_1 than their respective neighboring carbons (centered in the propylene spacer, C4 and C7) in the same layer. This is due to the nitrogen atom being in the trifurcate connection point in the dendrimer molecule, which has relatively slower motion (more confined or restricted by dendritic arms).

The T_1 values are also magnetic field dependent. T_1 relaxation can undergo through single quantum relaxation process, which requires magnetic field fluctuations, or magnetic noise, near the Larmor precession frequency ν_0. Thus the relaxation is the most efficient when the nuclei are tumbling at a rate of $(\tau_c)^{-1}$, or $\nu_0 \cdot \tau_c \approx 1/2\pi$. If we use the circular frequency ω_0 instead of frequency ν_0 ($\omega_0 = 2\pi\nu_0$), the relationship simplifies to: $\omega_0 \cdot \tau_c \approx 1$.[26] Because different carbons of the dendrimer molecule have different correlations times (τ_c), when the correlation time of a certain carbon matches the equation $\omega_0 \cdot \tau_c \approx 1$ in a certain magnetic field, the relaxation for this carbon will be the most efficient, or the corresponding T_1 value will be the shortest. In different magnetic fields, the Larmor precession frequency ν_0 is different. The relationship between ν_0 and magnetic field B_0 is $\nu_0 = \gamma B_0/2\pi$, which indicates in a higher magnetic field the Larmor precession frequency is higher. Therefore, the T_1 relaxations for a certain carbon nucleus will be different in different magnetic field. Generally, in lower field, the Larmor precession frequency (ν_0) or circular frequency (ω_0) is lower, the correlation time (τ_c) is larger, so the T_1 value is shorter. In the case of PPI-2 dendrimer, the relaxation of the carbons is more efficient at lower magnetic field, thus all the T_1 values obtained from the 500 MHz (^{1}H frequency, 125 MHz for ^{13}C frequency) spectrometer are longer than those from the 200 MHz (^{1}H frequency, 50 MHz for ^{13}C frequency) spectrometer of the same sample, as observed in Table 5.

Conclusion

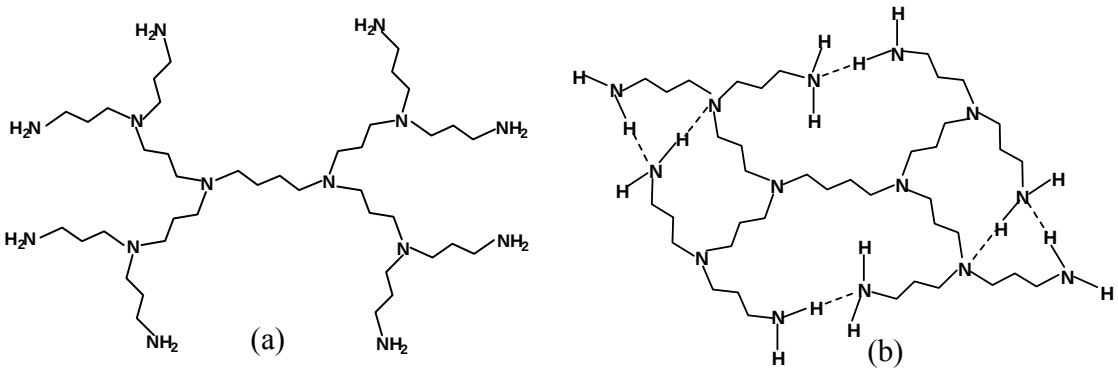

Figure 8. PPI-2 conformation schemes (a) in polar solvents (b) in nonpolar solvents.

The nature of solvent effects on the conformations of dendrimer has been probed via changes in both chemical shifts and T_1 values. Comparing the chemical shift differences at different concentrations in different solvents, it was concluded that the back-folded dendritic chains become more dominant in solution as the polarity of the solvent decreases (Figure 8). The ^{13}C T_1 study revealed that different mobilities are present in different portions of a PPI dendritic chain, with the core atoms possessing the least mobility, followed by the interior, and the exterior having the most mobility. This was supported by results of solvent properties study (viscosity, η, and polarity or dielectric constant, ε). The T_1 value results also confirm the conformations of dendrimers in different solvents obtained from the chemical shift analyses.

CHAPTER III – STUDY OF THE STRUCTURES OF SELF-ASSEMBLED INVERSE MICELLES FROM PPI DENDRIMER TEMPLATES

Introduction

In general, dendrimers contain dendritic voids in the core and interior parts. These dendritic voids are capable of encapsulating small guest molecules. As mentioned previously, PPI dendrimers have primary amine functional groups on their surfaces. With the modification of PPI-5 dendrimer's periphery with (*t*-Boc)-protected-phenylalanine residues, Meijer *et al.* was able to synthesize the "dendritic box" in 1994.[27] PPI dendrimers' periphery can also be modified with more apolar groups like palmitoyl or adamantyl moieties to form inverse micelle structures, which contain a polar center (PPI dendrimer moiety) and a nonpolar periphery (hydrocarbon chains). These inverse micelles can encapsulate small organic molecules such as fluorescent dyes within their dendritic voids. However, the aforementioned inverse micelles were built through the amide bonds between the primary amines on PPI surface and carboxylic groups of the acids.[28] This process is irreversible, since one has to break the amide bond through a chemical reaction to retrieve PPI dendrimers and the carboxylic acids. Similar inverse micelle structures have been made from PPI dendrimers and long chain carboxylic acids. These inverse micelles self-assemble through non-covalent electrostatic interactions between ammonium (from PPI moiety) and carboxylate ions (from the acid moiety).[29] Thus, a reversible system can be formed for the encapsulation of small molecules. The encapsulation of the small molecules is potentially controllable with the pH adjustment.

Currently, more attention has been devoted to the study of guest-host chemistry of dendrimer and dendrimer templated inverse micelles.[30] However, little work has been concerning the structural details of these inverse micelles; for example, the conformation of the nonpolar periphery of these inverse micelles in different solvents has not been investigated.

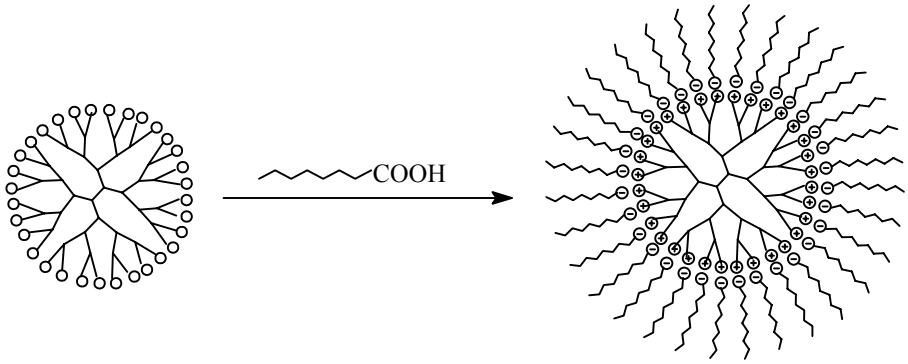

Figure 9. The inverse micelle formed by self-assembling of PPI-4 dendrimer and octanoic acid

In this study, methanol, benzene and toluene were selected as the examples of polar and nonpolar solvents. One-dimensional ^{1}H, ^{13}C NMR and ^{13}C T_1 relaxation (spin-lattice relaxation) measurements were used to investigate the structures of the reversible inverse micelle systems formed by the self-assembly of different generation PPI dendrimers and octanoic acid. Two-dimensional ^{1}H-^{1}H NOESY (**N**uclear **O**verhauser **E**ffect **S**pectroscop**Y**) spectra were also acquired for inverse micelles formed by PPI-1 dendrimers and hexanoic acids, to elucidate the conformation of the inverse micelles in these different solvents. Results from this study revealed the different conformations for PPI dendrimer and long aliphatic acid moieties in different solvent systems, and also proved the existence of these self-assembled inverse micelles in all studied solvents. AFM (**A**tomic **F**orce **M**icroscopy) images were also taken for the inverse micelles

formed by PPI-3 dendrimers and octanoic acids in different solvents for the morphology study.

Experimental

Chemicals and Sample Preparation. Inverse micelles for different generations of PPI dendrimers and octanoic acid were prepared at various concentrations in benzene-d_6, methanol-d_4 and toluene-d_8. PPI dendrimers and toluene-d_8 were obtained from Aldrich Chemical Co. All the other deuterated solvents were purchased from Cambridge Isotope Labs. Mica and double sided carbon adhesive materials used for AFM imaging were acquired from Structure Probe, Inc. Mica is pre-cut in 9.5 mm in diameter and 0.15 mm thick circles, and carbon adhesive materials are 1 cm circular carbon tape tabs and 0.5 cm wide conducting carbon tape. The concentration of each component of the inverse micelles used for the 1D NMR study are listed in Table 6. Samples for NOESY and AFM studies were prepared according to Table 7 and Table 8, respectively.

Table 6. Sample Concentrations of Different Generations of PPI Dendrimers and Octanoic Acids and the Respective Self-Assembled Systems

PPI Generation / Concentration (*M*)		PPI-1	PPI-1	PPI-1	PPI-2	PPI-3	PPI-4
Solvent		benzene-d_6	methanol-d_4			toluene-d_8	
PPI solution		0.18	0.36	0.053	0.026	0.013	0.0066
Octanoic acid solution		1.43	1.43	0.21	0.21	0.21	0.21
Self-assembly System	PPI	0.18	0.36	0.053	0.026	0.013	0.0066
	Octanoic acid	1.43*	1.43	0.21	0.21	0.42*	0.42*

* Non-stoichiometric mixing used.

Table 7. Sample Concentrations of Inverse Micelles for 2D NOESY NMR

Solvent / Concentration (*M*)	Benzene-d_6	acetonitrile-d_3	methanol-d_4
PPI-1	0.036	0.036	0.036
Hexanoic Acid	0.29	0.43	0.14

Table 8. Sample Concentrations of Inverse Micelles for AFM Imaging

Solvent*	PPI-3		Octanoic acid		Total
	Conc. (*M*)	Conc. (w/w %)	Conc. (*M*)	Conc. (w/w %)	Conc. (w/w %)
benzene	0.015	2.8 %	0.24	3.9 %	6.7 %
	0.015	2.8 %	0.48	7.8 %	10.6 %
acetonitrile	0.015	3.2 %	0.24	4.4 %	7.5 %
methanol	0.015	3.2 %	0.24	4.3 %	7.5 %

* Data based on solvent density: benzene 0.8787, acetonitrle 0.7856, and methanol 0.7914, which are from CRC Handbook of Chemistry and Physics (48th Edition, 1967-1968)

NMR Measurements. NMR spectra were obtained on a Varian 500 MHz spectrometer equipped with a Varian broadband probe and a Nalorac triple resonance $^{1}H/^{13}C/X$ (X can be tuned from ^{15}N to ^{31}P frequencies) probe. Solvents were also used as internal references for both ^{1}H and ^{13}C chemical shifts. The chemical shifts for the solvents are listed in Table 9. All data were processed with Varian VNMR software on a SUN Ultra-60 workstation.

Table 9. Different Solvent Chemical Shift as Referenced to TMS

Solvent	Chemical Shift (multiplicity) (ppm)*	
	^{1}H	^{13}C
acetonitrile-d_3	1.94 (5)	1.39 (7)
benzene-d_6	7.16 (1)	128.39 (3)
methanol-d_4	3.31 (5)	49.15 (7)
toluene-d_8	2.09 (5)	20.4 (7)

* Referenced to TMS, data from Cambridge Isotope Labs NMR Solvent Data Chart.

The 1D ^{1}H spectra of all solutions were acquired at 499.209 MHz, using 3.0 s acquisition time, 4000.0 Hz spectral width, 5 μs pulse width and 64 transients. All 1D ^{13}C spectra were acquired at 125.538 MHz, using 1.2 s acquisition time, 29996.3 Hz spectral width, 7.8 μs pulse width, 5 s relaxation delay and 1024 transients, with WALTZ-16 modulated ^{1}H decoupling. ^{13}C T_1 measurements were performed at 125.538 MHz, using 1.2 s acquisition time, 29996.3 Hz spectral width, 8.1 μs (90°) pulse width, 20 s

relaxation delay and 128 transients per spectrum with 12 different d_2 delays (range: 0.013 ~ 25.6 s) with WALTZ-16 modulated ^{1}H decoupling.

The 2D ^{1}H-^{1}H NOESY spectra were acquired at 499.209 MHz, using 0.5 ~ 1 s mixing time in order to detect the NOE interactions between protons of PPI-1 and hexanoic acid. ^{1}H 90° pulse widths were between 7.65 and 8.55 μs. All the 2D NOESY experiments were done with 5 s relaxation delay and 0.5 s acquisition time; 16 transients were averaged for each 2 × 256 complex t_1 increments. The data were processed with Gaussian weighting for both dimensions and with zero filling to display data on a 4096 × 1024 2D-matrix.

AFM Imaging Measurements. Two (2) μL of the sample solution or suspension, depending on the solvent (refer to Results and Discussion), was spread on the surface of a mica substrate and allowed to air dry. The mica was adhered to the sample plate with a piece of carbon tape. A Thermomicroscopes Topometrix Explorer AFM was used to image the dendrimer self-assemblies in the non-contact mode. A set point of 50% and a resolution of 400 points per line were used. Software from Thermomicroscopes was used to calculate the width and the height of the inverse micelle particles.

Results and Discussion

The ^{13}C T_1 Value Measurements. The structure of an inverse micelle normally has a polar center and nonpolar peripheries. In our study, the primary and tertiary amines from the PPI dendrimer could be considered as the polar center of the inverse micelle, and the nonpolar peripheries are comprised of the long aliphatic chains from octanoic acid moieties. Since the periphery of the inverse micelle is nonpolar, it should show

appreciable solubility in nonpolar solvents, such as benzene and toluene, which was observed in our study. However, the only solvent we found in this study that can solublize the inverse micelle at stoichiometric mixing of PPI and aliphatic acid is methanol. Stoichiometric mixing means the amount of aliphatic acids used is only enough to neutralize all the primary amine groups on the PPI surface. Because of the solvation of the ion pairs of the inverse micelle, methanol provides good solubility for different generation PPI dendrimer self-assembled systems.

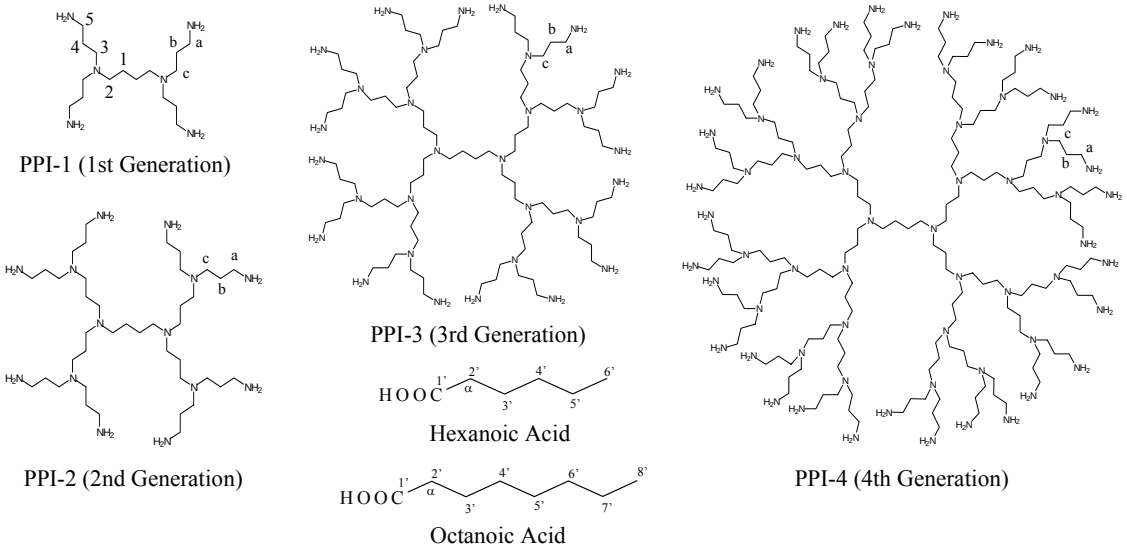

Figure 10. Labeled structures of PPI dendrimers and aliphatic acids

Two concentrated inverse micelles systems formed from the self-assembly of PPI-1 and octanoic acid were first prepared using the concentrations listed in the first two columns of Table 6. Significant differences have been observed between ^{13}C chemical shifts and ^{13}C spin-lattice relaxation time (T_1) of the exterior part (C3 ~ C5) of PPI-1 dendrimer and carboxylic acid end of octanoic acid with their corresponding moieties in the inverse micelles, as shown in Table 10 and 11. Comparing the "free" PPI-1 or "free" octanoic acid with the corresponding moieties in the self-assemblies of the concentrated

systems, regardless of the solvent used, the ^{13}C T_1 values of both groups near chain ends in PPI-1 dendrimer and carbonyl carbons in the octanoic acid moieties are reduced dramatically. This indicates the restricted motion at these sites due to the electrostatic interaction of the ammonium cation ($–NH_3^+$) and the carboxylate anion ($–COO^-$).

Table 10. The ^{13}C Chemical Shifts and ^{13}C T_1 Values of the Octanoic Acid Moieties of the Self-assemblies in Concentrated Solutions in Comparison with "Free" Octanoic Acid Solutions

Data	Solvent	System	-COOH	C2'	C3'	C4'	C5'	C6'	C7'	C8'
Chemical Shifts (ppm)	benzene-d_6	Self assembly	180.3	37.2	32.7	30.4	30.0	26.7	23.5	14.7
		"Free"	181.5	34.6	32.4	29.7	29.6	25.3	23.3	14.6
		Difference	-1.2	2.5	0.3	0.7	0.4	1.4	0.1	0.1
	methanol-d_4	Self assembly	182.7	39.3	33.1	30.9	30.4	27.8	23.8	14.7
		"Free"	177.7	35.1	33.0	30.3	30.2	26.2	23.7	14.6
		Difference	4.9	4.2	0.2	0.6	0.2	1.7	0.1	0.1
T_1 Values (s)	benzene-d_6	Self assembly	2.03	0.63	2.18	1.14	1.57	0.93	3.13	4.15
		"Free"	12.17	1.94	3.99	2.67	3.17	2.40	4.93	5.33
		% Difference	*-83*	*-68*	*-45*	*-57*	*-51*	*-61*	*-36*	*-22*
	methanol-d_4	Self assembly	6.13	1.04	2.57	1.48	1.92	1.26	3.59	4.87
		"Free"	22.30	2.84	4.98	3.38	4.11	3.15	6.18	6.37
		% Difference	*-73*	*-64*	*-48*	*-56*	*-53*	*-60*	*-42*	*-24*

Table 11. The ^{13}C Chemical Shifts and ^{13}C T_1 Values of the PPI-1 Moieties of the Self-assemblies in Concentrated Solutions in Comparison with "Free" PPI-1 Dendrimer Solutions

Data	Solvent	System	C1	C2	C3	C4	C5
Chemical Shifts (ppm)	benzene-d_6	Self assembly	25.9	54.4	52.9	25.6	39.4
		"Free"	26.2	55.0	52.8	32.1	41.4
		Difference	-0.2	-0.6	0.1	-6.5	-1.9
	methanol-d_4	Self assembly	25.8	54.9	52.7	26.1	39.6
		"Free"	26.0	55.3	53.1	31.1	41.4
		Difference	-0.2	-0.4	-0.5	-5.0	-1.7
T_1 Values (s)	benzene-d_6	Self assembly	0.198	0.115	0.143	0.218	0.148
		"Free"	1.133	1.184	1.202	1.822	2.492
		% Difference	*-82.5*	*-90.3*	*-88.1*	*-88.1*	*-94.1*
	methanol-d_4	Self assembly	0.219	0.199	0.227	0.267	0.323
		"Free"	0.558	0.508	0.535	0.792	1.220
		% Difference	*-60.7*	*-60.8*	*-57.6*	*-66.2*	*-73.5*

The ^{13}C chemical shifts of the penultimate methylene (C4 in PPI-1 as labeled in Figure 9) in all self-assembled systems significantly move upfield as shown in Figures 11 and 12, which indicates the possible chain conformational change of the PPI-1 moiety in the self-assembly to reduce the interaction of the ion pairs with solvent molecules.

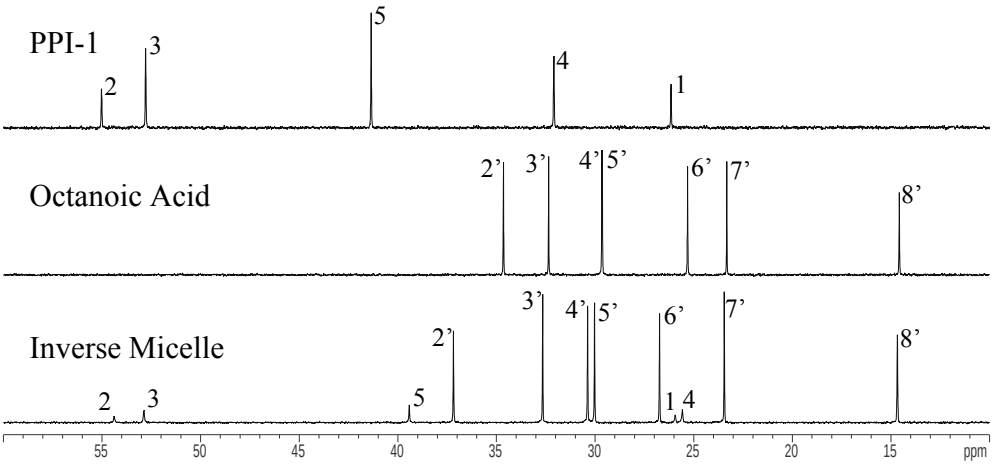

Figure 11. Labeled ^{13}C spectra of free PPI-1, free octanoic acid and inverse micelle in benzene-d_6

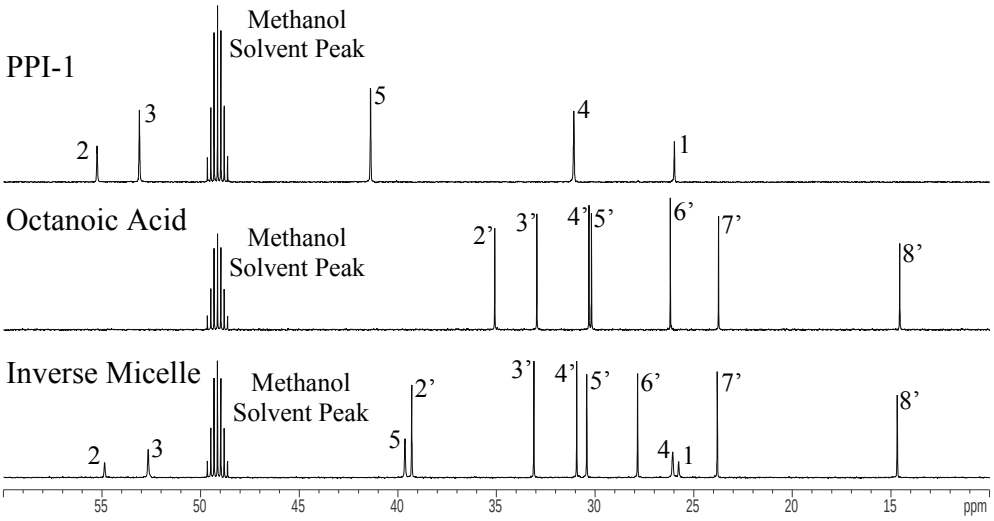

Figure 12. Labeled ^{13}C spectra of free PPI-1, free octanoic acid and inverse micelle in methanol-d_4

Another interesting observation for the self-assembled system in methanol is shown in Figure 13. The crowded resonances on PPI-1 in the hydrogen spectrum are more dispersed after the self-assembly is formed, probably because the inductive effect generated by the ion pairs influences the PPI-1 methylene groups.

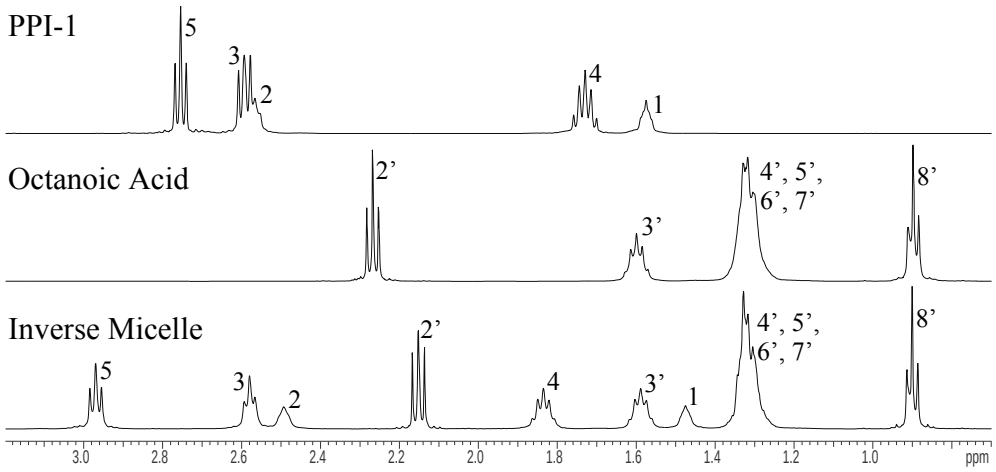

Figure 13. Labeled ^{1}H spectra of free PPI-1, free octanoic acid and inverse micelle in methanol-d_4

In the concentrated self-assembled systems, differences are observed mainly on the exterior part of PPI dendrimer moiety as well as on the carbonyl group and the α-methylene of carboxylate moiety. Solvent properties can account for the different behavior of the inverse micelles in solutions. Methanol is polar and protic compared with benzene (dielectric constant: methanol-32.7, benzene-2.3; and pK_a: methanol-15.5, benzene-43). Therefore, methanol has a significant interaction with PPI and acid molecules. Unlike in benzene or the other nonpolar solvents such as toluene (dielectric constant-2.4, pK_a-40), the inverse micelles cannot be intactly formed as in methanol solution. The NMR data show that the inverse micelles can be formed in methanol solution to a certain extent. Self-assemblies formed in nonpolar solvents tend to be better

inverse micelles than in polar solvents with the ion pairs wrapped inside and extended long aliphatic chains on the periphery. However, in polar solvents, the ion pairs tend to be exposed and have back-folded aliphatic chains.

Table 12. The ^{13}C Chemical Shifts and ^{13}C T_1 Values for Self-assembled System of PPI-1 Dendrimer and Octanoic Acid with Comparison to "Free" PPI-1 Dendrimer and Octanoic Acid Solutions

Data	Solvent	System	PPI-1			Octanoic Acid	
			C_a	C_b	C_c	-COOH	α-C
Chemical Shifts (ppm)	Methanol-d_4	Self-assembly	39.8	26.1	52.6	182.8	39.1
		"Free"	41.3	31.0	53.0	177.8	35.1
		Difference	-1.6	-4.8	-0.4	5.0	4.0
	Toluene-d_8	Self-assembly	39.3	25.1	52.8	179.9	36.4
		"Free"	41.0	31.8	52.4	180.9	34.2
		Difference	-1.7	-6.7	0.4	-0.9	2.2
T_1 Values (s)	Methanol-d_4	Self-assembly	0.454	0.394	0.277	9.885	1.644
		"Free"	1.192	0.766	0.521	10.93	2.991
		% Difference	-62.0	-48.5	-46.9	-9.6	-45.0
	Toluene-d_8	Self-assembly	0.150	0.154	0.142	2.101	0.682
		"Free"	2.317	1.705	1.137	11.28	2.219
		% Difference	-93.5	-91.0	-87.5	-81.4	-69.3

Table 13. The ^{13}C Chemical Shifts and ^{13}C T_1 Values for Self-assembled System of PPI-2 Dendrimer and Octanoic Acid with Comparison to "Free" PPI-2 Dendrimer and Octanoic Acid Solutions

Data	Solvent	System	PPI-2			Octanoic Acid	
			C_a	C_b	C_c	-COOH	α-C
Chemical Shifts (ppm)	Methanol-d_4	Self-assembly	39.6	26.2	52.4	182.8	39.2
		"Free"	41.3	31.0	53.0	177.8	35.1
		Difference	-1.7	-4.8	-0.7	5.0	4.1
	Toluene-d_8	Self-assembly	38.8	25.3	52.4	179.9	36.9
		"Free"	41.1	31.9	52.5	180.9	34.2
		Difference	-2.2	-6.5	-0.1	-1.0	2.7
T_1 Values (s)	Methanol-d_4	Self-assembly	0.336	0.262	0.199	6.71	1.423
		"Free"	0.952	0.569	0.371	10.93	2.991
		% Difference	-64.7	-54.0	-46.5	-38.6	-52.4
	Toluene-d_8	Self-assembly	0.166	0.161	0.153	1.844	0.572
		"Free"	1.569	1.006	0.580	11.28	2.219
		% Difference	-89.4	-84.0	-73.7	-83.7	-74.2

Table 14. The ^{13}C Chemical Shifts and ^{13}C T_1 Values for Self-assembled System of PPI-3 Dendrimer and Octanoic Acid with Comparison to "Free" PPI-3 Dendrimer and Octanoic Acid Solutions

Data	Solvent	System	PPI-3			Octanoic Acid	
			C_a	C_b	C_c	-COOH	α-C
Chemical Shifts (ppm)	Methanol-d_4	Self-assembly	39.6	26.3	52.4	182.7	39.2
		"Free"	41.3	31.0	53.1	177.8	35.1
		Difference	-1.7	-4.7	-0.7	4.8	4.0
	Toluene-d_8	Self-assembly	38.8	25.2	51.7	178.9	36.8
		"Free"	41.1	31.9	52.5	180.9	34.2
		Difference	-2.3	-6.6	-0.8	-2.0	2.6
T_1 Values (s)	Methanol-d_4	Self-assembly	0.288	0.240	0.172	6.083	1.152
		"Free"	0.811	0.494	0.323	10.93	2.991
		% Difference	-64.5	-51.3	-46.8	-44.3	-61.5
	Toluene-d_8	Self-assembly	0.157	0.199	0.153	1.192	0.554
		"Free"	1.202	0.729	0.389	11.28	2.219
		% Difference	-87.0	-72.8	-60.6	-89.4	-75.0

Table 15. The ^{13}C Chemical Shifts and ^{13}C T_1 Values for Self-assembled System of PPI-4 Dendrimer and Octanoic Acid with Comparison to "Free" PPI-4 Dendrimer and Octanoic Acid Solutions

Data	Solvent	System	PPI-4			Octanoic Acid	
			C_a	C_b	C_c	-COOH	α-C
Chemical Shifts (ppm)	Methanol-d_4	Self-assembly	39.5	26.2	52.4	182.3	39.0
		"Free"	41.4	31.1	53.1	177.8	35.1
		Difference	-1.8	-4.9	-0.7	4.5	3.9
	Toluene-d_8	Self-assembly	38.8	25.4	51.8	179.9	36.7
		"Free"	41.2	32.0	52.5	180.9	34.2
		Difference	-2.4	-6.6	-0.7	-1.0	2.5
T_1 Values (s)	Methanol-d_4	Self-assembly	0.249	0.217	0.165	4.548	0.965
		"Free"	0.707	0.449	0.268	10.93	2.991
		% Difference	-64.8	-51.8	-38.5	-58.4	-67.7
	Toluene-d_8	Self-assembly	0.166	0.247	0.211	2.155	0.591
		"Free"	1.127	0.633	0.337	11.28	2.219
		% Difference	-85.3	-61.0	-37.3	-80.9	-73.4

NMR studies were performed on the dilute systems of self-assemblies formed from PPI-1 to PPI-4 dendrimers. The NMR data for inverse micelles based on PPI-1 to PPI-4 are listed from Tables 12 to 15, respectively. The reduced ^{13}C T_1 values in the self-assembled system clearly demonstrate that the self-assemblies can be formed for all

generations of PPI dendrimers with octanoic acid in both polar and nonpolar solvents. The percentage difference of ^{13}C T_1 results between "free" PPIs or "free" ocatanoic acids with their corresponding moieties in the inverse micelles also indicate that the self-assembly is more efficient in nonpolar solvent than in polar solvents. It has also been observed that the ^{13}C chemical shifts of C_b (as labeled in Figure 10) in the dendrimer moieties of all generations displayed an obvious upfield shift in the self-assemblies.

Some interesting phenomena have been observed when performing the self-assemblies in different solvents. In nonpolar solvents such as benzene and toluene, mixing PPI dendrimer (for all generations) stoichiometrically with long chain carboxylic acid ($C_6 - C_{12}$) results in the formation of gel-like aggregates for the self-assemblies. In polar aprotic solvents such as acetonitrile and DMSO, powder-like aggregates (or precipitates) are obtained for the self-assemblies. But the self-assemblies are soluble in the polar protic organic solvent such as methanol. However, when non-stochiometrically mixing PPI dendrimer and the acid, *e.g.* adding twice more the amount of the acid than required for the self-assembly, the aggregation of the self-assemblies can be avoided and a clear solution can be obtained in nonpolar solvents (for polar aprotic solvent, only the first generation dendrimer PPI-1 yields a clear solution). Thus, the morphologies of these aggregates are interesting and 2D-NOESY NMR and AFM were used to study these self-assemblies.

NOESY study. Three kinds of solvents were selected for the NOE study, the protic solvent methanol, the nonpolar solvent benzene and the polar aprotic solvent acetonitrile. It is important to evaluate the effectiveness of the inverse micelle formation in a range of solvents before any conclusions can be drawn.

In methanol the components of self-assembly could be added stiochiometrically because of the solubility of the self-assemblies. According to the scheme in Figure 9, this should be the prefect ratio for inverse micelle formation. The polar protic methanol molecules can interact with both PPI-1 and hexanoic acid by strong hydrogen bonding, so the self-assemblies cannot be formed as tightly as in less polar and protic solvents. On the other hand, the enthalpy from hydrogen bonding provides a driving force to solublize the self-assemblies in methanol solution.

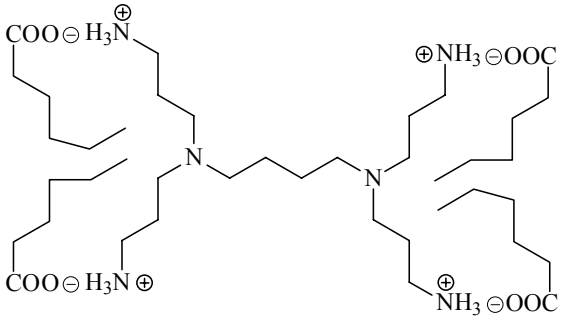

Figure 14. The possible scheme of inverse micelle in methanol solution (PPI-1 : hexanoic acid = 1:4)

The NOESY spectrum of the self-assembly in this solvent (Figure 15) is quite simple and all the NOE correlations have been observed are only between PPI-1 themselves and hexanoic acid themselves. This indicates in methanol, the PPI-1 moieties have extended conformations with extended alkyl chains of hexanoic acid. Hence the peripheral part of the self-assembly does not have a chance to get close to the central part. In this case, the alkyl chains of acid on the surface of self-assemblies maybe tangle with themselves, which gives the NOE cross peaks between the following protons: 2'/3', 2'/4', 2'/5', 3'/4', 3'/5', 3'/6', 4'/6', and 5'/6'. Because methanol has strong interaction with the PPI-1 moiety and the ion pairs of the self-assembly, the solvent molecules are able to move in and out of the self-assembly freely. Therefore, all the NOE interactions are positive,

indicating the solvated inverse micelles are segregated from each other by solvent molecules and can tumble fast in solution. No NOE interaction was observed between the PPI moiety and the acid moiety, which supported our previous prediction that strong interaction exists between the methanol solvent molecules and the components of inverse micelle (PPI-1s and hexanoic acids).

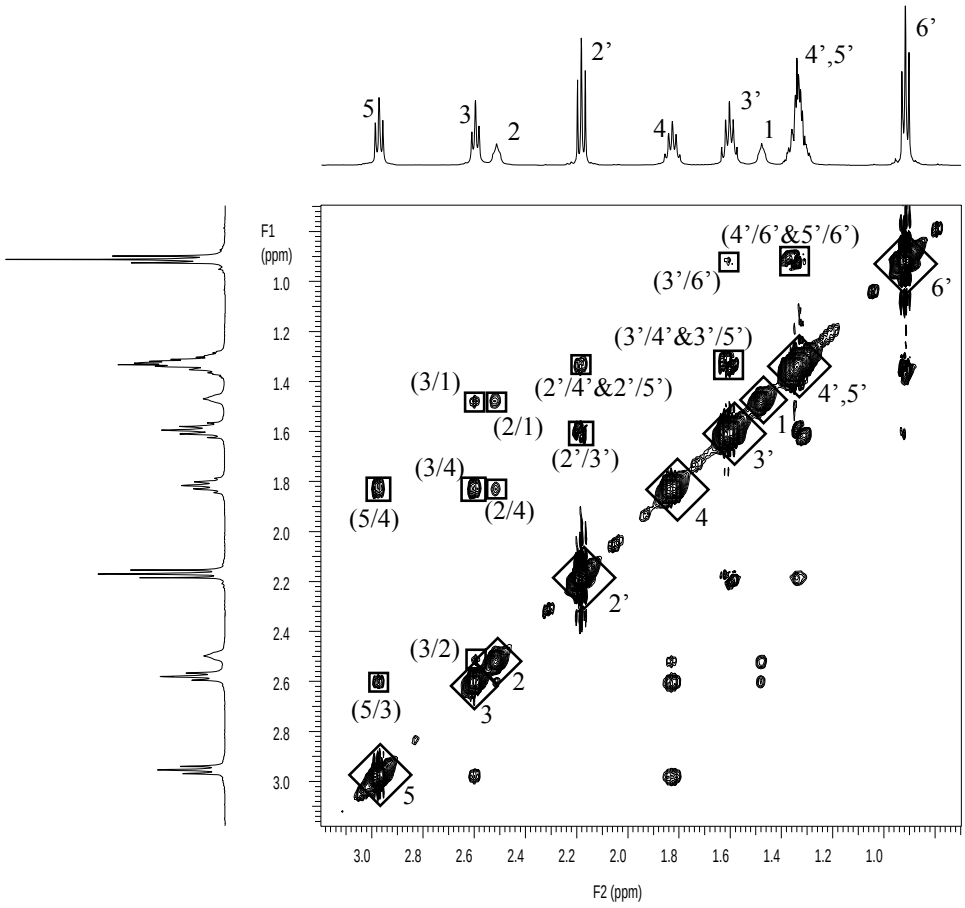

"◊" indicates diagonal peaks; "□" indicates positive NOE for the cross peak.

Figure 15. NOESY spectrum of PPI-1 – hexanoic acid inverse micelle in methanol solution. Diagonal peaks are labeled with the proton numbers shown in Figure 10, and cross peaks are marked based on the contributing protons' numbers in the inverse micelles. Frame shapes indicate the property of the peaks and the sign of NOE interaction.

In benzene, a solution of PPI-1 and hexanoic acid can be made by using twice the stoichiometric amount of hexanoic acid. Otherwise, a gel aggregation will be formed. Because of the hydrophobicity of the solvent, the ion pairs of the inverse micelles tend to be inside, away from solvent molecules as much as possible. With the stoichiometric mixing for the self-assembly, because the long aliphatic chains of hexanoic acid moieties can effectively interact with each other via van der Waal's forces, the interactions between long aliphatic chains of hexanoic acid from different inverse micelle particles can make large 3-D structure [Figure 16(a)]. This can explain why gel-like aggregates form when the amount of acid is stoichiometric.

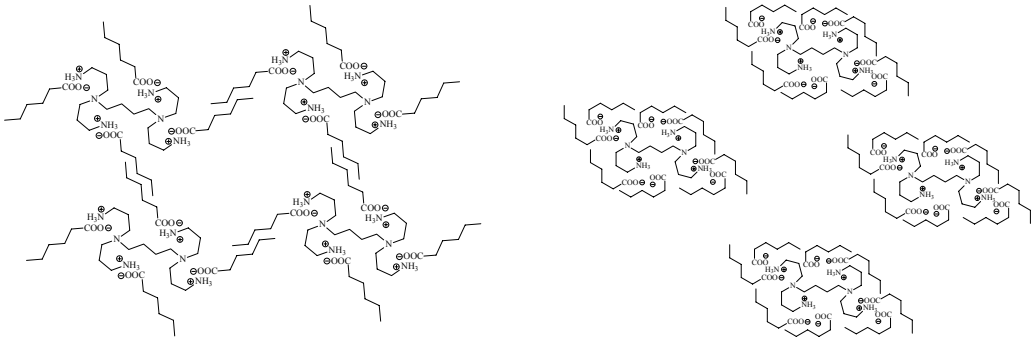

(a) (b)

Figure 16. The possible scheme of inverse micelle in benzene solution (a) stoichiometric mixing (1:4) (b) non-stoichiometric mixing (1:8): acid is in excess

However, the extra amount of hexanoic acid acts as "wrappers" to wrap the ion pairs inside the inverse micelles to form the small aggregates shown in Figure 16(b), which can be solvated by the benzene molecules. With excess hexanoic acid, the carboxyl groups can get close to the ion pairs, and their tails, the long aliphatic chains, can tangle around and provide a better shield for the hydrophilic part (ion pairs) of the inverse micelles in benzene. Hence, the solubility of inverse micelles can be increased in benzene. The same phenomenon also can happen in toluene, since the pK_a values and dielectric constants are

very similar for toluene and benzene. The NOESY study has proved that the extra acid solvates the self-assembly.

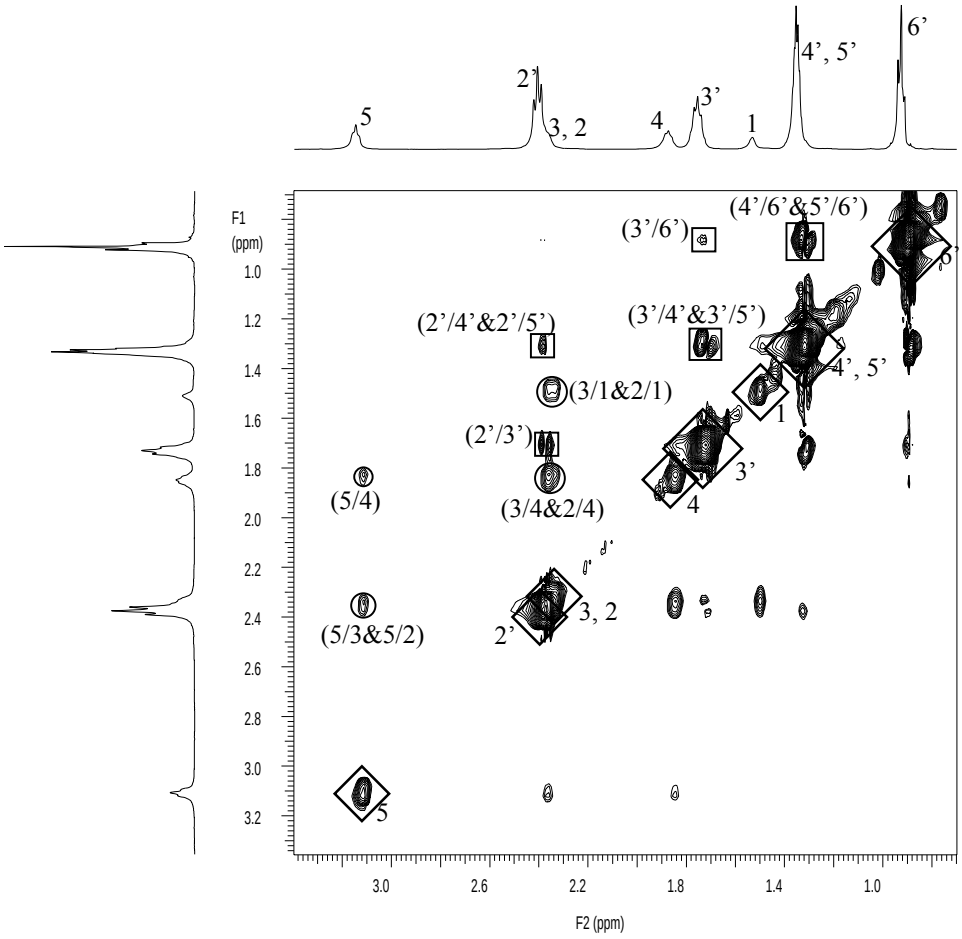

"◊" indicates diagonal peaks; "□" indicates positive NOE for the cross peak, "○" indicates negative NOE for the cross peak.

Figure 17. NOESY spectrum of PPI-1 – hexanoic acid inverse micelle in benzene solution. Diagonal peaks are labeled with the proton numbers shown in Figure 10, and cross peaks are marked based on the contributing protons' numbers in the inverse micelles. Frame shapes indicate the property of the peaks and the sign of NOE interaction.

In Figure 17, the NOE for PPI-1 moiety in the self-assembly is negative, indicating it is in an aggregate form with slow motion. Because the PPI-1 moiety is bundled tightly in

the inverse micelle as shown in Figure 16(b), it has to move with all the hexanoic acid "wrappers" on the periphery. However, the NOE for the hexanoic acid moiety is positive, which is typical for fast tumbling molecules, indicating the nonpolar long aliphatic chain still has a certain extent of freedom in the nonpolar benzene solvent. This is because the hexanoic acid moieties are on the periphery and interact with benzene molecules.

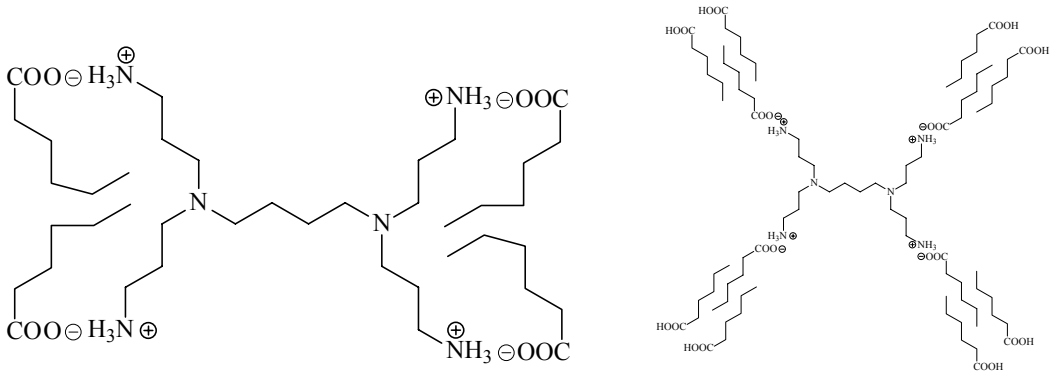

Figure 18. The possible scheme of inverse micelle in acetonitrile solution (a) stoichiometric mixing (1:4) and (b) non-stoichiometric mixing (1:12) (acid is in excess)

In acetonitrile, the hexanoic acid needs to be added in a three fold excess. Otherwise, a powder precipitate forms. The possible scheme of inverse micelles formed with stoichiometric mixing in acetonitrile is depicted in Figure 18(a), in which the ion pairs are exposed out with the aliphatic chains tangled around themselves. Considering the high polarity of acetonitrile, it is not easy to picture these self-assemblies. However, acetonitrile is an aprotic solvent, therefore its capacity to solvate is much lower than methanol because of the lack of hydrogen bonding. The ^{1}H NMR spectrum of the inverse micelle shows two sets of hexanoic acid resonances; one is from the "un-reacted" acid and the other is from the "reacted one", which can be identified based on the broad lines and lack of fine splitting patterns. Here "reacted" means those hexanoic acids moieties that have already formed ion pairs with PPI-1 dendrimers. They are in the inverse micelle

system and have a slow motion in the solution. Therefore, the relaxation of the nuclei in these acid moieties is fast, which gives broad NMR signal.

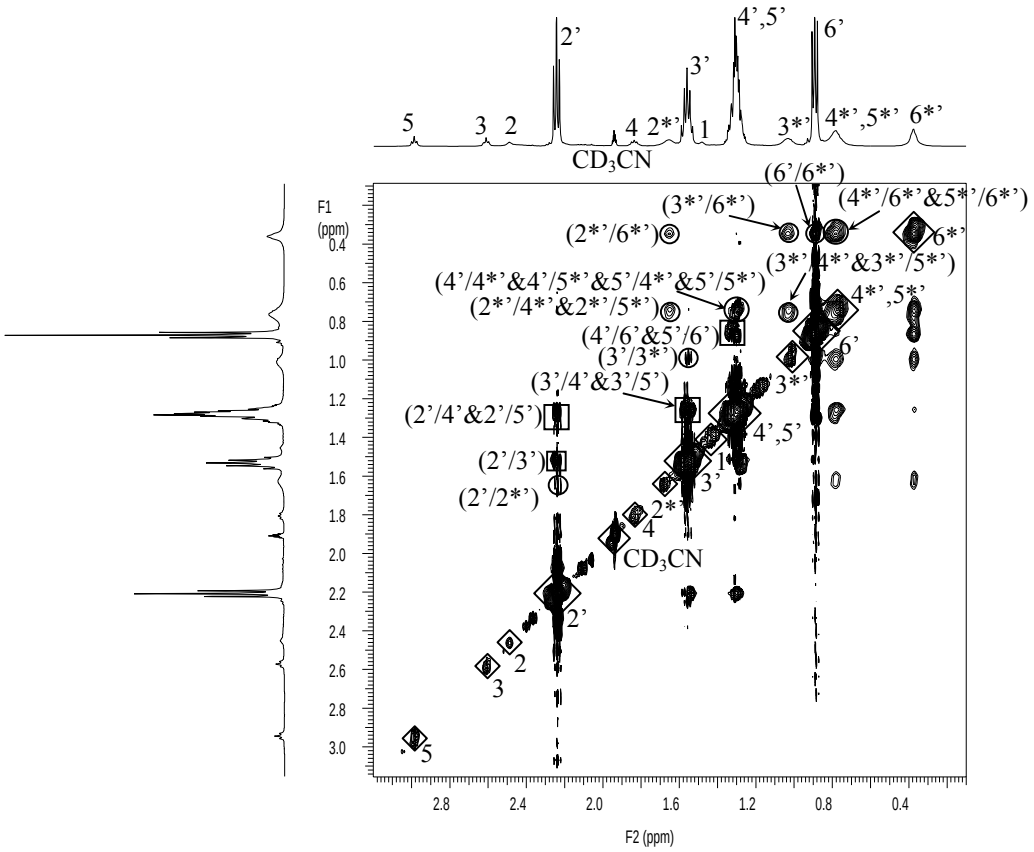

"◊" indicates diagonal peaks; "□" indicates positive NOE for the cross peak, "○" indicates negative NOE for the cross peak. "*" indicates the reacted hexanoic acids.

Figure 19. NOESY spectrum of PPI-1 – hexanoic acid inverse micelle in acetonitrile solution. Diagonal peaks are labeled with the proton numbers shown in Figure 10, and cross peaks are marked based on the contributing protons' numbers in the inverse micelles. Frame shapes indicate the property of the peaks and the sign of NOE interaction.

The NOESY spectrum of inverse micelles formed in acetonitrile (Figure 19) is very interesting. First, the NOE interactions of PPI-1 moiety itself are too weak to be observed with the scale for displaying the ones from the acid moiety. This suggests that dendrimer

is in the extended conformation and rigid. Also, the NOE interactions between "un-reacted" hexanoic acids are observed weakly and are all positive, indicating they are actually quite mobile in solution. This is also consistent with the ^{1}H NMR spectrum. Interestingly, the NOE interactions between "reacted" hexanoic acids are all negative, and are quite strong. This suggests that those acid moieties are associated with PPI-1 moieties quite tightly in the self-assembly. The weaker NOE interactions between "reacted" and "un-reacted" hexanoic acids indicate that the excess amounts of hexanoic acid assist the inverse micelle dissolving in this polar solvent. This is achieved by tangling the nonpolar tail (aliphatic chains) of these acids into the nonpolar periphery of the inverse micelle and pointing out their polar heads (carboxylate groups) into the polar solvent environment [Figure 18(b)]. This also indicates why the acid need be in large excess to get the inverse micelle to dissolve. Because the surface area is more crowded for higher generation PPI dendrimers, more nonpolar aliphatic chain on the dendrimer surface would be expected after the formation of inverse micelles. Therefore, more acids are required to "solvate" these inverse micelles; even a three-fold excess of long chain alphatic acid is not adequate. Another reason may be that the extra acids are more difficult to attach to the nonpolar periphery of the inverse micelles formed from higher generation PPI dendrimers since the surface is already quite crowded. Therefore, higher generation dendrimer based inverse micelles cannot be solublized with extra acids.

AFM imaging study. The inverse micelles have been studied in three solvents for AFM imaging: methanol, acetonitrile and benzene. Two ratios of self-assembly in benzene were used for the study. The concentrations of samples were listed in Table 8.

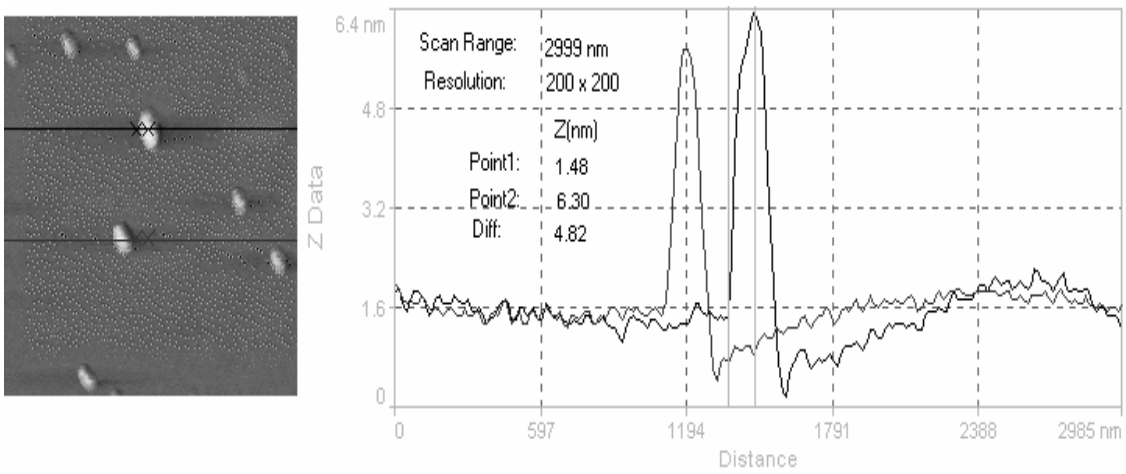

Figure 20. AFM image of inverse micelle in acetonitrile with stoichiometric mixing

As aforementioned, if the mixing ratio of PPI-3 and octanoic acid is stoichiometric in acetonitrile, a powder precipitate will be formed. The AFM image of the precipitates is shown in Figure 20. The particles of the precipitates are evenly formed and distributed with the height averaging from 4.5 to 5 nm. This supports the scheme proposed in Figure 18. The nonpolar periphery of these inverse micelles gives small contact area on the mica surface; this is also the reason why these particles give a relatively high height-to-width ratio in AFM image.

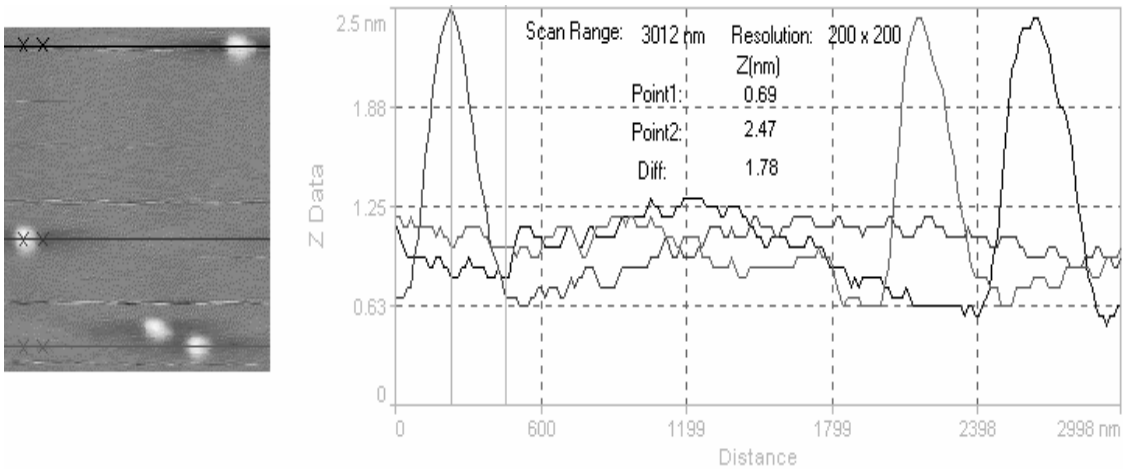

Figure 21. AFM image of inverse micelle in methanol with stoichiometric mixing

AFM image of the self-assembly in methanol is shown in Figure 21. In this solvent, the particles formed are shorter in height (1.5~2 nm). Because of the relatively high polarity and high hydrogen-bonding capability of methanol, the inverse micelle particles formed from self-assembly of PPI-3 and octanoic acid can be well solvated in methanol. So inverse micelles can spread out on the polar mica surface with larger contact areas and shorter height.

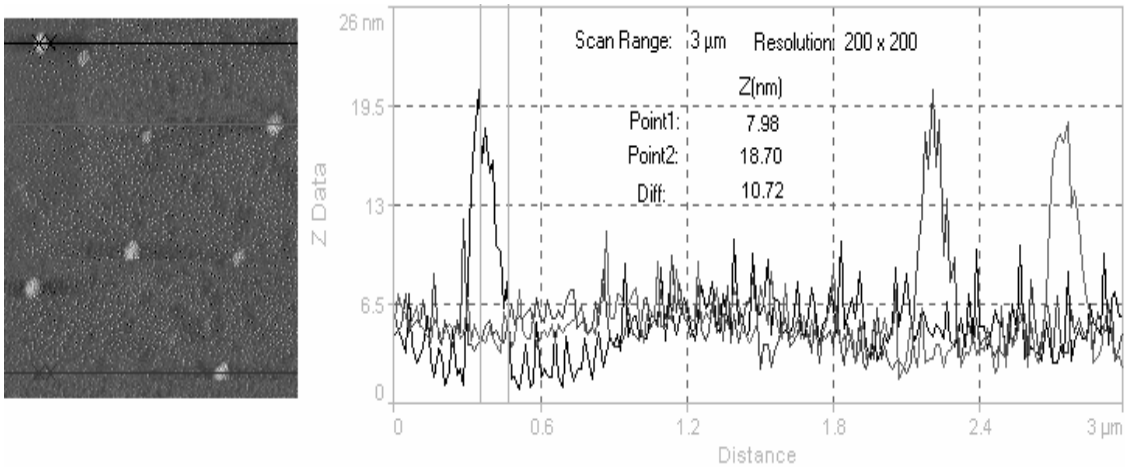

Figure 22. AFM image of inverse micelle in benzene with stoichiometric mixing

In benzene, which has proved to be the ideal solvent for the self-assembled inverse micelles (based on the ^{13}C T_1 results), the AFM images turned out to be very interesting. Actually, two different mixing ratios were used for AFM study in this solvent. When using stoichiometric mixing of PPI-3 and octanoic acid, the inverse micelles tend to form tall aggregated bundles (~11 nm) for the particles, which is shown by their AFM image in Figure 22. Here the benzene solvent for preparing AFM samples gives the fully hydrophobic self-assemblies which have rather small contact area with the mica surface. The height of the particles further supported the aggregation of the inverse micelles in benzene [Figure 16(a)].

It becomes more interesting when excess octanoic acid is added to the system. According to the scheme in Figure 16 (b), aggregations are smaller when extra octanoic acid is present in the system. The AFM image of the self-assembled inverse micelles is shown in Figure 23, which does indicate shorter height (~4 nm) than in the bundles (~11 nm) shown in Figure 22.

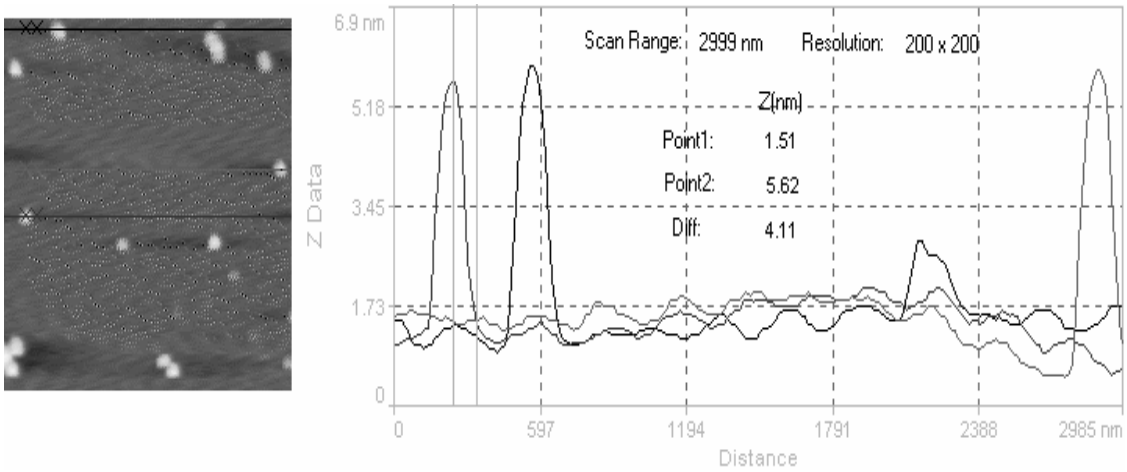

Figure 23. AFM image of inverse micelle in benzene with non-stoichiometric mixing

Conclusion

Different techniques, including ^{1}H and ^{13}C 1D NMR, ^{13}C T_1 values measurement and ^{1}H-^{1}H NOESY 2D NMR, and AFM imaging are used to confirm that inverse micelles between PPI dendrimers and long chain aliphatic acids can be formed through electrostatic self-assembling in all studied solvents. ^{13}C T_1 measurements showed the information of the restricted sites for the connection of two component moieties in those inverse micelle structures. The 2D NOESY and AFM imaging techniques provide enough information to further support the scheme proposed for the structures of inverse micelles in different solvents.

CHAPTER IV – STUDIES ON THE CATALYTIC PROPERTIES OF PPI DENDRIMERS

Introduction

Among the many potential applications of dendrimers, catalysis is one of the most promising fields.[31] The dendritic catalysts have spread into various areas, such as organic chemistry, inorganic chemistry, materials science, biochemistry, and polymer chemistry. Dendrimers have been used for both homogeneous and heterogeneous catalyses.[32] It is also possible to fine tune the structure, size, shape, and solubility of dendrimers and metallodendrimers for unique catalytic applications and to locate their catalytic sites either at the core or at the periphery of the dendrimer.[33]

PPI dendrimers have been extensively investigated for their potential as catalysts. By modifying PPI-3 with diphenylphosphine ligands, Reetz *et al.* made a 32-branch phosphine dendrimer that is capable of forming complexes with transition metal compounds such as $PdMe_2$ or $Rh(cod)BF_4$ (cod = 1,5-cyclooctadiene). These metal-dendrimer complexes showed better catalytic properties than the monomeric parent compound ($RN(CH_2PPh_2)_2PdMe_2$, R = *n*-C_3H_7 or Ph) for the hydroformylation of 1-octene because of the higher thermal stabilities of the dendritic complexes.[34] Peerlings and Meijer modified the periphery of PPI dendrimers with chiral (R)-phenyloxirane for exploring the possibility of catalyzing asymmetric addition of diethylzinc to benzaldehyde.[35] Crooks *et al.* reported the synthesis of PPI dendrimers encapsulating metal particles, and the use of them as homogeneous catalysts for hydrogenation. Because the surfaces of higher generation dendrimers are more sterically crowded, lower

generation dendrimers work better because the reactant has more chance of accessing the catalytic sites.[36] Froehling and Corstjens converted the primary amines of PPI-1 and PPI-2 dendrimers to tertiary amines to investigate the advantages of using these modified PPI dendrimers as catalysts for polyurethane synthesis. In fact, the modified dendrimers turned out to be no better than conventional tertiary amine catalysts, but the modified dendrimers are non-volatile and odorless so they could be used where the amine emission is problematic.[37] Jansen *et al.* showed the use of PPI dendrimers as photoinitiating systems in UV-curable coatings for various applications since dendrimers serve both as initiator and oxygen scavenger.[38]

The use of PPI dendrimers as catalysts for organic ester hydrolysis under mild conditions has not been reported. Accidentally, when PPI dendrimers were used for the encapsulation of a fluorescent dye, $DEBF_4$, a diester [Figure 24(b)], we discovered that PPI dendrimers can efficiently catalyze the ester hydrolysis at room temperature. In this work, the catalytic function of PPI dendrimers for ester hydrolysis was further investigated using NMR and UV-vis (**U**ltra**V**iolet **vis**ible light absorbance) spectroscopies.

Experimental

Materials. PPI dendrimers and DMSO-d_6 were obtained from Aldrich Chemical Co. Deuterium oxide and methanol-d_4 were purchased from Norell Inc. All fluorescent dyes used in this research were synthesized by Dr. Morgan's group at Marshall University. Methyl benzoate and benzoic acid were obtained from Fisher Scientific Company and The British Drug Houses Ltd., respectively. Ethyl amine and ethylene diamine were

purchased from Acros Organics. Sodium hydroxide and concentrated hydrochloric acid were obtained from VWR Scientific Products and Fisher Scientific Company, respectively. No special treatment for chemicals was performed prior to the UV-vis and NMR studies.

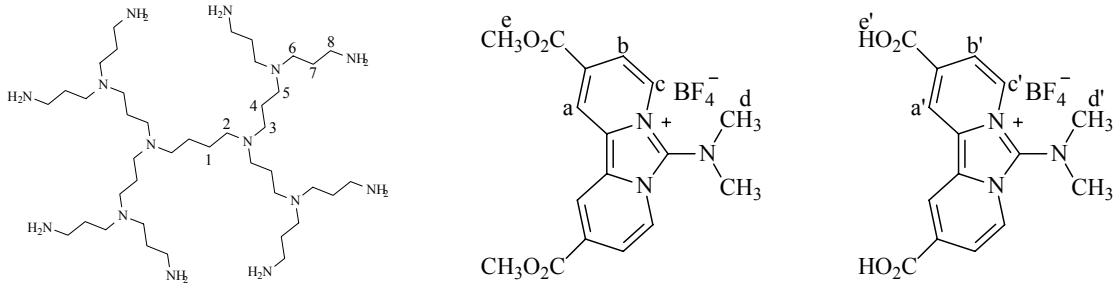

(a) PPI-2 (b) $DEBF_4$ (c) $DABF_4$

Figure 24. The labeled structures of (a) PPI-2 dendrimer, (b) fluorescence dye, $DEBF_4$ (dipyrido[1,2-c:2',1'-e] imidazol-5-ium, 6(dimethylamino)-2,10-bis (methoxycarbonyl), tetrafluoroborate), and (c) fluorescence dye, $DABF_4$ (dipyrido[1,2-c:2',1'-e] imidazol-5-ium, 6(dimethylamino)-2,10-bis (hydroxycarbonyl), tetrafluoroborate).

Kinetic Studies of the Hydrolysis of $DEBF_4$. *NMR Study.* Two different solvent systems (D_2O and methanol-d_4) were used for the NMR kinetic studies. In order to simplify the studies, both D_2O and methanol-d_4 were used in large excess so as to give pseudo-first-order reactions. In each system, the reactions were monitored through ^1H NMR by fixing the amount of dye and the amount of PPI dendrimer, respectively.

PPI dendrimers were dissolved in either D_2O or methanol-d_4 in a conical vial, and $DEBF_4$ dyes were dissolved in DMSO-d_6 in a 5 mm NMR tube. A stopwatch was started when the solutions were mixed, and ^1H 1D NMR spectra were acquired every five minutes till the reaction was completed. The initial concentrations of PPI-2 and $DEBF_4$ dye are listed in Table 16. The same procedure was used for acquiring the NMR spectra of $DABF_4$ and PPI-2 in the methanol-d_4 system, according to the concentrations listed in Table 17.

Table 16. $DEBF_4$ and PPI-2 Initial Concentration for NMR Studies

Molar Ratio of $DEBF_4$ to PPI-2	Initial Concentrations (*M*)*			
	D_2O System†		Methanol-d_4 System‡	
	$DEBF_4$	PPI-2	$DEBF_4$	PPI-2
1:16	0.01721	0.27535	0.00861	0.13768
1:8	0.01721	0.13768	0.00861	0.06884
1:4	0.01721	0.06884	0.00861	0.03442
1:2	0.01721	0.03442	0.00861	0.01721
1:1.5	0.01721	0.02591	0.00861	0.01295
1:1	0.01721	0.01721	0.00861	0.00851
1:0.75	0.01721	0.0195	0.00861	0.00648
1:0.5	0.01721	0.00851	0.00861	0.00426
1:0.25	0.01721	0.00426	0.00861	0.00241
4:1	0.06885	0.01721	0.03442	0.00851
2:1	0.03442	0.01721	0.01721	0.00851
0.5:1	0.00861	0.01721	0.00448	0.00851
0.25:1	0.00448	0.01721	0.00207	0.00851

* The volume of the solution was maintained at 0.7 mL. † In D_2O system, the mixed solvent ratio of D_2O to DMSO-d_6 was 1.63:1. Here DMSO-d_6 is used for the purpose of enhancing the solubility of the $DEBF_4$ dye in the aqueous solution. ‡ In methanol-d_4 system, the mixed solvent ratio of methanol-d_4 to DMSO-d_6 was 2.29:1.

Table 17. $DABF_4$ and PPI-2 Initial Concentration for NMR Studies

Molar Ratio of $DABF_4$ to PPI-2	Initial Concentrations (*M*)*		
	$DABF_4$	PPI-2	methanol†
1:4	0.00849	0.03442	0.1546

* The volume of the solution was maintained at 0.7 mL. The mixed solvent ratio of methanol-d_4 to DMSO-d_6 was 2.29:1. † Non-deuterated methanol was used to enhance the sensitivity of methoxy peaks.

NMR spectra were obtained on a Varian Unity 500 MHz spectrometer equipped with a Varian broadband probe. All experiments were performed at ambient temperature. ^1H NMR spectra were acquired at 499.212 MHz, using 3.0 s acquisition time, 5999.7 Hz spectral width, 5 μs (15º) pulse width and 1 transient for each spectrum. ^{13}C NMR spectra were acquired at 125.893 MHz, using 1.3 s acquisition time, 3 s relaxation delay, 29996.3 Hz spectral width, 7.8 μs (90º) pulse width and 1024 transient, with WALTZ-16

modulated ^{1}H decoupling. All data were processed with Varian VNMR software on a SUN Ultra 60 workstation.

UV-vis Study. The concentrations of reagents in aqueous stock solutions for the UV-vis study are as follows: PPI-2 – 0.0103 *M*, diester $DEBF_4$ – 0.00231 *M* and diacid $DABF_4$ – 0.00227 *M*. Different concentrations of $DABF_4$ solutions and $DEBF_4$ solutions were made from the stock solutions for the kinetic studies to obtain the absorbance of $DABF_4$ and $DEBF_4$ at wavelengths 399 nm (λ_{max} of $DABF_4$) and 419 nm (λ_{max} for $DEBF_4$), respectively.

Various concentrations of PPI-2 were also made by adding the different volume of the PPI-2 stock solution to 2 mL distilled water in a 1 cm cuvette. Each PPI-2 solution was used as blank for each individual UV-vis measurement. Later 20 μL $DEBF_4$ stock solution was added to the PPI-2 solution and the UV-vis spectra were taken every 5 minutes after the mixing for 12 hours.

Table 18. $DEBF_4$ and PPI-2 Initial Concentration for UV-vis Studies

Molar Ratio of $DEBF_4$ to PPI-2	Volume (μL)		Concentrations (*M*)	
	$DEBF_4$	PPI-2	$DEBF_4$	PPI-2
1:16	20	71.6	2.31×10^{-5}	3.70×10^{-4}
1:8	20	35.78	2.31×10^{-5}	1.85×10^{-4}
1:4	20	17.89	2.31×10^{-5}	9.24×10^{-5}
1:2	20	8.94	2.31×10^{-5}	4.62×10^{-5}
1:1	20	4.47	2.31×10^{-5}	2.31×10^{-5}
1:0.5	20	2.24	2.31×10^{-5}	1.16×10^{-5}
1:0.25	20	1.12	2.31×10^{-5}	5.78×10^{-6}

The Comparison of PPI-2 and Other Primary Amines as Catalysts for the Hydrolysis of $DEBF_4$ ester. The same $DEBF_4$ stock solution was used, and 1:2 molar ratio of $DEBF_4$ to PPI-2 was used. The concentrations of ethyl amine and ethylene diamine stocks were 0.01 *M*.

Table 19. Initial Concentrations for Comparison Studies

Amines	Molar Ratio of $DEBF_4$ to catalyst	Volume (μL)		Concentrations (*M*)		Initial pH value
		$DEBF_4$	Amine	$DEBF_4$	Amine	
PPI-2	1:2	20	8.94	2.31×10^{-5}	4.62×10^{-5}	8.2
PPI-2	1:2	20	8.94	2.31×10^{-5}	4.62×10^{-5}	7.0
Ethyl Amine	1:16*	20	73.9	2.31×10^{-5}	3.70×10^{-4}	8.2
Ethyl Amine	1:16*	20	73.9	2.31×10^{-5}	3.70×10^{-4}	7.0
Ethylene Diamine	1:8*	20	37.0	2.31×10^{-5}	1.85×10^{-4}	8.2
Ethylene Diamine	1:8*	20	37.0	2.31×10^{-5}	1.85×10^{-4}	7.0
None	1:0	20	0	2.31×10^{-5}	0	8.2
None	1:0	20	0	2.31×10^{-5}	0	7.0

* The ratios were chosen so that the number of primary amine groups in other amines is equivalent to the number of primary amine groups in PPI-2.

Samples were prepared according to the volumes in Table 19. At first, a volume of stock solution (PPI-2, ethyl amine or ethylene diamine) was added to 4 mL distilled water, then aqueous hydrochloric acid (0.1 *M*) was used to adjust the pH to the desired value. For comparison, solutions without amine (none) were also tested using aqueous sodium hydroxide (0.1 *M*) to adjust the pH. Blank spectra were obtained from 2 mL of the solutions prepared above in a 1 cm cuvette. Later 20 μL $DEBF_4$ stock solution were added to each solution and UV-vis spectra were taken every 5 minutes after mixing for 12 hours.

Study of PPI-2 Catalysis on the Hydrolysis of Other Esters. ^{13}C NMR spectra were taken for the methyl benzoate and methyl trifluoroacetate samples prepared according to Table 20 and 21, respectively, using the same parameters mentioned in the NMR kinetic study.

Table 20. NMR Samples for Methyl Benzoate Hydrolysis Study

Concentration (*M*)*				Waiting Time after Sample is Made
Methyl Benzoate	Benzoic Acid	Benzamide	PPI-2 Dendrimer	
0.115	—	—	0.115	0 min
0.115	—	—	0.115	46 hrs
0.115	—	—	0.115	147 hrs
—	0.115	—	0.115	0 min
—	—	0.115	0.115	0 min

* The mixed solvent ratio of D_2O to DMSO-d_6 was 1.10:1. DMSO-d_6 was used for enhancing the solubility of methyl benzoate and benzoic acid.

Table 21. NMR Sample for Methyl Trifluoroacetate Hydrolysis Study

Concentration (*M*)*		Waiting Time after Sample is Made
Methyl Trifluoroacetate	PPI-2 Dendrimer	
0.0284	—	0 min
0.0284	0.0142	4.3 hrs

* The mixed solvent ratio of D_2O to DMSO-d_6 was 0.895:1. DMSO-d_6 was used for enhancing the solubility of methyl trifluoroacetate.

Results and Discussion

Kinetic Study of the Hydrolysis of $DEBF_4$. The diester dye $DEBF_4$ was found to be very stable in either D_2O or DMSO-d_6 by monitoring it over a several-week period. As mentioned previously, the catalysis phenomenon was discovered when PPI-2 dendrimer was used to encapsulate the $DEBF_4$ dye. The resonance of the methoxy group of $DEBF_4$ disappeared in the ^1H NMR spectrum, and a peak at methanol's methoxy resonance appeared. Also the UV-vis spectra of the "encapsulated system" showed a significant blue shift in the λ_{max} of $DEBF_4$, which is towards the λ_{max} of the diacid fluorescence dye, $DABF_4$. Based on these results, the hydrolysis of the ester was proposed, and further investigations were performed.

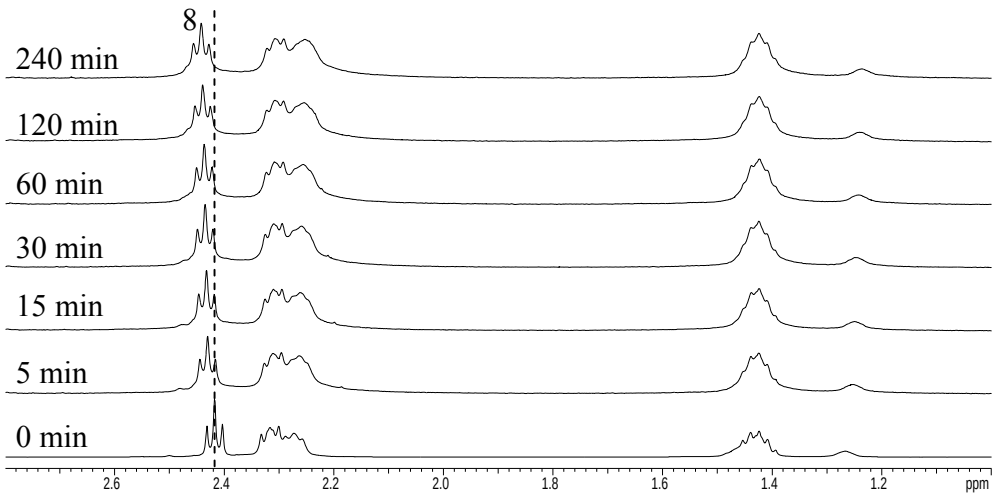

Figure 25. The ^{1}H NMR spectra of PPI-2 in D_2O system at different times (1:2 ratio of $DEBF_4$ and PPI-2).

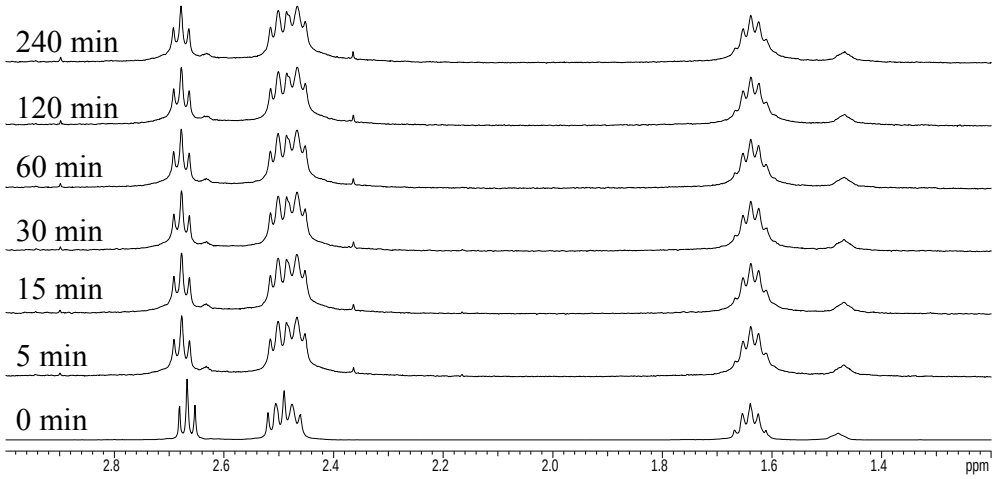

Figure 26. The ^{1}H NMR spectra of PPI-2 in methanol-d_4 system at different times (1:2 ratio of $DEBF_4$ and PPI-2).

NMR study. It is important to verify that PPI-2 dendrimer is truly a catalyst and not a reactant. NMR spectra of the PPI-2 dendrimer in both D_2O and methanol-d_4 systems at different reaction times were shown in Figures 25 and 26, respectively. It was clearly observed that the spectra of the PPI-2 dendrimer did not change substantially over the entire reaction period, and therefore the role of PPI-2 dendrimer is as a catalyst.

However, a slight downfield shift of the resonance of methylene group 8 [as labeled in Figure 24(a)] was observed. This may be because the primary amines in PPI-2 and the carboxylic acid groups in the product ($DABF_4$) can self-assemble through electrostatic interaction. This is similar to the formation of the inverse micelle mentioned in the previous chapter.

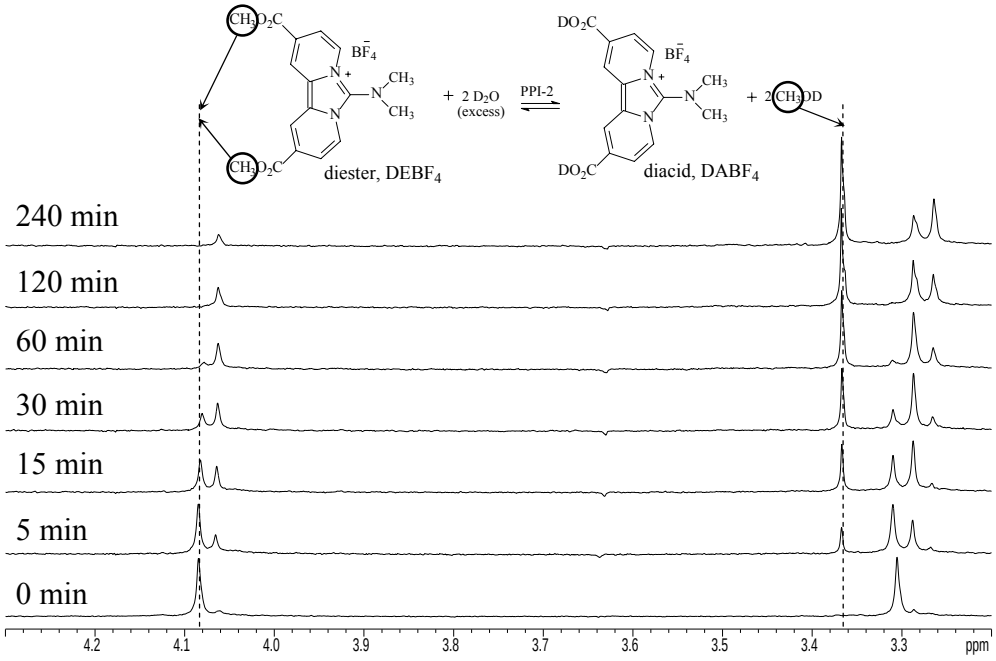

Figure 27. The ^{1}H NMR spectra of 1:2 ratio of $DEBF_4$ and PPI-2 in D_2O system at different times.

Figures 27 and 28 are stack plots of NMR spectra at different reaction times in D_2O and methanol-d_4 systems, respectively. A clear trend, the disappearance of the methoxy resonance of the diester dye $DEBF_4$ and the appearance of methanol's methoxy resonance, can be seen.

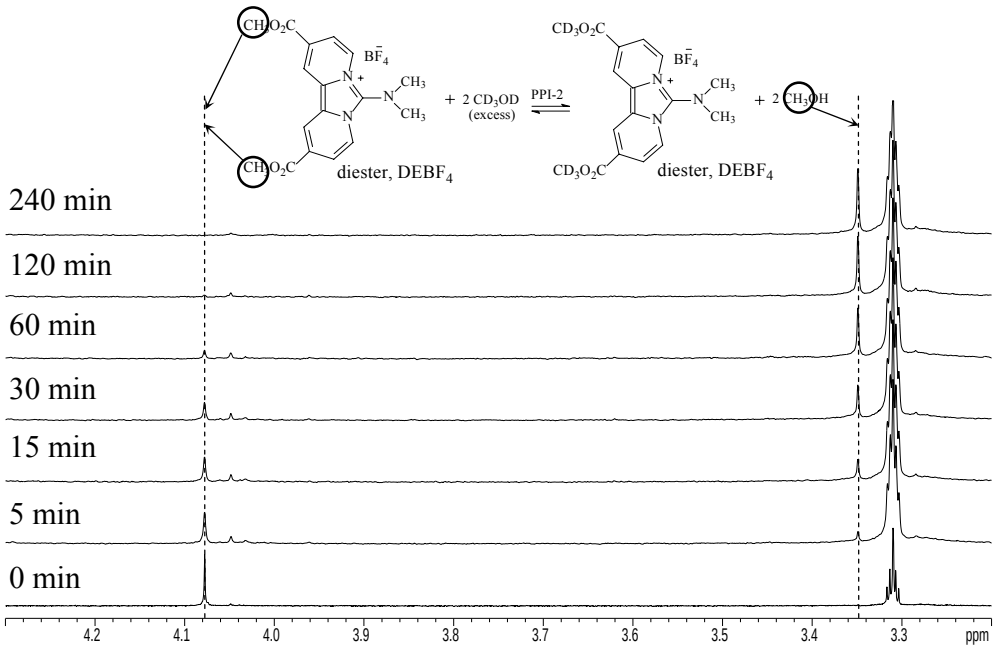

Figure 28. The ^{1}H NMR spectra of 1:2 ratio of $DEBF_4$ and PPI-2 in methanol-d_4 system at different times.

In quantitative NMR measurements, the area of each resonance peak is proportional to the number of contributing nuclei. So, all the NMR spectra were integrated, using the sum of integration values from all the aromatic peaks as the standard (because they do not change over the course of the reaction), so as to obtain an accurate ratio between the areas of the methoxy peak of the reactant and the methoxy peak of the product. The methoxy group of the diester represents the reactant (unhydrolyzed ester form), and the methoxy group of methanol represents one of the products (alcohol, the hydrolyzed form). Since each the hydrolysis of each mole of $DEBF_4$ gives 2 moles of methanol, but only one mole of the diacid $DABF_4$, the ratio between the areas of these two methoxy resonances actually is twice the ratio of reactant (diester dye $DEBF_4$) to the product (methanol), but equal to the ratio of diester dye $DEBF_4$ to the diacid dye $DABF_4$.

In organic chemistry, we know ester hydrolysis has a similar mechanism to that of transesterification. So, we also tested for PPI-2 catalysis at the transesterification in the methanol-d_4 system. In the methanol-d_4 system, the non-deuterated methoxy group (CH_3O–) in $DEBF_4$ is expected to be replaced by the deuterated methoxy group (CD_3O–) from the solvent, methanol-d_4. Actually, the same trend of the resonance changes (Figure 28) can be observed on NMR spectra. However, no λ_{max} shift would be observed in the UV-vis spectra because the product is actually the deuterated form of the reactant.

Based on NMR, the real-time concentration of $DEBF_4$ can be calculated to obtain the kinetics data using the following equation:

$$[DEBF_4] = [DEBF_4]_0 \times \frac{I_{MeO}}{I_{Aromatics}} \times \frac{63.05}{36.95}$$

In which $[DEBF_4]$ is the real time concentration of diester dye $DEBF_4$, $[DEBF_4]_0$ is the initial concentration of $DEBF_4$; I_{MeO} and $I_{Aromatics}$ are the integration value of the methoxy resonance and the total aromatic resonances, respectively, from the ^1H NMR spectra; 63.05/36.95 is the ratio of the integration of the total aromatic resonances to the methoxy resonance in pure diester dye $DEBF_4$ solution in the DMSO-d_6/D_2O mixed solvent (in DMSO-d_6/methanol-d_4 mixed solvent, the values are 58.03/41.97). All the integration values are listed in Appendix I; only the results of kinetic information are displayed here.

The kinetics data show a pseudo-1st order reaction in all cases, which is in accordance with the reaction rate equation we proposed as follows:

$$r = k \cdot [DEBF_4] \cdot [PPI\text{-}2] \cdot [D_2O]$$

where r is the reaction rate, k is the real (third order) reaction rate constant, $[DEBF_4]$, [PPI-2], and $[D_2O]$ is the concentration of $DEBF_4$, PPI-2 and D_2O, respectively. PPI-2 acts as the catalyst, so the concentration will not change during the whole reaction, and

its concentration can be taken as a constant. With the huge excess amount of D_2O or methanol-d_4 ($[D_2O]/[DEBF_4] = 2000$) in the reaction, only a very slight amount of D_2O is consumed after all the $DEBF_4$ has been converted, so we can also treat the D_2O concentration as a constant. In this way the reaction rate can be described in the following equation:

$$r = k_{obs} \cdot [DEBF_4]$$

where k_{obs} is the observed pseudo-1st order rate constant, and in fact,

$$k_{obs} = k \cdot [PPI\text{-}2] \cdot [D_2O]$$

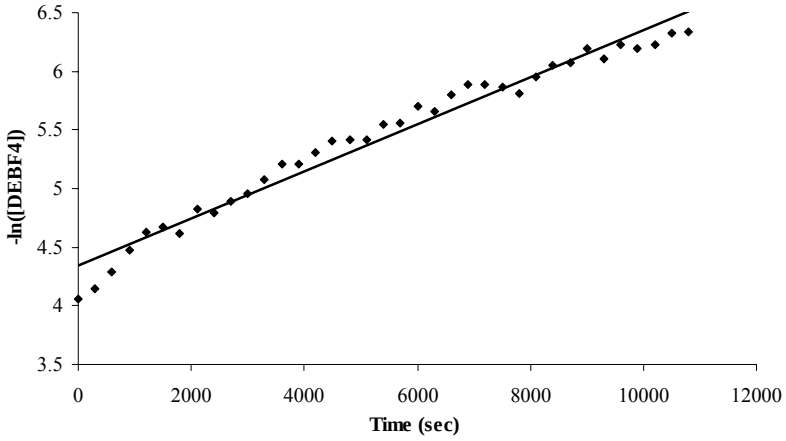

Figure 29. Linear relationship of $-\ln([DEBF_4])$ versus time, data obtained from 1:0.75 mixture of $DEBF_4$ and PPI-2 in D_2O system. The negative sign is to make all the values positive for easy processing.

If the natural logarithm of the concentration of $DEBF_4$ is plotted versus time, a linear relationship should be obtained, and the value of the slope should be k_{obs}. The k_{obs} values of different ratio mixtures are listed in Table 22 for D_2O system and Table 23 for methanol-d_4 system. The plot of pseudo-1st order reaction constant versus PPI-2 concentration generates another linear relationship, in which the slope is the pseudo-2nd

order reaction constant k_{obs2}, and $k_{obs2} = k \cdot [D_2O]$. With this information we can calculate the real rate constant k.

Table 22. Kinetic Data for Hydrolysis of $DEBF_4$ in D_2O System

Molar Ratio of $DEBF_4$ to PPI-2	Initial Concentrations (M)		Pseudo-1st Order Reaction Rate Constant ($\times 10^{-4}$ s^{-1})
	$DEBF_4$	PPI-2	
1:16	0.01721	0.27535	71.097
1:8	0.01721	0.13768	39.205
1:4	0.01721	0.06884	17.251
1:2	0.01721	0.03442	8.283
1:1.5	0.01721	0.02591	6.6171
1:1	0.01721	0.01721	4.3148
1:0.75	0.01721	0.0195	3.2317
1:0.5	0.01721	0.00851	2.2356
1:0.25	0.01721	0.00426	1.0554
4:1	0.06885	0.01721	4.2092
2:1	0.03442	0.01721	4.2863
1:1	0.01721	0.01721	4.3148
0.5:1	0.00861	0.01721	4.3302
0.25:1	0.00448	0.01721	4.2719

Table 23. Kinetic Data for Hydrolysis of $DEBF_4$ in Methanol-d_4 System

Molar Ratio of $DEBF_4$ to PPI-2	Initial Concentrations (M)		Pseudo-1st Order Reaction Rate Constant ($\times 10^{-4}$ s^{-1})
	$DEBF_4$	PPI-2	
1:16	0.01721	0.27535	45.92
1:8	0.01721	0.13768	10.646
1:4	0.01721	0.06884	10.146
1:2	0.01721	0.03442	6.23
1:1.5	0.01721	0.02591	5.0319
1:1	0.01721	0.01721	3.4318
1:0.75	0.01721	0.0195	2.6151
1:0.5	0.01721	0.00851	1.7306
1:0.25	0.01721	0.00426	1.1932
4:1	0.06885	0.01721	3.2809
2:1	0.03442	0.01721	3.3589
1:1	0.01721	0.01721	3.4318
0.5:1	0.00861	0.01721	3.3974
0.25:1	0.00448	0.01721	3.3376

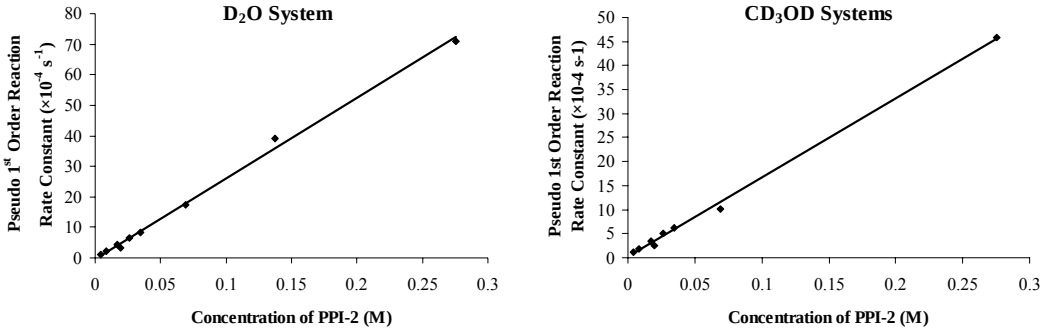

Figure 30. The plot of psuedo-1st order reaction constant versus PPI-2 concentration.

From the plot in Figure 30, the slope can be obtained as 0.0264 $mol^{-1}\cdot L\cdot s^{-1}$ for D_2O system, or k_{obs2_D2O} = 0.0264 $mol^{-1}\cdot L\cdot s^{-1}$, and the slope for methanol-d_4 system is 0.0165 $mol^{-1}\cdot L\cdot s^{-1}$, or k_{obs2_CD3OD} = 0.0165 $mol^{-1}\cdot L\cdot s^{-1}$. Using the equations proposed previously, the real rate constant can be calculated as:

$$k_{D2O} = k_{obs2\_D2O} / [D_2O] = 7.67\times10^{-4}\ mol^{-2}\cdot L^2\cdot s^{-1}$$

$$k_{CD3OD} = k_{obs2\_CD3OD} / [CD_3OD] = 9.59\times10^{-4}\ mol^{-2}\cdot L^2\cdot s^{-1}$$

From both Tables 21 and 22 it can also be noticed that at a fixed concentration of PPI-2, the pseudo-1st order reaction rate constants remain the same at different concentrations of $DEBF_4$. This supports the proposed pseudo-1st order reaction rate equation.

UV-vis Study. In this study, only the H_2O system was used because in methanol system, the reactant and the product differ only in isotopic substitution and the UV-vis spectrum does not change. A comparison of the UV-vis spectra of $DEBF_4$, $DABF_4$, and the mixture of $DEBF_4$ and PPI-2 at different times in H_2O system is shown in Figure 31. It shows that the reaction proceeds in the direction of hydrolysis. The λ_{max} for the diester dye $DEBF_4$, which is originally observed at 419 nm, was shifted towards 399 nm when mixed with PPI-2 dendrimer, which is the λ_{max} for diacid dye $DABF_4$. After mixing for

several hours (10 hrs), the resulting spectrum is almost identical to the $DABF_4$ spectrum, which provides evidence for the formation of $DABF_4$.

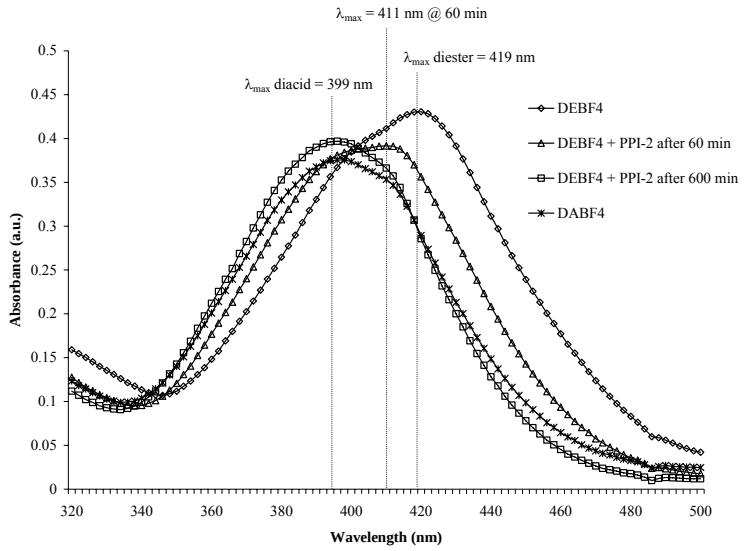

Figure 31. The UV-vis spectra of $DEBF_4$, $DABF_4$, and the mixture of $DEBF_4$ and PPI-2 (ratio = 1:4) after 1 hr and 10 hrs in aqueous solutions

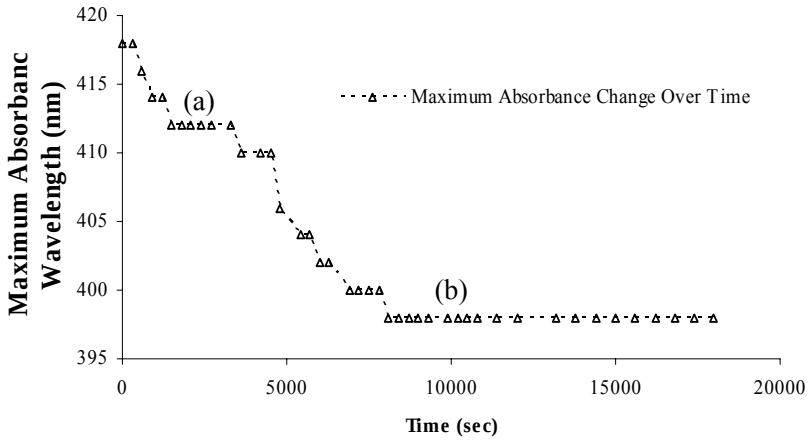

Figure 32. The λ_{max} change of the UV-vis absorbance with time for the system of 1:4 mixture of $DEBF_4$ and PPI-2 in aqueous solution.

As can be also observed in the λ_{max} versus time plot in Figure 32, the two ester groups in $DEBF_4$ react sequentially. The plot contains two periods, (a) and (b), in which λ_{max}

remains constant. Period (a) is the λ_{max} of the hybrid species with monoester and monoacid groups, and period (b) is the λ_{max} of diacid dye, $DABF_4$.

The exact concentrations of each component at a specific time for the catalysis study were obtained using the following equations:

$$A_{399} = \varepsilon_{DEBF_4 399} \times [DEBF_4] + \varepsilon_{DABF_4 399} \times [DABF_4]$$

$$A_{419} = \varepsilon_{DEBF_4 419} \times [DEBF_4] + \varepsilon_{DABF_4 419} \times [DABF_4]$$

In which A_{399} and A_{419} are the absorbance at 399 nm and 419 nm, respectively, $[DABF_4]$ and $[DEBF_4]$ are the concentrations at each time for $DABF_4$ and $DABF_4$, respectively, and $\varepsilon_{DABF_4 399}$, $\varepsilon_{DABF_4 419}$, $\varepsilon_{DEBF_4 399}$, and $\varepsilon_{DABF_4 419}$ are molar absorptivities for $DABF_4$ and $DEBF_4$ at the wavelengths of 399 nm and 419 nm, respectively. The logarithm of $[DEBF_4]$ versus time was graphed to obtain the reaction rate constant information. All the concentration values at different time are listed in Appendix II, and only the kinetic information is listed here.

Based on the same reasoning for the pseudo-1st order reaction as described in the NMR study, the same fitting technique is used to obtain the slope, the pseudo 1st order reaction rate constant k_{obs} (Figure 33). All the values of k_{obs} are listed in Table 24. Then the pseudo 2nd order reaction rate constant k_{obs2}, and the real rate constant can be calculated in the same way as in the NMR study.

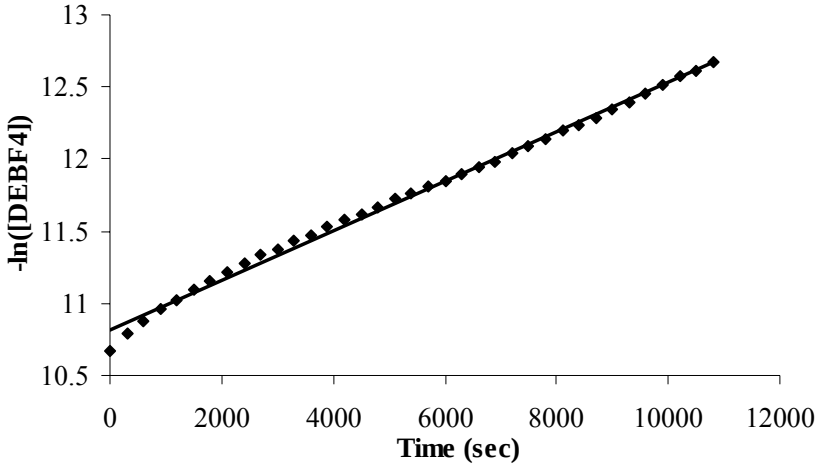

Figure 33. Linear relationship of –ln([$DEBF_4$]) versus time, data obtained from 1:4 mixture of $DEBF_4$ and PPI-2 in aqueous solution. The negative sign is to make all the values positive for easy processing.

Table 24. PPI-2 Concentration and Pseudo-1st Order Reaction Constants for UV-vis Kinetic Study

Ratio of $DEBF_4$ to PPI-2	PPI-2 Concentration ($\times 10^{-6}$ *M*)	Pseudo-1st Order Reaction Rate Constant ($\times 10^{-6}$ s^{-1})
1:64	1478	2377
1:32	739.1	1558
1:16	369.8	814.6
1:8	184.8	412.3
1:4	92.40	210.7
1:3.2	74.74	152.2
1:2	46.18	102.5
1:1	23.09	25.28
1:0.5	11.57	2.621
1:0.25	5.785	1.174

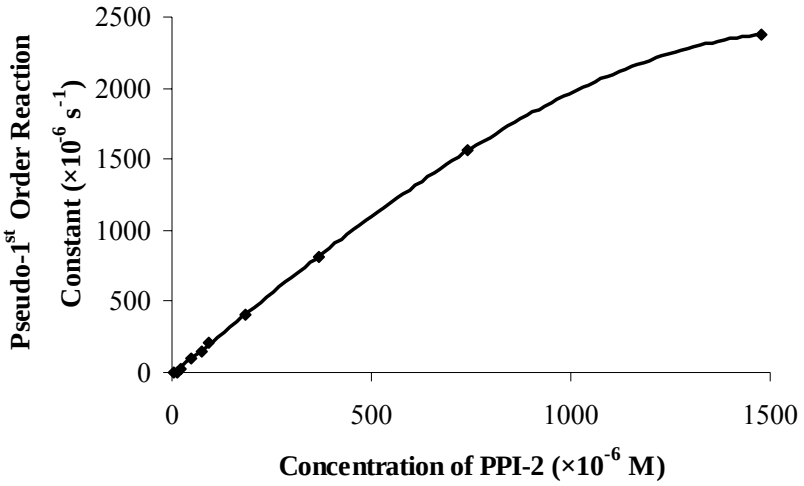

Figure 34. The plot of psuedo-1st order reaction constant versus PPI-2 concentration (the data from all ratio series are used).

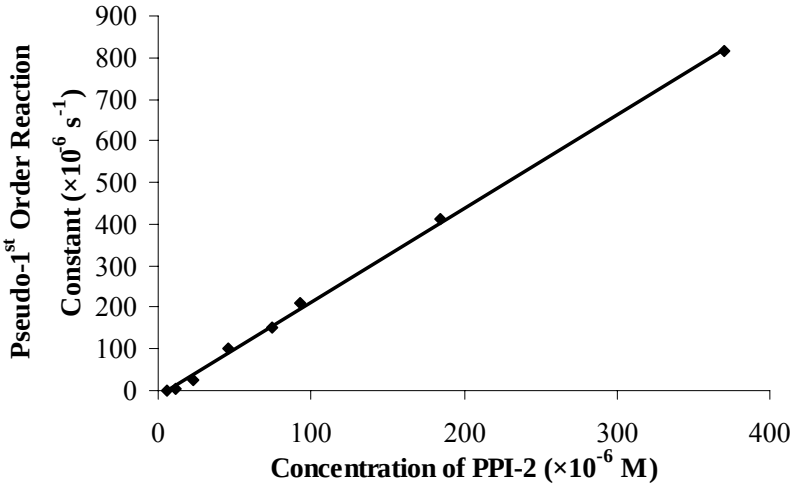

Figure 35. The plot of psuedo-1st order reaction constant versus PPI-2 concentration (the data from ratios 1 to 32 and 1 to 64 are excluded).

These pseudo-1st order reaction rate constants are plotted with PPI-2 concentrations for obtaining the pseudo-2nd order reaction rate constant, as shown in Figure 34. However, when the concentration of PPI-2 reaches a certain limit, it starts to deviate from the straight line. At higher PPI-2 concentration, the viscosity of the solution increases, which may cause more light to be reflected and less of the incident light to be absorbed by the sample. In this way, the absorbance detected by the UV-vis spectrometer is no

longer linearly related to the concentration change of the sample. The calculated concentration from Beer's Law will not accurately represent the real concentration of the samples based on the absorbance measured. Thus, the calculated rate constant for the reaction will not be reliable. If the data from the two highest PPI-2 concentration are excluded, a more linear plot can be obtained as displayed in Figure 35, which has a slope of 2.257 $mol^{-1} \cdot L \cdot s^{-1}$, or k_{obs2} = 2.257 $mol^{-1} \cdot L \cdot s^{-1}$, so we can calculate the real reaction constant as $k_{H2O} = k_{obs2} / [H_2O]$ = 0.04063 $mol^{-2} \cdot L^2 \cdot s^{-1}$.

There is about a 50 fold difference between the reaction rate constants obtained from the UV-vis study and the value obtained in the NMR study. The main reason is the concentrations used in the NMR study are about 1000 times more concentrated than those used in the UV-vis study. The diffusion becomes relatively difficult compared with that at lower concentrations. Because of the difficulty for the reactants to diffuse in the system, the reaction rate can be expected to be much slower. However, in the NMR study, experiments at different concentrations showed quite consistent results. This is because the diffusion effect is approximately the same for the reactions at these concentration ranges.

Comparison of Catalytic Property between PPI and Classic Primary Amines. To eliminate the pH effect from the basicity of primary amines in PPI-2, two classic primary amines, ethyl amine and ethylene diamine, were used for the study of the hydrolysis of $DEBF_4$, respectively. The amounts of ethyl amine or ethylene diamine were selected so they contained the same number of primary amine groups as PPI-2 dendrimer. Similarly to the previous UV-vis studies, the kinetic data was calculated and are listed in Appendix III.

Table 25. Catalyst Concentration and Pseudo-1st Order Reaction Constants

Amines	Concentration ($\times 10^{-6}$ *M*)	Initial pH Value	Pseudo-1st Order Reaction Rate Constant ($\times 10^{-6}$ s^{-1})	Real Rate Constant ($mol^{-2} \cdot L^2 \cdot s^{-1}$)
PPI-2	46.2	8.2	71.053	0.02768
Ethyl Amine	370	8.2	0.5981*	2.913×10^{-5}
Ethylene Diamine	185	8.2	1.4898*	1.451×10^{-4}
None	0	8.2	0.5806*	—
PPI-2	46.2	7.0	12.013	4.680×10^{-3}
Ethyl Amine	370	7.0	0.4374*	2.130×10^{-5}
Ethylene Diamine	185	7.0	1.2467*	1.214×10^{-4}
None	0	7.0	0.9615*	—

* The values listed are only approximations. These data are not reliable because the plot data points are scattered around instead of the clear linear trend.

The control of pH values for the study is important, which is shown in Table 25. As the pH was changed from slightly basic to neutral, all the reaction rate constants decreased. At pH=8.2, which is the pH value for the system of 1:2 ratio of $DEBF_4$ to PPI-2, it is clearly observed that the reaction rate constant for PPI-2 is much faster than those obtained for ethyl amine, ethylene diamine, and the blank solution (no amine). The significant reaction rate reduction for PPI-2 when pH changes from 8.2 to 7.0 is at least in part because the hydrochloric acid solution added to adjust the pH caused H^+ ions to react with some of the primary amines on the surface of PPI-2, which blocked some of the active sites for the catalysis.[39]

We noticed that few changes were observed for the rate constants of the classic primary amine systems and the blank system (no amine) when the pH changes. This indicates these substances actually do not have a catalytic effect on the ester hydrolysis. Further exploration of the UV-vis spectra of these systems reveals that only with the PPI-2 catalyst, noticeable changes of λ_{max} were observed, which is shown in Figure 36.

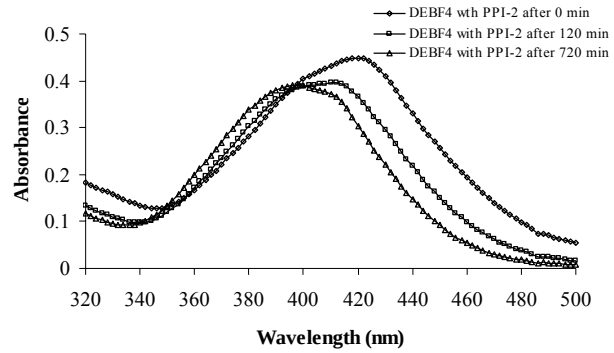

(a)

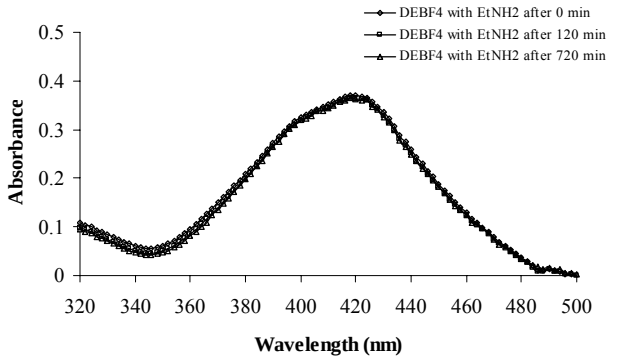

(b)

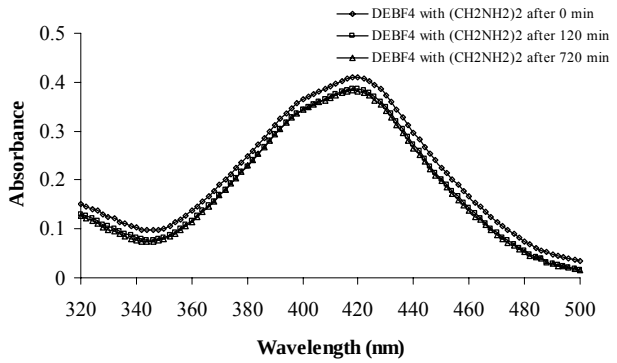

(c)

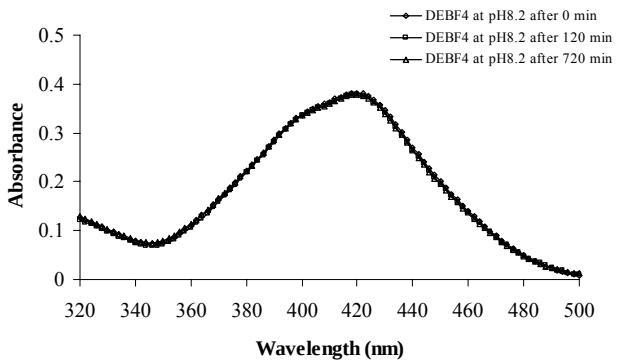

(d)

Figure 36. UV-vis spectra of $DEBF_4$ mixed with different amines after different times. The amines are (a) PPI-2 (b) ethyl amine (c) ethylene diamine (d) none.

Proposed Scheme for the Hydrolysis of $DEBF_4$ under the Catalysis of PPI-2 Dendrimer. In order to investigate the mechanism of the catalysis, we also tried to use NMR to study the system of PPI-2 mixed with the diacid dye $DABF_4$ to see whether the reverse reaction (esterification) can also be catalyzed in the methanol-d_4 system. The methanol-d_4 was pre-dried with 3A molecular sieves. However, no noticeable changes have been observed in either the aromatic region or the aliphatic region of the ^1H NMR spectra (Figure 27) acquired at different times. Also, no appearance of the methoxy resonance from the ester form (~4.08 ppm) can be observed. This can be explained as follows. The acid product of the hydrolysis can interact with PPI-2 to form "ammonium carboxylate" ion pairs. Therefore, the hydrolysis process is favored. The formation of these ion pairs can be further justified by the upfield shift of the resonances of a', b' and d' of $DABF_4$ [as labeled in Figure 24(c)] in the NMR spectra before and after mixing with PPI-2 dendrimer (Figure 37). The upfield shift of these resonances is due to the shielding effect of the negative charge on the carboxylate groups after the formation of the ion pairs. The formation of ion pairs also causes the downfield shift of the resonances of methylene group 8 [as labeled in Figure 24(a)] from the PPI-2 dendrimer (Figure 38) prior to and after mixing with $DABF_4$. This is due to the deshielding effect of the positive charge on the primary amine groups after the ion pairs are formed. Actually, this gives us a clue to the role of PPI-2 in this reaction, which is as a catalyst and, as well, a product scavenger.

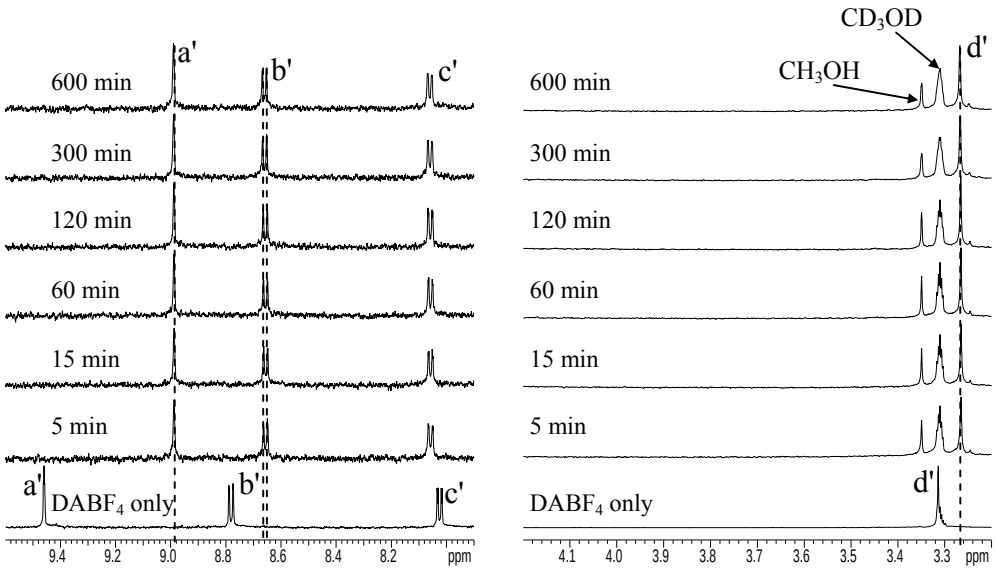

(a) Aromatic Region (7.9~9.6 ppm) (b) Aliphatic Region (3.2~4.2 ppm)

Figure 37. ^{1}H NMR spectra of $DABF_4$ before and after mixing with PPI-2 in methanol-d_4 system at different times.

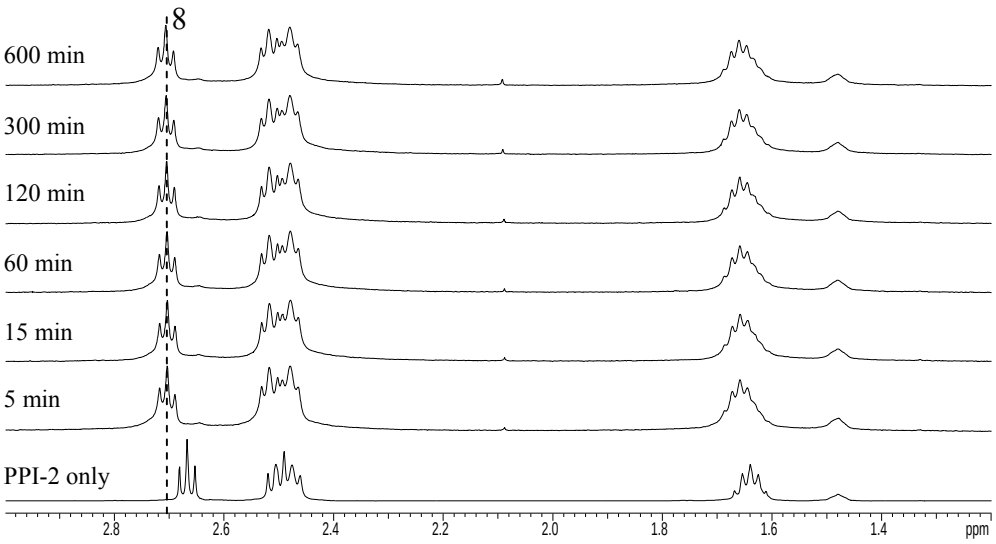

Figure 38. ^{1}H NMR spectra of PPI-2 before and after mixing with $DABF_4$ in methanol-d_4 system at different times

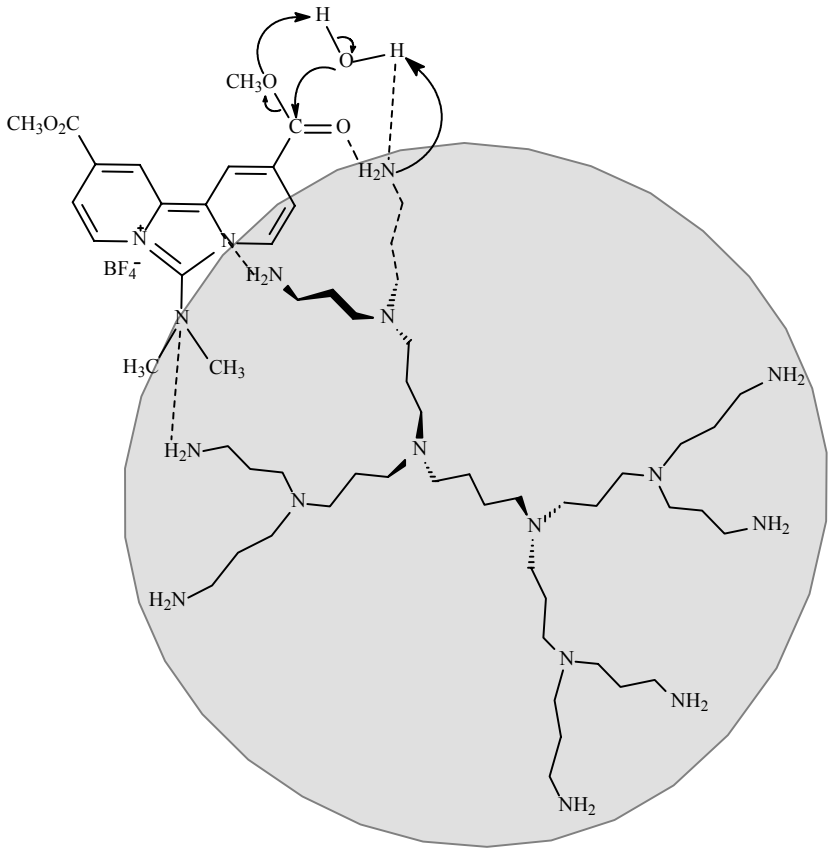

Figure 39. Electron-transfer scheme of PPI-2 as ester hydrolysis catalyst. The order of electron transfer is still uncertain.

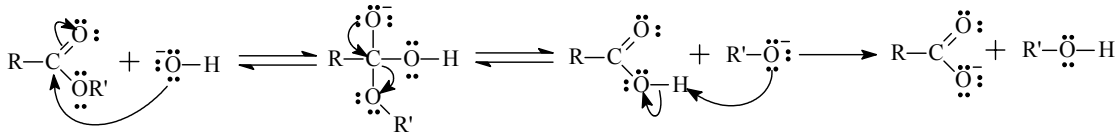

Figure 40. Traditional base ($^{-}$OH) catalyzed ester hydrolysis.

With all the evidence above, we can conclude that (1) PPI-2 is an effective catalyst for hydrolyzing the diester dye $DEBF_4$ under mild conditions (slight basic and room temperature) (2) The unique structure of PPI-2 dendrimer played an important role in the entire reaction because classic primary amines at same pH are ineffective. We proposed an electron-transfer scheme to understand this catalysis as shown in Figure 39, although the order of electron transfer is still uncertain. The traditional base catalyzed mechanism (usually by $^{-}$OH) is shown in Figure 40 for a comparison.

Study of PPI Catalysis on the Hydrolysis of Other Esters. In order to ascertain whether PPI dendrimers' catalytic properties towards ester hydrolysis are specific to diester dye $DEBF_4$ or more general, methyl benzoate and methyl trifluoroacetate were tested in PPI-2 dendrimer catalyzed hydrolysis.

Methyl Benzoate. It was also verified that PPI-2 dendrimer did not change over the reaction period via ^{13}C and ^{1}H NMR spectra shown in Figures 41 and 42, respectively. The PPI-2 resonances in these NMR spectra did not show any significant difference for the samples prepared by mixing PPI-2 with methyl benzoate or benzoic acid. However, a very small downfield shift of the resonance of methylene group 8 in PPI-2 [as labeled in Figure 24(a)] has been observed similar to the previous study.

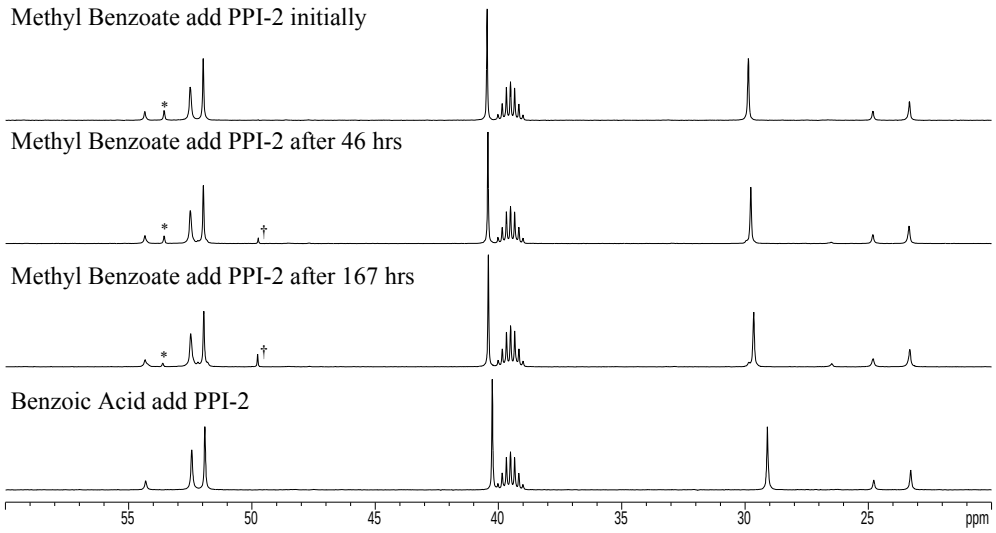

* Carbon resonance of the methoxy group in the reactant methyl benzoate
† Carbon resonance of the methoxy group in the product methanol

Figure 41. The ^{13}C spectra of PPI-2 dendrimer in the study of hydrolysis of methyl benzoate.

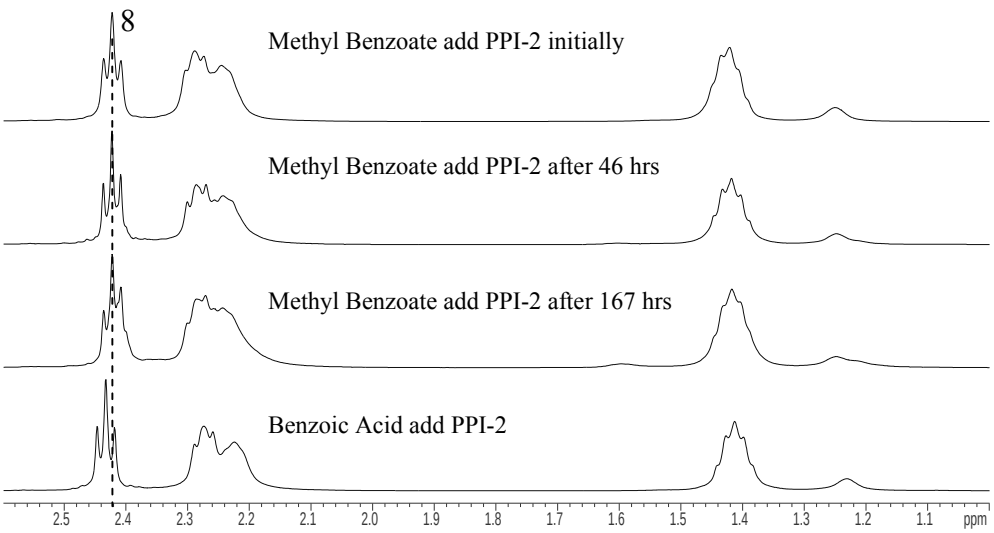

Figure 42. The ^{1}H spectra of PPI-2 dendrimer in the study of hydrolysis of methyl benzoate.

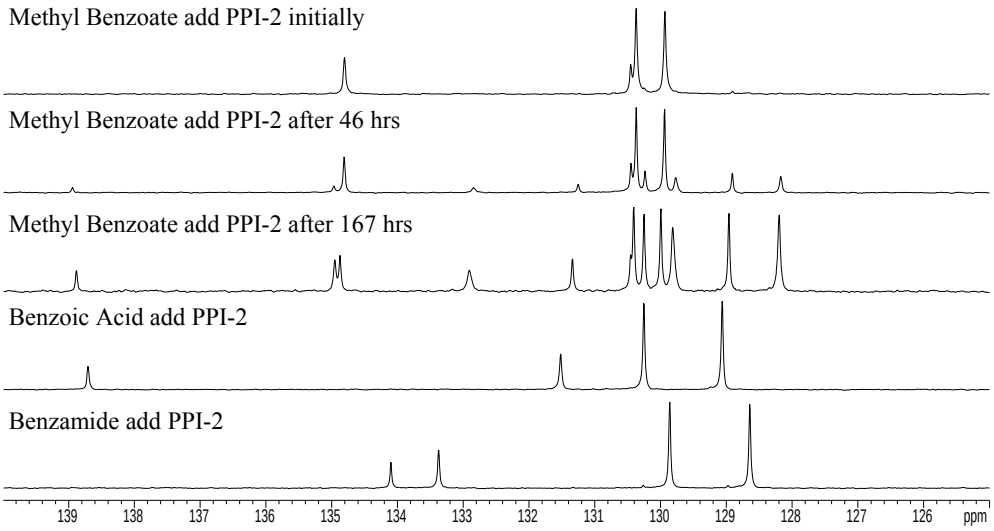

Figure 43. The aromatic region (125~140 ppm) of ^{13}C spectra in the study of hydrolysis of methyl benzoate.

The expansions of ^{13}C NMR spectra for the aromatic region and carbonyl region used in the study of the hydrolysis of methyl benzoate were shown in Figures 43 and 44,

respectively. The ^{1}H NMR spectra of the aromatic region and methoxy region for the study of methyl benzoate were shown in Figures 45 and 46, respectively.

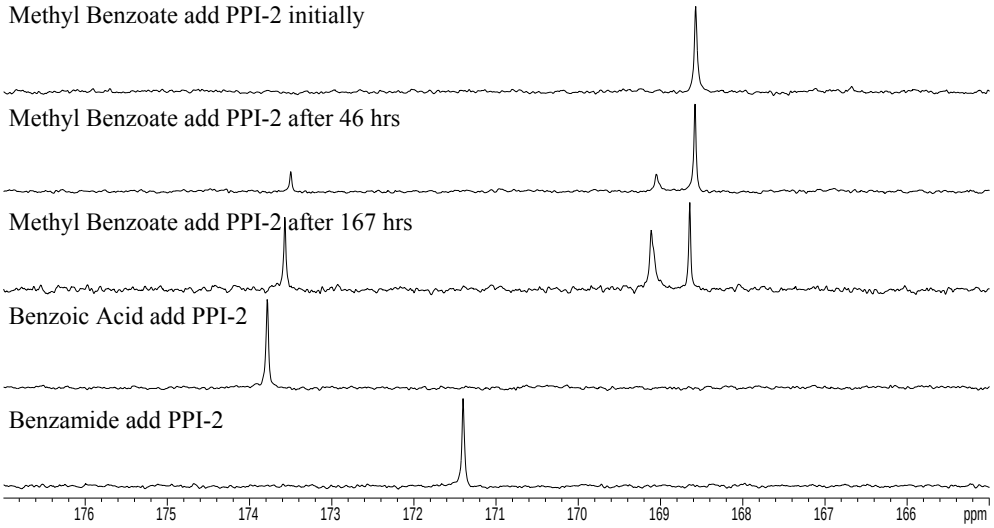

Figure 44. The carbonyl region (165~177 ppm) of ^{13}C spectra in the study of hydrolysis of methyl benzoate.

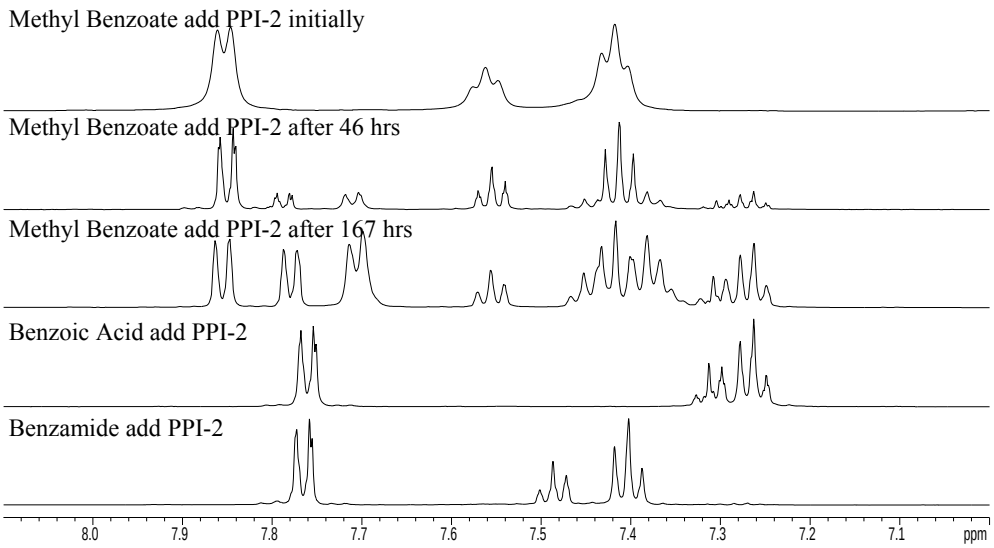

Figure 45. The aromatic region (7.0~8.1 ppm) of ^{1}H spectra in the study of hydrolysis of methyl benzoate.

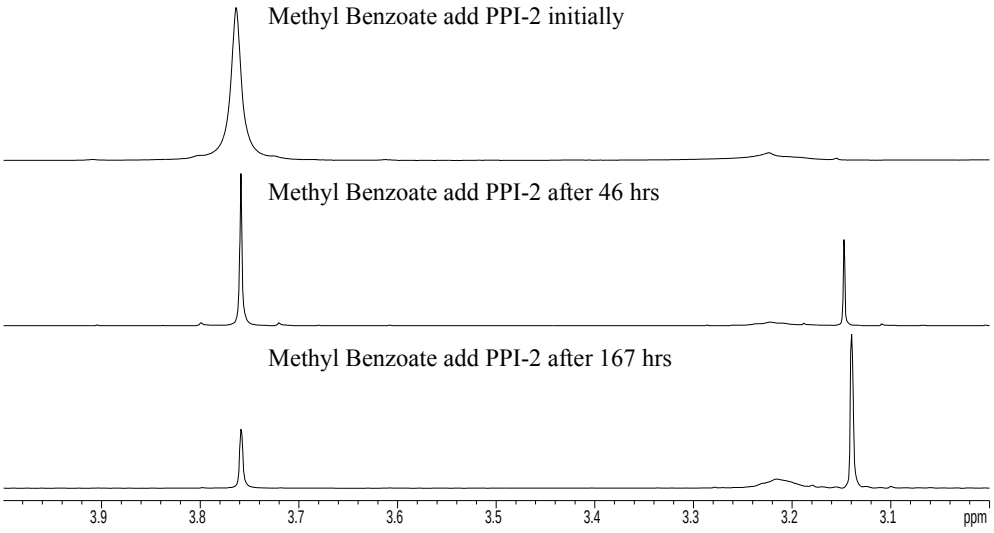

Figure 46. The methoxy region (3.0~4.0 ppm) of ^{1}H spectra in the study of hydrolysis of methyl benzoate.

Evidence for the formation of the reaction products (benzoic acid and methanol) is shown in those NMR spectra. From Figures 43 − 45, the appearance of resonances from benzoic acid can be clearly observed after mixing methyl benzoate and PPI-2 dendrimer for 46 hours. After 167 hours, the resonances of benzoic acid became stronger, which indicates the reaction is still in progress. The benzamide spectra were also displayed to exclude the possibility that amide may be formed as a by-product. In fact, even after mixing methyl benzoate and PPI-2 dendrimer for 167 hours, no resonances on the NMR spectra have been observed for the potential amide product. In Figure 46, a trend that is similar to those in Figures 26 and 27 can also be observed, which is the disappearance of methoxy resonance from the ester and the appearance of methanol's methoxy resonance. This also indicates the reaction is going towards the direction of hydrolysis.

Methyl Trifluoroacetate. ^{13}C NMR has been used to test the PPI-2 catalysis on the hydrolysis of methyl trifluoroacetate. The ^{13}C spectra of the carbonyl region are shown in Figure 47.

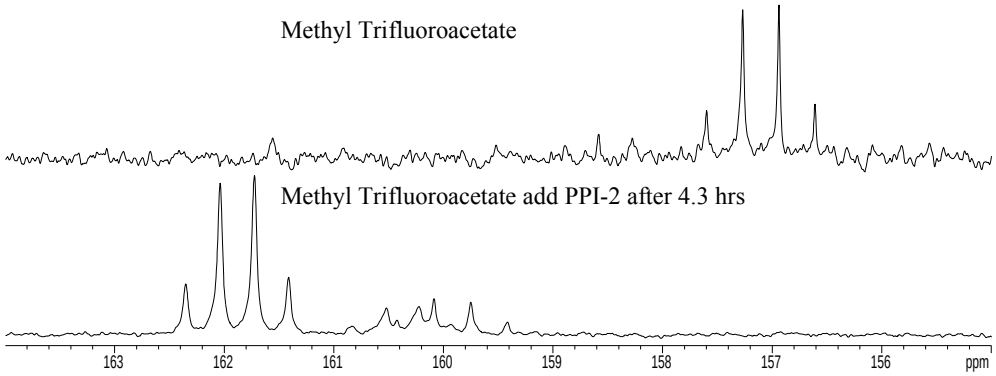

Figure 47. Carbonyl region (155~164 ppm) of ^{13}C spectra in the study of hydrolysis of methyl trifluoroacetate.

The carbonyl resonances have been assigned based on the Aldrich Library of ^{13}C and ^{1}H FT-NMR Spectra.[40] The chemical shift values from our experiments showed a good agreement with the values in Aldrich Library for both methyl trifluoroacetate and trifluoroacetic acid. The carbonyl resonances are quartets in all the ^{13}C NMR spectra because of the splitting from the three fluorine neighbors. This is also a strong proof that methyl trifluoroacetic acid is hydrolyzed under the presence of PPI-2 as a catalyst. In addition, the reaction rate for the catalysis of methyl trifluoroacetate acid is much faster than that of methyl benzoate. This may be because of the existence of the strong electron withdrawing group (fluorine) on the acid moiety of the ester.

Conclusion

The catalytic property of PPI dendrimers for organic ester hydrolysis and transesterification has been studied by NMR and UV-vis spectroscopies, which are

successful tools for monitoring the kinetics of these reactions. The results showed PPI dendrimers can generally catalyze the hydrolysis of organic esters at room temperature in a slightly basic environment, which is a rather mild condition compared with the one for ester soponification (strong basic condition with heating). However, different catalytic speeds have been observed for different structure esters. In addition, esters with stronger electron withdrawing group(s) in the acid moiety seem to be catalyzed faster by PPI-2 dendrimer. The reason for this is that the stronger electron withdrawing group(s) will enhance the acidity of the acid product from the hydrolysis, which can make more efficient self-assembly of the acid and the PPI-2 dendrimer.

BIBLIOGRAPHY

(1). Buhleier, E.; Wehner, W.;Vögtle, F. *Synthesis* **1978**, 155

(2). Wörner, C.; Mülhaupt, R. *Angew. Chem.* **1993**, *105*, 1367

(3). de Brabander-van den Berg, E. M. M. and Meijer E. W. *Angew. Chem., Int. Ed. Engl.* **1993**, *32*, 1308

(4). Frechet, J. M. J. *Science* **1994**, *263*, 1710

(5). Alper, J. *Science* **1991**, *251*, 1562

(6). Klajnert, B.; Bryszewska, M. *Acta Biochimica Polonica* **2001**, *48(1)*, 199

(7). Fischer, M.; Voegtle, F. *Angew. Chem., Int. Ed. Engl.* **1999**, *38*, 884

(8). (a) Wiener, E. C.; Auteri, F. P.,; Chen, J. W.; Brechbiel, M. W.; Gansow, O. A.; Schneider, D. S.; Belford, R. L.; Clarkson, R. B.; Lauterbur, P. C. *J. Am. Chem. Soc.* **1996**, *118*, 7774 (b) Bryant, L. H.; Brechbiel, M. W.; Wu, C.; Bulte, J. W. M.; Herynek, V.; Frank, J. A. *J. Magn. Reson. Imaging* **1999**, *9*, 348

(9). (a) Twyman, L. J.; Beezer, A .E.; Esfand, R.; Hardy, M. J.; Mitchell, J. C. *Tetrahedron Lett.* **1999**, *40*, 1743 (b) Liu, M.; Kono, K.; Frechet, J. M. J. *J. Controlled Release* **2000**, *65*, 121

(10). (a) Bielinska, A. U.; Kukowska-Latallo, J. F.; Johnson, J.; Tomalia, D. A.; Baker, J. R. *Nucleic Acids Res.* **1996**, *24*, 2176 (b) Kukowska-Latallo, J. F.; Raczka, E.; Quintana, A.; Chen, C. L.; Rymaszewski, M.; Baker, J. R. *Hum. Gene Therapy* **2000**, *11*, 1385

(11).Tomalia, D. A.; Dvornic, P. R. *Nature* **1994**, *372*, 617

(12). de Genes, P. G. and Heret, H. J. *Phys. Lett. Paris* **1983**, *44*, 351

(13). Lescanec. R. L.; Muthukumar. M. *Macromolecules* **1990**, *23*, 2280

(14). Mansfield, M. L.; Klushin, L. I. *Macromolecules* **1993**, *26*, 4262

(15). Wallace, E. J.; Buzza, D. M. A.; Read, D. J. *Macromolecules* **2001**, *34*, 7140

(16). Murat, M. and Grest, G. S. *Macromolecules* **1996**, *29*, 1278

(17). Boris, D.; Rubinstein, M. *Macromolecules* **1996,** 29, 7251

(18). Tande, B. M.; Wagner, N. J.; Mackay, M. E.; Hawker, C. J.; Jeong, M. *Macromolecules* **2001**, *34*, 8580

(19). Lee, I.; Athey, B. D.; Wetzel, A. W.; Meixner, W.; Baker Jr., J. R. *Macromolecules* **2002**, *35*, 4510

(20). Welch, P.; Muthukumar, M. *Macromolecules* **1998**, *31*, 5892

(21). Scherrenberg, R.; Coussens, B.; van Vliet, P.; Edouard, G.; Brackman, J.; de Brabander, E.; Mortensen, K. *Macromolecules* **1998**, *31*, 456

(22). Zacharopoulos, N.; Economou, I. G. *Macromolecules* **2002**, *35*, 1814

(23). Adhiya, A.; Wesdemiotis, C. *Int. J. Mass Spectrom.* **2002**, *214*, 75

(24). Chai, M.; Niu, Y.; Youngs, W. J. and Rinaldi, P. L. *J. Am. Chem. Soc.* **2001**, *123(20)*, 4670

(25). Neuhaus, D. and Williamson, M. P. *The Nuclear Overhauser Effect in Structural and Conformational Analysis 2nd Ed.* VCH **2000**.

(26). Sanders, J. K. M. and Hunter, B. K. *Modern NMR Spectroscopy* Oxford University Press **1993**.

(27). Jansen, J. F. G. A.; de Brabander-van den Berg E. M. M.; Meijer, E. W. *Science* **1994**, *266*, 1226

(28). (a) Schenning, A. P. H. J.; Elissen-Román, C.; Weener, J. W.; Baars, M. W. P. L.;van der Gaast, S. J.; Meijer, E. W. *J. Am. Chem. Soc.* **1998**, *120*, 8199 (b) Stevelmans, S.; van Hest, J. C. M.; Jansen, J. F. G. A.; van Boxtel, D. A. F. J.; de Brabander-van den Berg, E. M. M.; Meijer, E. W. *J. Am. Chem. Soc.* **1996**, *118*, 7398 (c) M. W. P. L. Baars, P. E. Froehling, E. W. Meijer *Chem. Commun.* **1997**, 1959-1960

(29). Chechik, V.; Zhao, M.; Crooks, R. M. *J. Am. Chem. Soc.* **1999**, *121(20)*, 4910-4911

(30). Baars, M. W. P. L.; Meijer, E. W. *Top. Curr. Chem.* **2000**, *210*, 131

(31). Astruc, D.; Chardac F. *Chem. Rev.*, **2001**, *101*, 2991

(32). (a) Cornils, B.; Herrmann, W. A.; Eds. *Applied Homogeneous Catalysis with Organometallic Compounds* VCH, Weinheim **1996**, (b) Tomalia, D. A.; Dvornic, P. R. *Nature* **1994**, 617

(33). (a) Janssen, H. M.; Meijer, E. W. *Chem. Rev.* **1999**, *99*, 1665 (b) Newkome, G. R.; He, E.; Moorefield, C. N. *Chem. Rev.* **1999**, *99*, 1689

(34). (a) Reetz, M. T.; Lohmer, G.; Schwickardi, R. *Angew. Chem., Int. Ed. Engl.* **1997**, *36*, 1526 (b) Brinkmann, N.; Giebel, D.; Lohmer, G.; Reetz, M. T.; Kragl, U. *J. Catal.* **1999**, *183*, 163

(35). Peerlings, H. W. I.; Meijer, E. W. *Chem. Eur. J.* **1997**, *3*, 1563

(36). Crooks, R. M.; Zhao, M.; Sun, L.; Chechik, V.; Yeung, L. K. *Acc.Chem. Res.* **2001**, *34*, 181

(37). Froehling, P. E.; Corstjens T. *Polym. Mater, Sci. Eng.* **1997**, *77*, 534

(38). Jansen, J. F. G. A.; Dias, A. A.; Hartwig, H.; Janssen, R. A. J. *Surf. Coat. Int.* **2000**, *83*, 119

(39). Koper, G. J. M.; van Genderen, M. H. P.; Elissen-Roma´n, C.; Baars, M. W. P. L.; Meijer, E. W.; Borkovec, M. *J. Am. Chem. Soc.* **1997,** *119,* 6512

(40). Pouchert, C. J.; Behnke J. *The Aldrich Library of ^{13}C and ^{1}H FT-NMR Spectra* Aldrich Chemical Company **1993**

APPENDICES

Appendix I – NMR Data for Kinetic Study of Hydrolysis of $DEBF_4$ Dye.

1. Data Table Index.

Data Table Index: $DEBF_4$ and PPI-2 for NMR Studies

Molar Ratio of $DEBF_4$ to PPI-2	Data Table Number	
	D_2O System	Methanol-d_4 System
1:16	1	14
1:8	2	15
1:4	3	16
1:2	4	17
1:1.5	5	18
1:1	6	19
1:0.75	7	20
1:0.5	8	21
1:0.25	9	22
4:1	10	23
2:1	11	24
0.5:1	12	25
0.25:1	13	26

***** Calculation of Relative Intensity of Methoxyl Peak is based on the following equation:

In D_2O system, $[\mathrm{Re}lativeIntensityOfMethoxylPeak] = \frac{[IntegrationOfMethoxylPeak] \times 63.05}{[IntegrationOfAromaticPeaks]} \times \frac{100}{36.95}$

In methanol-d_4 system, $[\mathrm{Re}lativeIntensityOfMethoxylPeak] = \frac{[IntegrationOfMethoxylPeak] \times 58.03}{[IntegrationOfAromaticPeaks]} \times \frac{100}{41.97}$

† Calculation of Real-time Concentration of $DEBF_4$ is based on the following equation:

$$[\mathrm{Re}alTimeConcentrationOfDEBF_4] = [InitialConcentrationOfDEBF_4] \times \frac{[\mathrm{Re}lativeIntensityOfMethoxylPeak]}{100}$$

2. Integration Data Tables

Data Table 1: Molar Ratio of $DEBF_4$ to PPI-2 = 1:16 in D_2O System

Time (sec)	Integration Values			Relative Intensity of Methoxyl Peak	Real-time Concentration of $DEBF_4$ (M)
	Aromatic Peaks	Methoxyl Peak	Methanol Peak		
0	63.05	36.95	0	100	0.017211704
300	81.94	5.69	12.37	11.84914339	0.002039439
600	81.87	4.17	13.96	8.691243403	0.001495911
900	78.07	4.3	17.63	9.398421631	0.001617629
1200	77.02	4.17	18.81	9.23853671	0.00159011
1500	76.99	3.96	19.05	8.776705268	0.001510621
1800	76.89	3.66	19.45	8.122353234	0.001397995
2100	76.26	3.73	20.01	8.34608261	0.001436503
2400	75.9	3.75	20.35	8.430632144	0.001451055
2700	76.82	3.48	19.7	7.729930502	0.001330453
3000	75.45	3.82	20.73	8.639224643	0.001486958
3300	76.96	3.16	19.88	7.006363603	0.001205915
3600	76.69	3.46	19.85	7.698533593	0.001325049

Data Table 2: Molar Ratio of $DEBF_4$ to PPI-2 = 1:8 in D_2O System

Time (sec)	Integration Values			Relative Intensity of Methoxyl Peak	Real-time Concentration of $DEBF_4$ (M)
	Aromatic Peaks	Methoxyl Peak	Methanol Peak		
0	63.05	36.95	0	100	0.017211704
300	78.42	6.51	15.07	14.1652681	0.002438084
600	78.55	4.38	17.07	9.514776019	0.001637655
900	77.98	3.66	18.36	8.008819443	0.001378454
1200	77.08	3.13	19.79	6.929043371	0.001192606
1500	77.38	2.97	19.65	6.549352597	0.001127255
1800	77.16	2.62	20.22	5.794016405	0.000997249
2100	76.29	2.68	21.03	5.994291067	0.00103172
2400	76.28	2.73	20.99	6.106925344	0.001051106
2700	75.14	2.74	22.12	6.222286734	0.001070962
3000	75.68	2.47	21.85	5.569118745	0.00095854
3300	75.75	2.34	21.91	5.271131714	0.000907252
3600	75.77	2.22	22.01	4.999497268	0.000860499
3900	74.91	2.22	22.87	5.056893712	0.000870378
4200	75.47	2.26	22.27	5.109809829	0.000879485
4500	74.87	2.35	22.78	5.355878019	0.000921838
4800	75.48	2.28	22.24	5.154346418	0.000887151
5100	75.18	2.17	22.65	4.925247516	0.000847719
5400	74.67	2.18	23.15	4.981739229	0.000857442
5700	75.17	2.06	22.77	4.676202592	0.000804854
6000	75.05	2.19	22.76	4.979251541	0.000857014
6300	73.78	2.18	24.04	5.041833399	0.000867785
6600	73.97	2.11	23.92	4.86740501	0.000837763
6900	74.36	2	23.64	4.589456552	0.000789924
7200	74.44	2.21	23.35	5.065899356	0.000871928

Data Table 3: Molar Ratio of $DEBF_4$ to PPI-2 = 1:4 in D_2O System

Time (sec)	Integration Values			Relative Intensity of Methoxyl Peak	Real-time Concentration of $DEBF_4$ (*M*)
	Aromatic Peaks	Methoxyl Peak	Methanol Peak		
0	63.05	36.95	0	100	0.017211704
300	60.41	21.1	18.49	59.59972663	0.010258129
600	63.78	14.46	21.76	38.68605334	0.006658529
900	63.51	10.99	25.5	29.52746938	0.005082181
1200	63.67	9.35	26.98	25.05805795	0.004312919
1500	61.35	8.25	30.4	22.94616064	0.003949425
1800	61.14	7.01	31.85	19.56425126	0.003367341
2100	60.81	6.35	32.84	17.81842732	0.003066855
2400	61.44	5.5	33.06	15.27503207	0.002629093
2700	60.94	4.84	34.22	13.55231726	0.002332585
3000	60.24	5.05	34.71	14.3046443	0.002462073
3300	61.72	4.48	33.8	12.38576241	0.002131801
3600	60.36	4.38	35.26	12.3821348	0.002131176
3900	58.12	4.26	37.62	12.50704296	0.002152675
4200	59.66	4.21	36.13	12.04119238	0.002072494
4500	57.49	4.38	38.13	13.00027233	0.002237568
4800	57.97	3.94	38.09	11.59747833	0.001996124
5100	58.24	3.68	38.08	10.78194471	0.001855756
5400	57.46	3.83	38.71	11.37375321	0.001957617
5700	59.26	3.74	37	10.76912959	0.001853551
6000	58.55	3.6	37.85	10.49170932	0.001805802
6300	57.56	3.47	38.97	10.2867773	0.00177053
6600	58.49	3.75	37.76	10.94007488	0.001882973
6900	57.51	3.24	39.25	9.61329547	0.001654612
7200	57.98	3.04	38.98	8.946764808	0.001539891
7500	55.54	3.17	41.29	9.739216832	0.001676285
7800	55.29	3.12	41.59	9.628943807	0.001657305
8100	55.9	3.19	40.91	9.737546024	0.001675998
8400	54.95	3.24	41.81	10.06115782	0.001731697
8700	55.4	3.32	41.28	10.22583939	0.001760041
9000	55.51	3.39	41.1	10.42075341	0.001793589
9300	55.23	3.11	41.66	9.608508839	0.001653788
9600	56.98	3.1	39.92	9.283460569	0.001597842
9900	56.25	2.76	40.99	8.372539468	0.001441057
10200	56.86	2.96	40.18	8.882914949	0.001528901
10500	55.02	2.82	42.16	8.745792525	0.0015053
10800	55.8	2.81	41.39	8.592959584	0.001478995

Data Table 4: Molar Ratio of $DEBF_4$ to PPI-2 = 1:2 in D_2O System

Time (sec)	Integration Values			Relative Intensity of Methoxyl Peak	Real-time Concentration of $DEBF_4$ (*M*)
	Aromatic Peaks	Methoxyl Peak	Methanol Peak		
0	63.05	36.95	0	100	0.017211704
300	55.45	30.89	13.66	95.05763522	0.016361039
600	61.51	21.93	16.56	60.83640646	0.010470982
900	61.51	18.8	19.69	52.1534173	0.008976492
1200	61.37	16.73	21.9	46.516868	0.008006346
1500	57.83	15.79	26.38	46.59073758	0.00801906
1800	59.59	13.25	27.16	37.94138158	0.006530358
2100	61.98	10.82	27.2	29.78834239	0.005127081
2400	60.38	10.04	29.58	28.37339161	0.004883544
2700	56.56	9.7	33.74	29.2639524	0.005036825
3000	62.95	7.56	29.49	20.49258331	0.003527123
3300	56.18	8.04	35.78	24.41996078	0.004203091
3600	57.1	7.47	35.43	22.32313274	0.003842192
3900	60.08	5.97	33.95	16.9556739	0.00291836
4200	59.74	5.87	34.39	16.76654316	0.002885808
4500	59.4	5.73	34.87	16.46034089	0.002833105
4800	58.91	4.78	36.31	13.84552799	0.002383051
5100	59.16	4.45	36.39	12.83519567	0.002209156
5400	57.73	4.3	37.97	12.70976575	0.002187567
5700	58.98	3.87	37.15	11.19635977	0.001927084
6000	61.39	3.54	35.07	9.83957356	0.001693558
6300	55.72	3.93	40.35	12.03516617	0.002071457
6600	59.88	3.72	36.4	10.60063293	0.00182455
6900	57.37	3.68	38.95	10.94544989	0.001883898
7200	58.9	3.33	37.77	9.647162343	0.001660441
7500	57.31	3.35	39.34	9.974360179	0.001716757
7800	58.1	3.01	38.89	8.840178033	0.001521545
8100	56.24	3.4	40.36	10.31583182	0.00177553
8400	56.85	3.22	39.93	9.664870758	0.001663489
8700	57.56	3.15	39.29	9.338140774	0.001607253
9000	51.18	3.24	45.58	10.80227867	0.001859256
9300	57.17	2.8	40.03	8.357194068	0.001438416
9600	56.81	3.14	40.05	9.431385724	0.001623302
9900	50.64	2.47	46.89	8.322885202	0.00143251
10200	52.29	2.39	45.32	7.799197305	0.001342375
10500	52.21	2.29	45.5	7.48432154	0.001288179
10800	56.24	2.54	41.22	7.706533184	0.001326426

Data Table 5: Molar Ratio of $DEBF_4$ to PPI-2 = 1:1.5 in D_2O System

Time (sec)	Integration Values			Relative Intensity of Methoxyl Peak	Real-time Concentration of $DEBF_4$ (*M*)
	Aromatic Peaks	Methoxyl Peak	Methanol Peak		
0	63.05	36.95	0	100	0.017211704
300	69.14	20.15	10.71	49.72975544	0.008559338
600	69.45	16.87	13.68	41.44894498	0.00713407
900	72.22	12.98	14.8	30.66816962	0.005278515
1200	71.17	12	16.83	28.7709981	0.004951979
1500	72.47	9.86	17.67	23.21610193	0.003995887
1800	72.65	8.67	18.68	20.36357981	0.003504919
2100	72.28	7.86	19.86	18.55560207	0.003193735
2400	72.29	6.91	20.8	16.31062004	0.002807336
2700	72.5	6.2	21.3	14.59231954	0.002511587
3000	72.92	5.58	21.5	13.05744446	0.002247409
3300	71.86	5.22	22.92	12.39521141	0.002133427
3600	72.55	4.6	22.85	10.81909821	0.001862151
3900	72.53	3.72	23.75	8.7517703	0.001506329
4200	71.93	3.73	24.34	8.848495201	0.001522977
4500	71.74	3.58	24.68	8.515149995	0.001465602
4800	71.89	3.15	24.96	7.476747572	0.001286876
5100	71.36	3.12	25.52	7.460542364	0.001284086
5400	70.84	3.05	26.11	7.346693725	0.001264491
5700	72.18	2.74	25.08	6.477453937	0.00111488
6000	71.2	2.53	26.27	6.063329583	0.001043602
6300	71.14	2.6	26.26	6.236345037	0.001073381
6600	70.34	2.27	27.39	5.506734542	0.000947803
6900	70.02	2.43	27.55	5.921814722	0.001019245
7200	70.58	2.31	27.11	5.584714473	0.000961225
7500	71.38	1.96	26.66	4.685437789	0.000806444
7800	70.09	1.95	27.96	4.747327571	0.000817096
8100	70.59	2.25	27.16	5.438886355	0.000936125
8400	70.99	2.09	26.92	5.02365444	0.000864657
8700	69.4	1.86	28.74	4.573241353	0.000787133
9000	69.89	2.11	28	5.151551704	0.00088667
9300	69.71	1.83	28.46	4.479470235	0.000770993
9600	69.57	1.84	28.59	4.513011787	0.000776766
9900	69.39	1.94	28.67	4.770627317	0.000821106
10200	70.01	1.78	28.21	4.338409804	0.000746714
10500	69.66	1.69	28.65	4.139747787	0.000712521
10800	68.83	1.92	29.25	4.759859213	0.000819253

Data Table 6: Molar Ratio of $DEBF_4$ to PPI-2 = 1:1 in D_2O System

Time (sec)	Integration Values			Relative Intensity of Methoxyl Peak	Real-time Concentration of $DEBF_4$ (*M*)
	Aromatic Peaks	Methoxyl Peak	Methanol Peak		
0	63.05	36.95	0	100	0.017211704
300	62.06	29.19	8.75	80.25885727	0.013813917
600	63.38	25.94	10.68	69.83745187	0.012020215
900	64.01	23.18	12.81	61.7925692	0.010635554
1200	64.29	21.27	14.44	56.45399914	0.009716695
1500	64.96	19.47	15.57	51.14351623	0.008802671
1800	64.28	18.74	16.98	49.74671031	0.008562257
2100	64.04	17.47	18.49	46.5492009	0.008011911
2400	66.51	15.2	18.29	38.99664889	0.006711988
2700	64.91	15.14	19.95	39.80016882	0.006850287
3000	65.57	14.01	20.42	36.45890322	0.006275198
3300	65.73	13.41	20.86	34.81254659	0.005991832
3600	65.18	12.38	22.44	32.40984371	0.005578286
3900	64.63	12.19	23.18	32.18401321	0.005539417
4200	65.67	10.88	23.45	28.27043736	0.004865824
4500	66.79	9.96	23.25	25.4459426	0.00437968
4800	66.44	9.87	23.69	25.34884507	0.004362968
5100	65.76	9.71	24.53	25.19579543	0.004336626
5400	63.86	9.86	26.28	26.34624032	0.004534637
5700	67.21	8.05	24.74	20.43772886	0.003517681
6000	65.46	8.14	26.4	21.21871366	0.003652102
6300	65.08	8.24	26.68	21.60480325	0.003718555
6600	65.43	7.59	26.98	19.79408832	0.0034069
6900	65.9	7.17	26.93	18.56540336	0.003195422
7200	64.67	6.9	28.43	18.20609808	0.00313358
7500	65.68	6.8	27.52	17.66633318	0.003040677
7800	64.42	6.6	28.98	17.48211059	0.003008969
8100	64.71	6.28	29.01	16.55994508	0.002850249
8400	65.16	6.14	28.7	16.07895959	0.002767463
8700	64.74	5.79	29.47	15.26077245	0.002626639
9000	65.51	5.73	28.76	14.92511447	0.002568867
9300	63.96	5.97	30.07	15.9270933	0.002741324
9600	66.54	5.31	28.15	13.61702932	0.002343723
9900	64.71	5.23	30.06	13.79116445	0.002373694
10200	63.85	5.32	30.83	14.21743917	0.002447064
10500	62.62	5.19	32.19	14.14245947	0.002434158
10800	62.85	4.67	32.48	12.67891957	0.002182258

Data Table 7: Molar Ratio of $DEBF_4$ to PPI-2 = 1:0.75 in D_2O System

Time (sec)	Integration Values			Relative Intensity of Methoxyl Peak	Real-time Concentration of $DEBF_4$ (*M*)
	Aromatic Peaks	Methoxyl Peak	Methanol Peak		
0	63.05	36.95	0	100	0.017211704
300	59.99	32.28	7.73	91.817468	0.015803351
600	61.46	28.72	9.82	79.73748397	0.01372418
900	64.09	24.83	11.08	66.10846849	0.011378394
1200	66.19	21.92	11.89	56.50915548	0.009726189
1500	65.51	20.91	13.58	54.46494652	0.009374345
1800	63.22	21.19	15.59	57.19355782	0.009843986
2100	66.35	18.15	15.5	46.67736702	0.00803397
2400	64.59	18.2	17.21	48.08136091	0.008275622
2700	65.24	16.76	18	43.83597899	0.007544919
3000	65.26	15.64	19.1	40.89406919	0.007038566
3300	66.66	14.18	19.16	36.29790584	0.006247488
3600	68.09	12.7	19.21	31.82665782	0.00547791
3900	66.45	12.37	21.18	31.76474421	0.005467254
4200	67.59	11.36	21.05	28.67916701	0.004936173
4500	68.24	10.48	21.28	26.20552789	0.004510418
4800	67.12	10.17	22.71	25.85470895	0.004450036
5100	66.39	10	23.61	25.70206275	0.004423763
5400	67.66	8.93	23.41	22.52112669	0.00387627
5700	67.06	8.81	24.13	22.4172847	0.003858397
6000	68.74	7.83	23.43	19.43671571	0.00334539
6300	67.13	8	24.87	20.33499116	0.003499998
6600	68.78	7.12	24.1	17.66397618	0.003040271
6900	69.13	6.56	24.31	16.19227722	0.002786967
7200	68.58	6.46	24.96	16.07332349	0.002766493
7500	67.15	6.51	26.34	16.54267051	0.002847275
7800	66.11	6.74	27.15	17.39656033	0.002994244
8100	67.22	5.97	26.81	15.15466956	0.002608377
8400	68.2	5.45	26.35	13.6358676	0.002346965
8700	68.13	5.32	26.55	13.32428433	0.002293336
9000	68.76	4.79	26.45	11.8869461	0.002045946
9300	67.86	5.16	26.98	12.97497395	0.002233214
9600	67.31	4.54	28.15	11.509247	0.001980938
9900	68.65	4.77	26.58	11.85628105	0.002040668
10200	67.05	4.51	28.44	11.47752924	0.001975478
10500	67.53	4.11	28.36	10.38522046	0.001787473
10800	66.53	4	29.47	10.25919102	0.001765782

Data Table 8: Molar Ratio of $DEBF_4$ to PPI-2 = 1:0.5 in D_2O System

Time (sec)	Integration Values			Relative Intensity of Methoxyl Peak	Real-time Concentration of $DEBF_4$ (*M*)
	Aromatic Peaks	Methoxyl Peak	Methanol Peak		
0	63.05	36.95	0	100	0.017211704
300	63.89	29.81	6.3	79.61588666	0.013703251
600	66.05	26.6	7.35	68.71941644	0.011827783
900	66.77	25.09	8.14	64.11947138	0.011036054
1200	66.25	25.03	8.72	64.46821048	0.011096078
1500	66.32	23.72	9.96	61.02964101	0.010504241
1800	67.07	23.07	9.86	58.69349031	0.01010215
2100	66.47	22.77	10.76	58.45316078	0.010060785
2400	66.96	21.72	11.32	55.3496685	0.009526621
2700	67.73	20.67	11.6	52.0750924	0.008963011
3000	68.46	19.59	11.95	48.82791607	0.008404116
3300	67.8	19.62	12.58	49.37873472	0.008498922
3600	68.94	18.47	12.59	45.71579373	0.007868467
3900	68.6	18.32	13.08	45.56926269	0.007843247
4200	67.95	18.09	13.96	45.42759591	0.007818863
4500	69.04	17.24	13.72	42.60956759	0.007333833
4800	68.82	16.86	14.32	41.80358717	0.00719511
5100	68.58	16.74	14.68	41.65130577	0.007168899
5400	68.45	16.51	15.04	41.15705289	0.00708383
5700	69.08	15.86	15.06	39.1761273	0.006742879
6000	68.64	15.7	15.66	39.02950342	0.006717643
6300	69.45	15.13	15.42	37.17383151	0.00639825
6600	69.76	14.7	15.54	35.95683946	0.006188785
6900	68.21	15.15	16.64	37.89965281	0.006523176
7200	69.77	14.15	16.08	34.60655473	0.005956378
7500	68.74	14.6	16.66	36.24215189	0.006237892
7800	69.96	13.42	16.62	32.73206185	0.005633746
8100	69.72	13.61	16.67	33.30975167	0.005733176
8400	69.21	13.37	17.42	32.96349151	0.005673579
8700	69.69	12.78	17.53	31.29183543	0.005385858
9000	69.88	12.74	17.38	31.10908087	0.005354403
9300	69.57	12.89	17.54	31.61560975	0.005441585
9600	69.44	12.54	18.02	30.8147375	0.005303741
9900	69.53	12.05	18.42	29.57232468	0.005089901
10200	68.95	12.43	18.62	30.76149982	0.005294578
10500	69.11	12.19	18.7	30.09771052	0.005180329
10800	69.75	11.64	18.61	28.47602834	0.00490121

Data Table 9: Molar Ratio of $DEBF_4$ to PPI-2 = 1:0.25 in D_2O System

Time (sec)	Integration Values			Relative Intensity of Methoxyl Peak	Real-time Concentration of $DEBF_4$ (*M*)
	Aromatic Peaks	Methoxyl Peak	Methanol Peak		
0	63.05	36.95	0	100	0.017211704
300	66.48	29.69	3.83	76.20611732	0.013116371
600	67.35	28.62	4.03	72.51079681	0.012480344
900	65.79	30.22	3.99	78.37999326	0.013490532
1200	68.18	27.43	4.39	68.64982886	0.011815805
1500	67.18	28.14	4.68	71.47509508	0.012302082
1800	67.8	27.62	4.58	69.51277538	0.011964333
2100	67.78	27.07	5.15	68.14866293	0.011729546
2400	67.4	27.92	4.68	70.6848215	0.012166062
2700	67.01	27.65	5.34	70.40867408	0.012118533
3000	67.66	26.71	5.63	67.36162305	0.011594083
3300	68.69	25.75	5.56	63.96676169	0.01100977
3600	66.81	27.51	5.68	70.26188012	0.012093267
3900	68.52	25.39	6.09	63.22895363	0.01088278
4200	67.9	26.12	5.98	65.64082737	0.011297905
4500	68.26	25.34	6.4	63.3448008	0.01090272
4800	68.95	24.63	6.42	60.95380053	0.010491188
5100	68.44	25.13	6.43	62.65462513	0.010783929
5400	68.58	24.84	6.58	61.80516339	0.010637722
5700	68.73	24.54	6.73	60.92546642	0.010486311
6000	68.41	24.73	6.86	61.68437577	0.010616932
6300	68.23	24.85	6.92	62.1472148	0.010696595
6600	66.81	25.29	7.9	64.59189198	0.011117365
6900	69.34	23.53	7.13	57.90402297	0.009966269
7200	68.81	23.68	7.51	58.7219932	0.010107056
7500	69.26	23.28	7.46	57.35498057	0.009871769
7800	69.12	23.4	7.48	57.767394	0.009942753
8100	69.25	23.13	7.62	56.99365422	0.009809579
8400	69.36	22.94	7.7	56.43583789	0.009713569
8700	69.58	22.67	7.75	55.59525722	0.009568891
9000	68.56	23.53	7.91	58.56279102	0.010079654
9300	68.72	23	8.28	57.11041728	0.009829676
9600	67.98	23.78	8.24	59.68996692	0.01027366
9900	68.85	22.86	8.29	56.65561127	0.009751396
10200	69.11	22.97	7.92	56.71406158	0.009761456
10500	69.03	22.57	8.4	55.79102416	0.009602586
10800	68.37	23.37	8.26	58.32621316	0.010038935

Data Table 10: Molar Ratio of $DEBF_4$ to PPI-2 = 4:1 in D_2O System

Time (sec)	Integration Values			Relative Intensity of Methoxyl Peak	Real-time Concentration of $DEBF_4$ (*M*)
	Aromatic Peaks	Methoxyl Peak	Methanol Peak		
0	63.05	36.95	0	100	0.068846816
300	68.9	25.8	5.3	63.89562642	0.043990104
600	69.68	24.37	5.95	59.67851877	0.04108676
900	70.46	22.83	6.71	55.28838712	0.038064294
1200	71.4	21.41	7.19	51.16689978	0.035226781
1500	71.98	20.22	7.8	47.93359003	0.03300075
1800	72.17	19.58	8.25	46.29420499	0.031872086
2100	73.06	18.46	8.48	43.1144328	0.029682914
2400	73.19	17.77	9.04	41.42917917	0.028522671
2700	73.58	17.22	9.2	39.93411018	0.027493363
3000	73.86	16.55	9.59	38.2348458	0.026323474
3300	74.12	16.14	9.74	37.15683962	0.025581301
3600	74.36	15.72	9.92	36.0731285	0.0248352
3900	74.42	15.35	10.23	35.19568015	0.024231105
4200	74.64	14.95	10.41	34.17749356	0.023530116
4500	74.8	14.48	10.72	33.03220858	0.022741624
4800	74.65	14.4	10.95	32.91571764	0.022661424
5100	75.06	13.75	11.19	31.25825907	0.021520316
5400	75.2	13.56	11.24	30.76893732	0.021183434
5700	75.09	13.28	11.63	30.17773349	0.020776409
6000	75.47	12.87	11.66	29.09878429	0.020033586
6300	75.48	12.56	11.96	28.39411887	0.019548447
6600	75.59	12.3	12.11	27.7658782	0.019115923
6900	76.04	11.83	12.13	26.54686765	0.018276673
7200	75.7	11.74	12.56	26.46323086	0.018219092
7500	75.92	11.35	12.73	25.50999129	0.017562817
7800	76.13	11.12	12.75	24.92410692	0.017159454
8100	76.35	10.76	12.89	24.04771843	0.016556088
8400	76.38	10.6	13.02	23.68082669	0.016303495
8700	76.44	10.36	13.2	23.12649011	0.015921852
9000	76.57	10.07	13.36	22.44096207	0.015449888
9300	76.73	9.88	13.39	21.97163595	0.015126772
9600	76.96	9.59	13.45	21.26298321	0.014638887
9900	76.81	9.46	13.73	21.0157077	0.014468646
10200	76.86	9.28	13.86	20.60242037	0.01418411
10500	76.54	9.32	14.14	20.7777302	0.014304806
10800	76.63	9.23	14.14	20.55291961	0.014150031

Data Table 11: Molar Ratio of $DEBF_4$ to PPI-2 = 2:1 in D_2O System

Time (sec)	Integration Values			Relative Intensity of Methoxyl Peak	Real-time Concentration of $DEBF_4$ (*M*)
	Aromatic Peaks	Methoxyl Peak	Methanol Peak		
0	63.05	36.95	0	100	0.034423408
300	66.25	26.82	6.93	69.07860188	0.023779209
600	67.03	24.72	8.25	62.92886448	0.02166226
900	67.63	23.04	9.33	58.13179529	0.020010945
1200	67.08	22.53	10.39	57.31110552	0.019728436
1500	68.05	20.79	11.16	52.13111429	0.017945306
1800	68.46	19.78	11.76	49.30148953	0.016971253
2100	68.36	19.03	12.61	47.50150639	0.016351637
2400	68.56	18.11	13.33	45.07318935	0.015515728
2700	68.84	17.25	13.91	42.75814798	0.014718812
3000	68.92	16.74	14.34	41.44582921	0.014267067
3300	69.38	15.83	14.79	38.93294601	0.013402047
3600	69.21	15.28	15.51	37.67256173	0.01296818
3900	69.18	14.81	16.01	36.52961954	0.01257474
4200	70.22	13.77	16.01	33.46137348	0.011518545
4500	69.86	13.65	16.49	33.34070035	0.011477005
4800	69.3	13.38	17.32	32.94530458	0.011340897
5100	69.45	12.86	17.69	31.5965283	0.010876602
5400	70.28	12.22	17.5	29.66949138	0.01021325
5700	69.7	11.92	18.38	29.18193767	0.010045417
6000	70.18	11.37	18.45	27.6450735	0.009516376
6300	70.37	11	18.63	26.67324059	0.009181838
6600	69.49	11.05	19.46	27.13379969	0.009340379
6900	69.82	10.6	19.58	25.90577976	0.008917652
7200	71.21	9.72	19.07	23.29141788	0.0080177
7500	70.3	9.91	19.79	24.05409255	0.008280238
7800	70.42	9.46	20.12	22.92269964	0.007890774
8100	69.91	9.35	20.74	22.82143541	0.007855916
8400	70.75	8.86	20.39	21.36869134	0.007355832
8700	70.28	8.82	20.9	21.41447741	0.007371593
9000	70.8	8.34	20.86	20.10034174	0.006919223
9300	70.14	8.23	21.63	20.0218739	0.006892211
9600	71.33	7.98	20.69	19.08979724	0.006571359
9900	70.65	7.66	21.69	18.50066127	0.006368558
10200	70.83	7.57	21.6	18.23682732	0.006277737
10500	71.08	7.33	21.59	17.59653686	0.006057328
10800	70.07	7.25	22.68	17.65535837	0.006077576

Data Table 12: Molar Ratio of $DEBF_4$ to PPI-2 = 0.5:1 in D_2O System

Time (sec)	Integration Values			Relative Intensity of Methoxyl Peak	Real-time Concentration of $DEBF_4$ (*M*)
	Aromatic Peaks	Methoxyl Peak	Methanol Peak		
0	63.05	36.95	0	100	0.008605852
300	65.65	23.32	11.03	60.61281636	0.005216249
600	71.27	16.45	12.28	39.38490404	0.003389407
900	72.74	13.41	13.85	31.45763937	0.002707198
1200	73.14	11.76	15.1	27.43614023	0.002361114
1500	72.76	10.6	16.64	24.85900966	0.00213933
1800	69.75	10.34	19.91	25.2957159	0.002176912
2100	70.27	9.19	20.54	22.31599246	0.001920481
2400	70.55	8.28	21.17	20.02644983	0.001723447
2700	67.85	8.36	23.79	21.02456765	0.001809343
3000	71.29	6.6	22.11	15.79741288	0.001359502
3300	69.09	6.21	24.7	15.33723442	0.0013199
3600	73.13	5	21.87	11.66662072	0.001004012
3900	69.15	5.67	25.18	13.99141127	0.00120408
4200	69.69	5.15	25.16	12.60977719	0.001085179
4500	72.63	4.08	23.29	9.585499902	0.000824914
4800	71.1	4.57	24.33	10.96774255	0.000943868
5100	68.78	3.95	27.27	9.799537345	0.000843334
5400	67.91	4.22	27.87	10.60350312	0.000912522
5700	69.46	3.36	27.18	8.254203021	0.000710344
6000	68.6	4.12	27.28	10.2481093	0.000881937
6300	71.23	3.43	25.34	8.216783117	0.000707124
6600	64.46	4.45	31.09	11.77986621	0.001013758
6900	71.36	3.08	25.56	7.364894385	0.000633812
7200	70.4	3.06	26.54	7.416848628	0.000638283
7500	70.21	2.99	26.8	7.266794243	0.00062537
7800	67.4	3.4	29.2	8.607750469	0.00074077
8100	70.92	2.96	26.12	7.121863282	0.000612897
8400	68.79	3.1	28.11	7.689658137	0.000661761
8700	67.92	2.96	29.12	7.436433215	0.000639968
9000	67.06	2.76	30.18	7.022895095	0.00060438
9300	67.4	2.92	29.68	7.392538638	0.000636191
9600	67.45	3.26	29.29	8.247195587	0.000709741
9900	68.18	2.66	29.16	6.657256462	0.000572914
10200	65.94	2.89	31.17	7.478586963	0.000643596
10500	72.3	2.04	25.66	4.814625573	0.00041434
10800	71.54	2.84	25.62	6.77391983	0.000582954

Data Table 13: Molar Ratio of $DEBF_4$ to PPI-2 = 0.25:1 in D_2O System

Time (sec)	Integration Values			Relative Intensity of Methoxyl Peak	Real-time Concentration of $DEBF_4$ (*M*)
	Aromatic Peaks	Methoxyl Peak	Methanol Peak		
0	63.05	36.95	0	100	0.004475043
300	87.43	6.04	6.53	11.78818949	0.000527527
600	87.67	4.99	7.34	9.712257477	0.000434628
900	86.06	5.05	8.89	10.01291858	0.000448082
1200	87.54	3.77	8.69	7.348614343	0.000328854
1500	87.27	3.71	9.02	7.254033917	0.000324621
1800	85.74	2.89	11.37	5.751551485	0.000257384
2100	87.05	2.18	10.77	4.27325064	0.00019123
2400	84.17	3.22	12.61	6.527835364	0.000292123
2700	86.53	1.61	11.86	3.174898316	0.000142078
3000	84.42	1.96	13.62	3.96169805	0.000177288
3300	85.13	2.27	12.6	4.550025933	0.000203616
3600	83.95	1.54	14.51	3.130189776	0.000140077
3900	84.27	1.92	13.81	3.88775495	0.000173979
4200	82.89	1.32	15.79	2.717330352	0.000121602
4500	83.87	0.95	15.18	1.932803086	8.64938E-05
4800	84.02	1.63	14.35	3.310362666	0.00014814
5100	84.83	0.52	14.65	1.045982756	4.68082E-05
5400	82.39	1.44	16.17	2.982350191	0.000133461
5700	84.06	1.2	14.74	2.435917125	0.000109008
6000	83.03	1.83	15.14	3.760855957	0.0001683
6300	82.12	0.81	17.07	1.683087623	7.53189E-05
6600	82.92	1.04	16.04	2.140152368	9.57727E-05
6900	82.96	0.87	16.17	1.789456549	8.0079E-05
7200	83.87	0.64	15.49	1.302098921	5.82695E-05
7500	79.99	1.46	18.55	3.114496213	0.000139375
7800	80.25	1.05	18.7	2.23262049	9.99107E-05
8100	83.1	1.04	15.86	2.135516659	9.55653E-05
8400	81.42	0.87	17.71	1.823302816	8.15936E-05
8700	81.73	0.59	17.68	1.231802726	5.51237E-05
9000	80.98	0.57	18.45	1.201068374	5.37483E-05
9300	81.6	0.43	17.97	0.899184775	4.02389E-05
9600	80.77	1.49	17.74	3.147797845	0.000140865
9900	80.11	0.69	19.2	1.469714596	6.57704E-05
10200	80.75	0.9	18.35	1.901825327	8.51075E-05
10500	80.69	1.36	17.95	2.876006353	0.000128703
10800	79.89	1.39	18.72	2.96888262	0.000132859

Data Table 14: Molar Ratio of $DEBF_4$ to PPI-2 = 1:16 in Methanol-d_4 System

Time (sec)	Integration Values			Relative Intensity of Methoxyl Peak	Real-time Concentration of $DEBF_4$ (M)
	Aromatic Peaks	Methoxyl Peak	Methanol Peak		
0	58.03	41.97	0	100	0.008605852
600	91.31	4.2	4.49	6.359815971	0.000547316
900	91.55	3.73	4.72	5.633315623	0.000484795
1200	91.75	3.19	5.06	4.807266641	0.000413706
1500	92.02	2.83	5.15	4.252240386	0.000365942
1800	92.08	2.64	5.28	3.964169517	0.000341151
2100	91.96	2.56	5.48	3.849059318	0.000331244
2400	92.13	2.31	5.56	3.466765852	0.000298345
2700	92.26	2.2	5.54	3.297029492	0.000283737
3000	92.36	2.03	5.61	3.038965117	0.000261529
3300	91.99	2.15	5.86	3.231554186	0.000278103
3600	92.31	1.96	5.73	2.93576252	0.000252647
3900	92.13	1.97	5.9	2.956505943	0.000254433
4200	92.53	1.7	5.77	2.540270475	0.000218612
4500	92.36	1.69	5.95	2.529975886	0.000217726
4800	92.31	1.69	6	2.531346255	0.000217844
5100	92.24	1.67	6.09	2.503287774	0.000215429
5400	92.33	1.59	6.08	2.381046572	0.000204909

Data Table 15: Molar Ratio of $DEBF_4$ to PPI-2 = 1:8 in Methanol-d_4 System

Time (sec)	Integration Values			Relative Intensity of Methoxyl Peak	Real-time Concentration of $DEBF_4$ (M)
	Aromatic Peaks	Methoxyl Peak	Methanol Peak		
0	58.03	41.97	0	100	0.008605852
300	54.67	28.73	16.6	72.66079637	0.006253081
600	46.55	32.7	20.75	97.12737885	0.008358638
900	48.41	28.63	22.96	81.77110503	0.0070371
1200	49.92	25.62	24.46	70.96074233	0.006106776
1500	51.61	22.81	25.58	61.10897899	0.005258948
1800	47.6	23.57	28.83	68.46462459	0.005891964
2100	46.75	23.41	29.84	69.23622807	0.005958367
2400	49.1	21.78	29.12	61.33240356	0.005278176
2700	48.08	21.47	30.45	61.74207014	0.005313431
3000	51.34	19.76	28.9	53.21630018	0.004579716
3300	46.66	21.37	31.97	63.32473617	0.005449633
3600	49.03	20.08	30.89	56.62593897	0.004873144
3900	50.93	18.84	30.23	51.14707751	0.004401642
4200	46.79	20.86	32.35	61.64173587	0.005304797
4500	47.54	20.04	32.42	58.28437465	0.005015867
4800	47.94	19.73	32.33	56.90398182	0.004897072
5100	48.95	19.21	31.84	54.26105957	0.004669626
5400	50.65	18.08	31.27	49.35516155	0.004247432
5700	49.78	18.92	31.3	52.55086163	0.004522449
6000	48.97	19.88	31.15	56.13062492	0.004830518
6300	52.6	17.76	29.64	46.6842965	0.004017581
6600	48.2	20	31.8	57.37154676	0.00493731
6900	49.96	18.54	31.5	51.30986848	0.004415651
7200	54.83	16.24	28.93	40.95259066	0.003524319

Data Table 16: Molar Ratio of $DEBF_4$ to PPI-2 = 1:4 in Methanol-d_4 System

Time (sec)	Integration Values			Relative Intensity of Methoxyl Peak	Real-time Concentration of $DEBF_4$ (M)
	Aromatic Peaks	Methoxyl Peak	Methanol Peak		
0	58.03	41.97	0	100	0.008605852
300	63.41	24.92	11.67	54.33802962	0.00467625
600	60.59	23.84	15.57	54.4025053	0.004681799
900	63.32	18.89	17.79	41.24816691	0.003549756
1200	62.41	17.05	20.54	37.77320208	0.003250706
1500	62.38	15.22	22.4	33.73516847	0.002903199
1800	62.51	13.38	24.11	29.59512754	0.002546913
2100	60.13	13.22	26.65	30.39861889	0.00261606
2400	64.31	10.8	24.89	23.21981992	0.001998263
2700	58.48	11.56	29.96	27.33153803	0.002352112
3000	60.3	10.12	29.58	23.20474508	0.001996966
3300	64.35	8.75	26.9	18.80066033	0.001617957
3600	63.72	8.45	27.83	18.33557539	0.001577932
3900	62.59	8.45	28.96	18.66660591	0.00160642
4200	61.62	7.82	30.56	17.54682967	0.001510054
4500	61.91	7.37	30.72	16.45963822	0.001416492
4800	65.63	6.98	27.39	14.70505387	0.001265495
5100	62.52	7.17	30.31	15.85673571	0.001364607
5400	59.11	7.91	32.98	18.50244515	0.001592293
5700	63.31	7.23	29.46	15.78990747	0.001358856
6000	58.51	7.75	33.74	18.31408417	0.001576083
6300	59.14	6.99	33.87	16.34215995	0.001406382
6600	64.82	6.07	29.11	12.94771901	0.001114262
6900	65.91	5.99	28.1	12.56577017	0.001081392
7200	62.91	6.69	30.4	14.70347657	0.001265359
7500	61.77	6.99	31.24	15.64635486	0.001346502
7800	63.82	6.87	29.31	14.88379016	0.001280877
8100	64.53	6.2	29.27	13.28445144	0.00114324
8400	64.39	6.25	29.36	13.42070078	0.001154966
8700	61.99	6.77	31.24	15.10012817	0.001299495
9000	60.24	6.57	33.19	15.07974535	0.001297741
9300	62.36	6.92	30.72	15.34311673	0.001320406
9600	65.2	6.92	27.88	14.67479693	0.001262891
9900	59.84	6.76	33.4	15.619557	0.001344196
10200	63.87	6.43	29.7	13.91962893	0.001197903
10500	61.6	6.49	31.91	14.56725042	0.001253636
10800	58.74	7.28	33.98	17.13606254	0.001474704

Data Table 17: Molar Ratio of $DEBF_4$ to PPI-2 = 1:2 in Methanol-d_4 System

Time (sec)	Integration Values			Relative Intensity of Methoxyl Peak	Real-time Concentration of $DEBF_4$ (M)
	Aromatic Peaks	Methoxyl Peak	Methanol Peak		
0	58.03	41.97	0	100	0.008605852
300	62.38	23.27	14.35	51.57801382	0.004438728
600	60.54	21.21	18.25	48.44086094	0.004168749
900	61.13	18.72	20.15	42.34138404	0.003643837
1200	58.43	18.32	23.25	43.3514057	0.003730758
1500	62.34	14.21	23.45	31.51671042	0.002712281
1800	62.55	13.12	24.33	29.0014774	0.002495824
2100	62.08	11.61	26.31	25.85795128	0.002225297
2400	63.01	10.07	26.92	22.09701407	0.001901636
2700	60.19	11.38	28.43	26.14156117	0.002249704
3000	60.97	9.4	29.63	21.31695949	0.001834506
3300	61.73	8.5	29.77	19.03865439	0.001638438
3600	62.42	7.05	30.53	15.61632914	0.001343918
3900	62.18	6.86	30.96	15.25411441	0.001312747
4200	60.73	7.28	31.99	16.57454822	0.001426381
4500	60.25	6.55	33.2	15.03134525	0.001293575
4800	61.26	5.96	32.78	13.45187641	0.001157649
5100	56.62	6.28	37.1	15.33569209	0.001319767
5400	59.46	5.42	35.12	12.60340764	0.001084631
5700	61.21	4.64	34.15	10.48115642	0.000901993
6000	61.86	4.39	33.75	9.812240988	0.000844427
6300	62.1	4.09	33.81	9.106370358	0.000783681
6600	59.57	4.53	35.9	10.51439294	0.000904853
6900	58.59	4.51	36.9	10.6430633	0.000915926
7200	60.51	3.81	35.68	8.705854892	0.000749213
7500	57.78	4.47	37.75	10.69654659	0.000920529
7800	59.27	3.67	37.06	8.561399015	0.000736781
8100	60.82	3.95	35.23	8.979750729	0.000772784
8400	55.37	3.89	40.74	9.713789303	0.000835954
8700	60.28	3.79	35.93	8.693197925	0.000748124
9000	58.22	3.56	38.22	8.454567547	0.000727588
9300	57.51	3.04	39.45	7.308761957	0.000628981
9600	59.38	2.8	37.82	6.519757452	0.000561081
9900	56.62	3.13	40.25	7.643426151	0.000657782
10200	58.18	3.34	38.48	7.937547756	0.000683094
10500	58.08	2.87	39.05	6.832330879	0.00058798
10800	57.73	3.36	38.91	8.047320925	0.000692541

Data Table 18: Molar Ratio of $DEBF_4$ to PPI-2 = 1:1.5 in Methanol-d_4 System

Time (sec)	Integration Values			Relative Intensity of Methoxyl Peak	Real-time Concentration of $DEBF_4$ (M)
	Aromatic Peaks	Methoxyl Peak	Methanol Peak		
0	58.03	41.97	0	100	0.008605852
300	55.55	31.79	12.66	79.12615565	0.00680948
600	55.87	27.49	16.64	68.03144097	0.005854685
900	55.73	24.06	20.21	59.69255679	0.005137053
1200	57.07	20.18	22.75	48.89077152	0.004207467
1500	56.23	17.79	25.98	43.74429946	0.00376457
1800	57.4	15.38	27.22	37.04742644	0.003188247
2100	56.2	14.2	29.6	34.93539276	0.003006488
2400	57.13	12.42	30.45	30.05875393	0.002586812
2700	58.82	9.83	31.35	23.10692204	0.001988548
3000	58.44	9.3	32.26	22.00322515	0.001893565
3300	56.52	8.94	34.54	21.87000926	0.001882101
3600	58	8.02	33.98	19.11877121	0.001645333
3900	57.35	6.9	35.75	16.63524762	0.001431605
4200	57.05	6.23	36.72	15.09892401	0.001299391
4500	55.67	6.76	37.57	16.78955077	0.001444884
4800	53.46	6.06	40.48	15.67318541	0.001348811
5100	54.83	5.47	39.7	13.79376052	0.001187071
5400	58.16	4.18	37.66	9.937233283	0.000855184
5700	56.42	4.4	39.18	10.78284087	0.000927955
6000	55.49	3.96	40.55	9.867202985	0.000849157
6300	55.7	3.81	40.49	9.457653133	0.000813912
6600	54.36	3.78	41.86	9.614483382	0.000827408
6900	53.74	3.55	42.71	9.133648461	0.000786028
7200	56.72	3.66	39.62	8.921922873	0.000767807
7500	55.62	3.08	41.3	7.656553709	0.000658912
7800	55.18	3.49	41.33	8.744950029	0.000752577
8100	55.41	3.11	41.48	7.760430971	0.000667851
8400	55.54	3.12	41.34	7.767161224	0.00066843
8700	56.07	3.06	40.87	7.545785781	0.000649379
9000	56.8	2.44	40.76	5.939571189	0.000511151
9300	54.07	2.6	43.33	6.648605733	0.000572169
9600	57.09	2.32	40.59	5.61877373	0.000483543
9900	56.12	2.59	41.29	6.38110224	0.000549148
10200	55.85	2.44	41.71	6.040602391	0.000519845
10500	55.54	2.35	42.11	5.850265666	0.000503465
10800	53.08	2.79	44.13	7.267530958	0.000625433

Data Table 19: Molar Ratio of $DEBF_4$ to PPI-2 = 1:1 in Methanol-d_4 System

Time (sec)	Integration Values			Relative Intensity of Methoxyl Peak	Real-time Concentration of $DEBF_4$ (M)
	Aromatic Peaks	Methoxyl Peak	Methanol Peak		
0	58.03	41.97	0	100	0.008605852
300	70.37	21.1	8.53	41.45801512	0.003567815
600	69.03	19.95	11.02	39.95936958	0.003438844
900	69.71	18.59	11.7	36.87210301	0.003173159
1200	71.16	16.08	12.76	31.24378973	0.002688794
1500	70.11	15.56	14.33	30.68620817	0.00264081
1800	68.3	15.36	16.34	31.09453835	0.00267595
2100	69.42	13.66	16.92	27.20693953	0.002341389
2400	69.04	12.58	18.38	25.19378737	0.00216814
2700	70.03	12.2	17.77	24.08736567	0.002072923
3000	67.28	11.63	21.09	23.90051908	0.002056843
3300	69.48	10.7	19.82	21.29303506	0.001832447
3600	69.05	10.19	20.76	20.40441286	0.001755974
3900	70.64	9.42	19.94	18.43800012	0.001586747
4200	68.59	9.23	22.18	18.60606353	0.00160121
4500	69.22	8.15	22.63	16.27944576	0.001400985
4800	68.66	8.02	23.32	16.150433	0.001389882
5100	68.9	7.88	23.22	15.81323034	0.001360863
5400	69.29	7.21	23.5	14.38726705	0.001238147
5700	66.89	7.37	25.74	15.23420843	0.001311033
6000	69.78	6.28	23.94	12.4434922	0.001070869
6300	70.72	5.95	23.33	11.63290858	0.001001111
6600	69.48	5.58	24.94	11.10421829	0.000955613
6900	68.47	5.94	25.59	11.99498526	0.001032271
7200	69.57	5.46	24.97	10.85136172	0.000933852
7500	68.75	5.19	26.06	10.43778283	0.00089826
7800	69.14	4.98	25.88	9.958950389	0.000857053
8100	68.54	4.88	26.58	9.844401621	0.000847195
8400	68.98	4.46	26.56	8.939747861	0.000769341
8700	70.14	4.43	25.43	8.73276083	0.000751528
9000	69.09	4.29	26.62	8.585304455	0.000738839
9300	67.85	4.26	27.89	8.681071805	0.00074708
9600	67.62	3.79	28.59	7.749570703	0.000666917
9900	68.65	3.68	27.67	7.411751987	0.000637844
10200	67.84	4.25	27.91	8.661970337	0.000745436
10500	69.45	3.69	26.86	7.346284063	0.00063221
10800	69.05	3.47	27.48	6.94831331	0.000597962

Data Table 20: Molar Ratio of $DEBF_4$ to PPI-2 = 1:0.75 in Methanol-d_4 System

Time (sec)	Integration Values			Relative Intensity of Methoxyl Peak	Real-time Concentration of $DEBF_4$ (M)
	Aromatic Peaks	Methoxyl Peak	Methanol Peak		
0	58.03	41.97	0	100	0.008605852
300	55.74	33.67	10.59	83.51985917	0.007187595
600	57.64	29.8	12.56	71.48351397	0.006151765
900	53.65	30.15	16.2	77.70182003	0.006686904
1200	57.4	25.48	17.12	61.37636058	0.005281959
1500	52.11	26.69	21.2	70.81758328	0.006094456
1800	57.73	21.79	20.48	52.18783422	0.004491208
2100	56.34	20.46	23.2	50.21140665	0.004321119
2400	57.49	18.34	24.17	44.10833091	0.003795898
2700	58.97	16.63	24.4	38.99192916	0.003355588
3000	61.37	14.73	23.9	33.18640622	0.002855973
3300	55.05	15.62	29.33	39.23171627	0.003376223
3600	57.01	14.57	28.42	35.33638452	0.003040997
3900	55.19	13.55	31.26	33.9463045	0.002921369
4200	56.67	11.89	31.44	29.00963358	0.002496526
4500	56.42	11.21	32.37	27.47173776	0.002364177
4800	55.5	11.34	33.16	28.25099009	0.002431238
5100	58.36	9.56	32.08	22.64937438	0.001949172
5400	57.88	8.7	33.42	20.78281308	0.001788538
5700	57.29	8.55	34.16	20.63482993	0.001775803
6000	56.77	8.32	34.91	20.2636667	0.001743861
6300	57.66	7.39	34.95	17.72080317	0.001525026
6600	56.2	7.02	36.78	17.27087727	0.001486306
6900	54.06	7.72	38.22	19.74489644	0.001699217
7200	56.92	6.4	36.68	15.5463587	0.001337897
7500	56.31	6.54	37.15	16.05853129	0.001381973
7800	52.08	6.98	40.94	18.53096554	0.001594747
8100	56.89	5.81	37.3	14.12062111	0.0012152
8400	54.95	5.4	39.65	13.58750336	0.00116932
8700	56.96	4.85	38.19	11.77295162	0.001013163
9000	55.58	4.88	39.54	12.13989361	0.001044741
9300	56.42	4.91	38.67	12.03267015	0.001035514
9600	55.83	4.15	40.02	10.27765583	0.00088448
9900	55.56	4.74	39.7	11.79586262	0.001015134
10200	57.31	3.74	38.95	9.023079734	0.000776513
10500	54.8	3.73	41.47	9.411132213	0.000809908
10800	55.68	3.64	40.68	9.038903678	0.000777875

Data Table 21: Molar Ratio of $DEBF_4$ to PPI-2 = 1:0.5 in Methanol-d_4 System

Time (sec)	Integration Values			Relative Intensity of Methoxyl Peak	Real-time Concentration of $DEBF_4$ (M)
	Aromatic Peaks	Methoxyl Peak	Methanol Peak		
0	58.03	41.97	0	100	0.008605852
300	42.52	40.73	16.75	132.4447523	0.011397999
600	43.84	39.23	16.93	123.7261115	0.010647686
900	51.41	32.71	15.88	87.97242053	0.007570776
1200	44.03	36.87	19.1	115.7812019	0.009963959
1500	48.78	30.95	20.27	87.7268345	0.007549642
1800	49.55	29.7	20.75	82.87554394	0.007132147
2100	52.14	26.61	21.25	70.56469181	0.006072693
2400	41.69	31.32	26.99	103.8731877	0.008939173
2700	48.83	25.92	25.25	73.39422252	0.006316198
3000	42.16	28.93	28.91	94.87710681	0.008164983
3300	51.88	22.61	25.51	60.2579283	0.005185708
3600	44.65	25.05	30.3	77.57108541	0.006675653
3900	47.66	22.35	29.99	64.83911684	0.005579958
4200	43	24.15	32.85	77.65372276	0.006682764
4500	43.83	22.64	33.53	71.41978742	0.006146281
4800	51.28	18.74	29.98	50.52835637	0.004348396
5100	37.22	23.86	38.92	88.63549448	0.007627839
5400	47.97	19.43	32.6	56.00369523	0.004819595
5700	42.54	20.81	36.65	67.63760108	0.005820792
6000	36.36	21.52	42.12	81.83366347	0.007042484
6300	51.7	15.29	33.01	40.89126478	0.003519042
6600	51.18	15.58	33.24	42.09017904	0.003622219
6900	53.32	13.87	32.81	35.96664445	0.003095236
7200	50.76	14.39	34.85	39.19699575	0.003373235
7500	38.03	17.51	44.46	63.66099497	0.005478571
7800	42.04	16.21	41.75	53.31309664	0.004588046
8100	50.81	12.93	36.26	35.18543554	0.003028007
8400	49.51	13.13	37.36	36.6678462	0.003155581
8700	37.06	15.52	47.42	57.90284505	0.004983033
9000	48.04	13.02	38.94	37.47326954	0.003224894
9300	49.87	11.86	38.27	32.88205278	0.002829781
9600	36.43	15.37	48.2	58.33487849	0.005020213
9900	47.56	11.73	40.71	34.1012083	0.0029347
10200	37.2	13.04	49.76	48.46723594	0.004171019
10500	37.58	12.5	49.92	45.99036312	0.003957863
10800	48.72	9.86	41.42	27.98228894	0.002408114

Data Table 22: Molar Ratio of $DEBF_4$ to PPI-2 = 1:0.25 in Methanol-d_4 System

Time (sec)	Integration Values			Relative Intensity of Methoxyl Peak	Real-time Concentration of $DEBF_4$ (M)
	Aromatic Peaks	Methoxyl Peak	Methanol Peak		
0	58.03	41.97	0	100	0.008605852
300	57.76	32.97	9.27	78.92332325	0.006792024
600	63.59	27.8	8.61	60.44627913	0.005201917
900	54.99	33.04	11.97	83.07491782	0.007149304
1200	58.07	29.26	12.67	69.66844178	0.005995563
1500	56.42	32.12	11.46	78.71473834	0.006774074
1800	58.83	28.45	12.72	66.86471898	0.005754279
2100	54.36	33.69	11.95	85.69099078	0.00737444
2400	53.78	33.08	13.14	85.04686404	0.007319007
2700	54.63	32.81	12.56	83.04024679	0.007146321
3000	54.18	31.04	14.78	79.21297297	0.006816951
3300	47.51	36.66	15.83	106.6893407	0.009181527
3600	47.11	36.33	16.56	106.626682	0.009176134
3900	53.42	32.86	13.72	85.05057944	0.007319327
4200	51.48	32.67	15.85	87.74536757	0.007551236
4500	52.56	32.62	14.82	85.81084953	0.007384755
4800	53.21	30.77	16.02	79.95540706	0.006880844
5100	55.53	30.31	14.16	75.46956804	0.006494799
5400	55.11	29.23	15.66	73.33511978	0.006311112
5700	56.54	28.53	14.93	69.76852939	0.006004176
6000	54.72	30.07	15.21	75.98028894	0.006538751
6300	52.59	30.07	17.34	79.05764234	0.006803584
6600	43.31	36.75	19.94	117.3228923	0.010096634
6900	49.21	31.73	19.06	89.15183947	0.007672275
7200	45.78	35.49	18.73	107.1874187	0.009224391
7500	56.43	28.4	15.17	69.58600295	0.005988468
7800	56.66	26.73	16.61	65.22828948	0.00561345
8100	51.02	31.59	17.39	85.60966015	0.007367441
8400	57.41	25.69	16.9	61.87143071	0.005324564
8700	58.2	26.08	15.72	61.95811605	0.005332024
9000	59.69	24.44	15.87	56.61261606	0.004871998
9300	46.9	32.7	20.4	96.40254766	0.008296261
9600	49.03	31.98	18.99	90.18413986	0.007761114
9900	44.78	33.71	21.51	104.0850283	0.008957403
10200	55.19	28.04	16.77	70.24755558	0.006045401
10500	46.11	31.89	22	95.62534133	0.008229375
10800	42.06	35.15	22.79	115.5499235	0.009944055

Data Table 23: Molar Ratio of $DEBF_4$ to PPI-2 = 4:1 in Methanol-d_4 System

Time (sec)	Integration Values			Relative Intensity of Methoxyl Peak	Real-time Concentration of $DEBF_4$ (M)
	Aromatic Peaks	Methoxyl Peak	Methanol Peak		
0	58.03	41.97	0	100	0.034423408
300	61.07	34.27	4.66	77.58893412	0.026708755
600	61.51	32.96	5.53	74.08922934	0.025504038
900	61.32	32.44	6.24	73.14628953	0.025179446
1200	60.3	32.32	7.38	74.10843487	0.025510649
1500	61.71	30.57	7.72	68.49415207	0.023578021
1800	60.53	30.95	8.52	70.69742255	0.024336462
2100	60.75	29.97	9.28	68.21094433	0.023480532
2400	60.1	29.71	10.19	68.35051342	0.023528576
2700	60.54	28.57	10.89	65.25013659	0.022461321
3000	60.95	27.86	11.19	63.20057121	0.02175579
3300	60.99	27.17	11.84	61.594879	0.021203056
3600	61.54	26.08	12.38	58.59542337	0.020170542
3900	61.32	25.75	12.93	58.06155843	0.019986767
4200	61.53	24.85	13.62	55.84098615	0.01922237
4500	61.17	24.52	14.31	55.42370912	0.019078729
4800	62.05	23.55	14.4	52.4762421	0.018064111
5100	60.33	23.97	15.7	54.93489643	0.018910463
5400	60.98	23.1	15.92	52.3767035	0.018029846
5700	61.1	22.54	16.36	51.00659149	0.017558207
6000	61.42	21.88	16.7	49.25508886	0.01695528
6300	61.44	21.36	17.2	48.06884009	0.016546933
6600	61.05	21.05	17.9	47.67382887	0.016410957
6900	60.91	20.62	18.47	46.80730781	0.016112671
7200	60.77	20.32	18.91	46.23257348	0.015914827
7500	60.17	20.22	19.61	46.46380169	0.015994424
7800	60.56	19.57	19.87	44.68055515	0.01538057
8100	61.2	18.66	20.14	42.15740001	0.014512014
8400	61.48	18.32	20.2	41.20075854	0.014182705
8700	60.78	18.31	20.91	41.65251696	0.014338216
9000	60.09	18.12	21.79	41.69361873	0.014352364
9300	60.95	17.34	21.71	39.33589034	0.013540754
9600	60.09	17.36	22.55	39.94487976	0.013750389
9900	61.32	16.6	22.08	37.42997553	0.012884673
10200	61.42	16.05	22.53	36.13090385	0.012437488
10500	60.41	16.12	23.47	36.89519441	0.012700583
10800	60.98	15.68	23.34	35.55267147	0.012238441

Data Table 24: Molar Ratio of $DEBF_4$ to PPI-2 = 2:1 in Methanol-d_4 System

Time (sec)	Integration Values			Relative Intensity of Methoxyl Peak	Real-time Concentration of $DEBF_4$ (M)
	Aromatic Peaks	Methoxyl Peak	Methanol Peak		
0	58.03	41.97	0	100	0.017211704
300	60.84	33.23	5.93	75.51874034	0.012998062
600	63.07	29.35	7.58	64.34263997	0.011074465
900	62.54	28	9.46	61.9032935	0.010654612
1200	63.06	26.11	10.83	57.24881568	0.009853497
1500	63.29	24.61	12.1	53.76382012	0.00925367
1800	63.22	23.28	13.5	50.91457065	0.008763265
2100	63.04	22.06	14.9	48.3841265	0.008327733
2400	63.06	21.06	15.88	46.17617994	0.007947707
2700	64.93	18.92	16.15	40.2892637	0.006934469
3000	65.1	17.92	16.98	38.06016074	0.006550802
3300	64.58	17.42	18	37.29612497	0.006419299
3600	64.54	16.38	19.08	35.09122568	0.006039798
3900	66.13	14.84	19.03	31.02765684	0.005340388
4200	64.48	14.63	20.89	31.37132765	0.00539954
4500	63.93	14.16	21.91	30.62472166	0.005271036
4800	65.11	13	21.89	27.60636707	0.004751526
5100	65.9	12.41	21.69	26.03754109	0.004481504
5400	65.46	11.91	22.63	25.15645041	0.004329854
5700	64.1	11.85	24.05	25.56076939	0.004399444
6000	66.42	10.26	23.32	21.3580742	0.003676089
6300	65.53	10.42	24.05	21.98574327	0.003784121
6600	65.24	9.95	24.81	21.08738512	0.003629498
6900	65.27	9.42	25.31	19.95496137	0.003434589
7200	66.76	8.66	24.58	17.93556926	0.003087017
7500	64.88	8.77	26.35	18.689701	0.003216816
7800	65.03	8.38	26.59	17.81738096	0.003066675
8100	65.61	8.14	26.25	17.15410122	0.002952513
8400	65.44	7.72	26.84	16.31126378	0.002807446
8700	65.85	7.22	26.93	15.15985403	0.002609269
9000	65.8	6.84	27.36	14.37288032	0.002473818
9300	65.29	6.79	27.92	14.37926565	0.002474917
9600	65.67	6.33	28	13.32754922	0.002293898
9900	65.33	6.23	28.44	13.18526886	0.002269409
10200	65.72	5.92	28.36	12.45482854	0.002143688
10500	66.76	5.64	27.6	11.68090192	0.002010482
10800	65.45	5.45	29.1	11.51331674	0.001981638

Data Table 25: Molar Ratio of $DEBF_4$ to PPI-2 = 0.5:1 in Methanol-d_4 System

Time (sec)	Integration Values			Relative Intensity of Methoxyl Peak	Real-time Concentration of $DEBF_4$ (M)
	Aromatic Peaks	Methoxyl Peak	Methanol Peak		
0	58.03	41.97	0	100	0.004475043
300	71.25	19.62	9.13	38.07393251	0.001703825
600	72.78	16.59	10.63	31.51722239	0.001410409
900	75.7	14.92	9.38	27.25125735	0.001219505
1200	71.78	14.89	13.33	28.68169711	0.001283518
1500	73.82	12.29	13.89	23.01926451	0.001030122
1800	69.06	13.64	17.3	27.30872334	0.001222077
2100	72.12	11.18	16.7	21.43382531	0.000959173
2400	70.64	10.73	18.63	21.00209568	0.000939853
2700	74.33	8.51	17.16	15.82993125	0.000708396
3000	70.73	9.33	19.94	18.23860371	0.000816185
3300	72.68	8.03	19.29	15.27616104	0.000683615
3600	72.95	6.76	20.29	12.81253312	0.000573366
3900	73.46	6.23	20.31	11.72602252	0.000524745
4200	70.75	6.57	22.68	12.83963053	0.000574579
4500	71.75	5.98	22.27	11.52372484	0.000515692
4800	70.76	5.36	23.88	10.47346937	0.000468692
5100	71.46	5.77	22.77	11.16416901	0.000499601
5400	72.13	4.7	23.17	9.009392903	0.000403174
5700	73.83	4.35	21.82	8.146479892	0.000364558
6000	68.35	4.36	27.29	8.819857567	0.000394692
6300	73.41	3.96	22.63	7.458535535	0.000333773
6600	72.85	3.68	23.47	6.984444391	0.000312557
6900	72.35	3.9	23.75	7.453146758	0.000333532
7200	70.98	3.77	25.25	7.343768137	0.000328637
7500	73.28	3.55	23.17	6.698175058	0.000299746
7800	71.34	3.36	25.3	6.512080698	0.000291418
8100	72.59	3.78	23.63	7.199935482	0.0003222
8400	73.92	2.62	23.46	4.900641512	0.000219306
8700	72.01	2.82	25.17	5.414643884	0.000242308
9000	72.37	2.11	25.52	4.031229134	0.000180399
9300	73.75	2.86	23.39	5.361886416	0.000239947
9600	71.16	3.24	25.6	6.295390468	0.000281721
9900	71.64	2.4	25.96	4.632007628	0.000207284
10200	70.36	3.41	26.23	6.701039062	0.000299874
10500	72.74	2.47	24.79	4.69501796	0.000210104
10800	70.41	2.64	26.95	5.184217144	0.000231996

Data Table 26: Molar Ratio of $DEBF_4$ to PPI-2 = 0.25:1 in Methanol-d_4 System

Time (sec)	Integration Values			Relative Intensity of Methoxyl Peak	Real-time Concentration of $DEBF_4$ (M)
	Aromatic Peaks	Methoxyl Peak	Methanol Peak		
0	58.03	41.97	0	100	0.002065404
300	42.38	27.9	29.72	91.02419614	0.001880018
600	78.13	9.44	12.43	16.70581899	0.000345043
900	77.7	8.12	14.18	14.44936001	0.000298438
1200	76.14	8.25	15.61	14.98147857	0.000309428
1500	79.91	7.2	12.89	12.45790363	0.000257306
1800	78.19	7.96	13.85	14.07587677	0.000290724
2100	77.64	7.12	15.24	12.67967343	0.000261887
2400	78.85	6.49	14.66	11.38037572	0.000235051
2700	79.51	6	14.49	10.43381419	0.0002155
3000	78.46	6.81	14.73	12.00086111	0.000247866
3300	78.51	6.59	14.9	11.60577211	0.000239706
3600	78.16	6.92	14.92	12.24151432	0.000252837
3900	80.64	5.13	14.23	8.795903324	0.000181671
4200	79.16	5.24	15.6	9.152486623	0.000189036
4500	77.28	6.54	16.18	11.70103386	0.000241674
4800	79.51	4.61	15.88	8.016647235	0.000165576
5100	80.21	4.16	15.63	7.170978421	0.00014811
5400	79.12	5.12	15.76	8.947408869	0.0001848
5700	80.35	4.55	15.1	7.829591736	0.000161713
6000	81.08	4.43	14.49	7.55446281	0.00015603
6300	78.65	5.05	16.3	8.877818307	0.000183363
6600	80.98	4.99	14.03	8.519936826	0.000175971
6900	80.17	4.7	15.13	8.105868905	0.000167419
7200	79.62	4.33	16.05	7.519333106	0.000155305
7500	80.86	4.59	14.55	7.848606395	0.000162105
7800	80.55	4.4	15.05	7.55267389	0.000155993
8100	79.49	4.38	16.13	7.618600746	0.000157355
8400	79.92	4.8	15.28	8.304229891	0.000171516
8700	79.75	4.61	15.64	7.992521901	0.000165078
9000	79.51	3.81	16.68	6.62547201	0.000136843
9300	79.46	4.05	16.49	7.047256256	0.000145554
9600	77.83	4.43	17.74	7.869919628	0.000162546
9900	80.59	3.52	15.89	6.03914016	0.000124733
10200	77.27	4.91	17.82	8.78585803	0.000181464
10500	78.35	4.01	17.64	7.076507531	0.000146159
10800	80.08	3.37	16.55	5.818612529	0.000120178

Appendix II – UV-vis Data for Kinetic Study of Hydrolysis of $DEBF_4$ Dye.

1. Data Table Index.

Data Table Index: $DEBF_4$ and PPI-2 for UV-vis Studies

Molar Ratio of $DEBF_4$ to PPI-2	Data Table Number
1:64	27
1:32	28
1:16	29
1:8	30
1:4	31
1:3.2	32
1:2	33
1:1	34
1:0.5	35
1:0.25	36

* Calculation of Real-time Concentration of $DEBF_4$ is based on the following equation:

$$[DEBF_4] = \frac{A_{399}\varepsilon_{DABF_4 419} - A_{419}\varepsilon_{DABF_4 399}}{\varepsilon_{DEBF_4 399}\varepsilon_{DABF_4 419} - \varepsilon_{DEBF_4 419}\varepsilon_{DABF_4 399}}$$

$$[DEBF_4] = \frac{A_{399} \times 4903.389085 - A_{419} \times 6180.761844}{16687.71521 \times 4903.389085 - 18764.70267 \times 6180.761844}$$

In which A_{399} and A_{419} are the absorbance at 399 nm and 419 nm, respectively; $[DEBF_4]$ is the real-time concentration of $DEBF_4$; and $\varepsilon_{DABF_4 399}$, $\varepsilon_{DABF_4 419}$, $\varepsilon_{DEBF_4 399}$, and $\varepsilon_{DABF_4 419}$ are molar absorptivities for $DABF_4$ and $DEBF_4$ at 399 nm and 419 nm wavelength, respectively. The molar absorptivity values are:

$\varepsilon_{DEBF_4 399} = 16687.71521$ L·mol^{-1}·cm^{-1}, $\varepsilon_{DABF_4 399} = 6180.761844$ L·mol^{-1}·cm^{-1},

$\varepsilon_{DEBF_4 419} = 18764.70267$ L·mol^{-1}·cm^{-1}, $\varepsilon_{DABF_4 419} = 4903.389085$ L·mol^{-1}·cm^{-1}.

2. Absorbance Data Tables

Data Table 27: Molar Ratio of $DEBF_4$ to PPI-2 = 1:64

Time (sec)	Absorbance		Real-time Concentration of $DEBF_4$ ($\times 10^{-6}$ *M*)
	At 399 nm	At 419 nm	
0	0.331962585	0.36832428	18.99592
300	0.344696045	0.325050354	9.33659
600	0.34551239	0.304336548	5.470842
900	0.345100403	0.289344788	2.816954
1200	0.345062256	0.279151917	0.977842

Data Table 28: Molar Ratio of $DEBF_4$ to PPI-2 = 1:32

Time (sec)	Absorbance		Real-time Concentration of $DEBF_4$ ($\times 10^{-6}$ *M*)
	At 399 nm	At 419 nm	
0	0.336158752	0.377220154	20.00336
300	0.346229553	0.338500977	11.55057
600	0.346221924	0.318511963	7.93428
900	0.346153259	0.305274963	5.548658
1200	0.347434998	0.295837402	3.65674
1500	0.347312927	0.287757874	2.212125
1800	0.347366333	0.281066895	0.993601
2100	0.348220825	0.277099609	0.15297

Data Table 29: Molar Ratio of $DEBF_4$ to PPI-2 = 1:16

Time (sec)	Absorbance		Real-time Concentration of $DEBF_4$ ($\times 10^{-6}$ *M*)
	At 399 nm	At 419 nm	
0	0.366004944	0.41293335	22.18137
300	0.376411438	0.383758545	15.40761
600	0.377708435	0.365272522	11.87602
900	0.379882813	0.353569031	9.445882
1200	0.378135681	0.34185791	7.57737
1500	0.376541138	0.332611084	6.132911
1800	0.375205994	0.324554443	4.866596
2100	0.376098633	0.319442749	3.813386
2400	0.37562561	0.313323975	2.773992
2700	0.374961853	0.307739258	1.858628
3000	0.374977112	0.303924561	1.166097
3300	0.374450684	0.300254822	0.577568

Data Table 30: Molar Ratio of $DEBF_4$ to PPI-2 = 1:8

Time (sec)	Absorbance		Real-time Concentration of $DEBF_4$ ($\times 10^{-6}$ *M*)
	At 399 nm	At 419 nm	
0	0.38596344	0.43221283	22.80495
300	0.385719299	0.406532288	18.19263
600	0.3881073	0.392311096	15.2762
900	0.389152527	0.381622314	13.19181
1200	0.389656067	0.373809814	11.7057
1500	0.390434265	0.367134094	10.38588
1800	0.389839172	0.360664368	9.300501
2100	0.389381409	0.354873657	8.318285
2400	0.390235901	0.350105286	7.332682
2700	0.389152527	0.345809937	6.710897
3000	0.389282227	0.341957092	5.995033
3300	0.38936615	0.338142395	5.292644
3600	0.38709259	0.332931519	4.676049
3900	0.386940002	0.32925415	4.032468
4200	0.3878479	0.327644348	3.6108
4500	0.388191223	0.325248718	3.127976
4800	0.388183594	0.322502136	2.632027
5100	0.387878418	0.320358276	2.287869
5400	0.38910675	0.319046021	1.874043
5700	0.388160706	0.316619873	1.570808
6000	0.388679504	0.315010071	1.205002
6300	0.389511108	0.313301086	0.776338
6600	0.388381958	0.311302185	0.576709
6900	0.389076233	0.309715271	0.189852
7200	0.390182495	0.309616089	0.01308

Data Table 31: Molar Ratio of $DEBF_4$ to PPI-2 = 1:4

Time (sec)	Absorbance		Real-time Concentration of $DEBF_4$ ($\times 10^{-6}$ *M*)
	At 399 nm	At 419 nm	
0	0.380813599	0.430297852	23.19775
300	0.375854492	0.411590576	20.52429
600	0.376525879	0.403083801	18.88844
900	0.378013611	0.396362305	17.45847
1200	0.38004303	0.391418457	16.27243
1500	0.380325317	0.385452271	15.15221
1800	0.381698608	0.381790161	14.29233
2100	0.382324219	0.377754211	13.47213
2400	0.38318634	0.374214172	12.70772
2700	0.384552002	0.371040344	11.93729
3000	0.384757996	0.368492126	11.44657
3300	0.385536194	0.365814209	10.85023
3600	0.385429382	0.363212585	10.39475
3900	0.386245728	0.360618591	9.80812
4200	0.387397766	0.3592453	9.394202
4500	0.387077332	0.357032776	9.039809
4800	0.387161255	0.35459137	8.585942
5100	0.38760376	0.352348328	8.116493
5400	0.388130188	0.351051331	7.806199
5700	0.388130188	0.349067688	7.447222
6000	0.388916016	0.348152161	7.168721
6300	0.388648987	0.346160889	6.8467
6600	0.389083862	0.344459534	6.476374
6900	0.389205933	0.343200684	6.231037
7200	0.389411926	0.341651917	5.921185
7500	0.389442444	0.340164185	5.647571
7800	0.389381409	0.338615417	5.376055
8100	0.389793396	0.337059021	5.035248
8400	0.38999176	0.336349487	4.878366
8700	0.390037537	0.335113525	4.648124
9000	0.390350342	0.333610535	4.331221
9300	0.3904953	0.332832336	4.169581
9600	0.390701294	0.331596375	3.916336
9900	0.390640259	0.330253601	3.682099
10200	0.391174316	0.329528809	3.474261
10500	0.390533447	0.328300476	3.34398
10800	0.391471863	0.32787323	3.131935
11400	0.391296387	0.325408936	2.711169
12000	0.391479492	0.323745728	2.383892
12600	0.391174316	0.322227478	2.15295
13200	0.392349243	0.320640564	1.697087
13800	0.392211914	0.318969727	1.414434
14400	0.392066956	0.317878723	1.237808
15000	0.392608643	0.316139221	0.845244
15600	0.392738342	0.315032959	0.626425
16200	0.393112183	0.314224243	0.426401
16800	0.393280029	0.312858582	0.155162

Data Table 32: Molar Ratio of $DEBF_4$ to PPI-2 = 1:3.2

Time (sec)	Absorbance		Real-time Concentration of $DEBF_4$ ($\times 10^{-6}$ *M*)
	At 399 nm	At 419 nm	
0	0.356254578	0.406242371	22.37035
300	0.352027893	0.39276123	20.53751
600	0.352813721	0.38609314	19.21797
900	0.354774475	0.380317688	17.8913
1200	0.355171204	0.374992371	16.87063
1500	0.356666565	0.371574402	16.03739
1800	0.357788086	0.368309021	15.28545
2100	0.359313965	0.364685059	14.41056
2400	0.359466553	0.361473083	13.80739
2700	0.359909058	0.358329773	13.17502
3000	0.360862732	0.356391907	12.68741
3300	0.361434937	0.353927612	12.1593
3600	0.361938477	0.351402283	11.63
3900	0.362052917	0.349006653	11.18004
4200	0.36252594	0.346923828	10.7352
4500	0.362731934	0.345176697	10.38945
4800	0.363708496	0.343559265	9.956542
5100	0.363265991	0.341278076	9.607248
5400	0.363731384	0.339622498	9.240825
5700	0.357574463	0.332267761	8.793786
6000	0.357818604	0.329734802	8.300349
6300	0.358474731	0.329071045	8.086031
6600	0.358665466	0.327415466	7.75904
6900	0.360679626	0.328460693	7.659025
7200	0.365386963	0.330970764	7.437446
7500	0.365890503	0.329452515	7.090398
7800	0.365875244	0.328475952	6.915862
8100	0.365074158	0.32711792	6.785111
8400	0.365112305	0.324829102	6.365431
8700	0.365310669	0.324211121	6.225117
9000	0.364952087	0.322212219	5.914859
9300	0.365020752	0.321372986	5.753126
9600	0.365119934	0.320404053	5.563541
9900	0.365272522	0.319801331	5.43256
10200	0.366020203	0.318763733	5.137445
10500	0.365020752	0.317604065	5.07107
10800	0.365684509	0.316635132	4.80043
11400	0.366104126	0.314865112	4.419869
12000	0.366241455	0.313545227	4.161295
12600	0.366317749	0.311050415	3.698859
13200	0.366630554	0.309509277	3.375053
13800	0.367034912	0.308311462	3.100233
14400	0.366844177	0.306228638	2.750691
15000	0.367172241	0.304611206	2.410887
15600	0.367256165	0.303024292	2.111657
16200	0.367759705	0.3021698	1.884729
16800	0.367507935	0.300735474	1.661307
17400	0.367752075	0.299499512	1.402586
18000	0.368583679	0.298606873	1.121655
19800	0.368186951	0.294692993	0.470323

Data Table 33: Molar Ratio of $DEBF_4$ to PPI-2 = 1:2

Time (sec)	Absorbance		Real-time Concentration of $DEBF_4$ ($\times 10^{-6}$ *M*)
	At 399 nm	At 419 nm	
0	0.398994446	0.449142456	23.99785
300	0.387077332	0.431480408	22.51249
600	0.387084961	0.426513672	21.61257
900	0.386306763	0.421218872	20.7661
1200	0.386894226	0.417747498	20.05355
1500	0.387573242	0.414237976	19.32095
1800	0.385848999	0.409362793	18.68624
2100	0.387268066	0.406906128	18.03793
2400	0.387161255	0.404380798	17.59626
2700	0.387390137	0.401199341	16.98766
3000	0.387634277	0.398468018	16.45832
3300	0.386444092	0.395278931	16.05207
3600	0.386764526	0.393348694	15.65675
3900	0.387313843	0.391609192	15.2631
4200	0.386863708	0.388916016	14.84034
4500	0.387557983	0.387268066	14.44244
4800	0.386871338	0.384880066	14.10887
5100	0.387290955	0.383659363	13.82771
5400	0.387649536	0.382019043	13.47939
5700	0.386054993	0.378929138	13.14914
6000	0.386512756	0.377601624	12.84318
6300	0.386489868	0.375694275	12.50129
6600	0.385169983	0.373596191	12.3111
6900	0.385490417	0.3723526	12.04004
7200	0.38609314	0.371986389	11.88724
7500	0.385597229	0.369987488	11.5967
7800	0.385803223	0.368873596	11.36555
8100	0.385704041	0.367965698	11.21548
8400	0.385765076	0.366195679	10.8864
8700	0.385246277	0.365028381	10.74964
9000	0.385307312	0.36315918	10.40261
9300	0.385032654	0.362442017	10.31226
9600	0.385139465	0.361839294	10.18785
9900	0.384910583	0.360420227	9.963906
10200	0.385505676	0.359962463	9.795629
10500	0.385871887	0.358970642	9.563565
10800	0.385574341	0.358451843	9.512396
11400	0.385231018	0.356010437	9.119869
12000	0.385414124	0.354576111	8.834013
12600	0.386108398	0.353111267	8.469247
13200	0.386062622	0.351539612	8.191399
13800	0.386032104	0.350357056	7.981775
14400	0.386405945	0.348823547	7.650586
15000	0.386413574	0.347702026	7.446531
15600	0.386169434	0.346221924	7.21373
16200	0.386199951	0.344680786	6.930451
16800	0.386306763	0.343788147	6.753577
17400	0.386817932	0.342735291	6.489655
18000	0.386611938	0.34173584	6.33836
19800	0.387168884	0.338226318	5.623288
21600	0.387664795	0.33530426	5.023291
23400	0.388130188	0.333129883	4.562981
25200	0.388198853	0.330314636	4.043652
27000	0.388656616	0.328071594	3.572012
28800	0.38848114	0.326019287	3.225802
30600	0.388275146	0.323616028	2.820462
32400	0.389381409	0.322044373	2.377218
34200	0.388442993	0.319923401	2.128115
36000	0.389503479	0.318962097	1.801898
37800	0.390159607	0.31690979	1.336296
39600	0.390670776	0.316184998	1.131744
41400	0.390426636	0.314788818	0.91413
43200	0.390480042	0.313064575	0.594429

Data Table 34: Molar Ratio of $DEBF_4$ to PPI-2 = 1:1

Time (sec)	Absorbance		Real-time Concentration of $DEBF_4$ ($\times 10^{-6}$ *M*)
	At 399 nm	At 419 nm	
0	0.418395996	0.467521667	24.53846
300	0.412559509	0.461013794	24.19868
600	0.411277771	0.458503723	23.92845
900	0.411888123	0.457832336	23.71932
1200	0.411651611	0.456611633	23.53237
1500	0.411277771	0.455429077	23.37203
1800	0.411026001	0.454116821	23.1707
2100	0.411598206	0.453094482	22.90354
2400	0.413619995	0.453834534	22.7472
2700	0.412605286	0.452308655	22.61675
3000	0.412727356	0.451934814	22.53157
3300	0.413101196	0.451393127	22.37987
3600	0.412780762	0.450317383	22.2312
3900	0.412414551	0.448905945	22.02835
4200	0.413162231	0.448913574	21.92239
4500	0.413551331	0.448036194	21.70775
4800	0.413566589	0.447181702	21.55092
5100	0.413658142	0.446403503	21.39694
5400	0.413833618	0.445625305	21.23092
5700	0.413856506	0.445579529	21.21935
6000	0.414115906	0.444824219	21.04542
6300	0.413734436	0.444351196	21.01459
6600	0.414535522	0.44392395	20.82226
6900	0.414604187	0.442970276	20.63982
7200	0.414459229	0.442810059	20.63163
7500	0.414649963	0.441986084	20.45514
7800	0.415458679	0.442146301	20.36803
8100	0.415351868	0.440795898	20.13898
8400	0.415176392	0.440139771	20.04543
8700	0.415962219	0.440368652	19.97404
9000	0.41595459	0.439735413	19.86053
9300	0.415878296	0.439109802	19.75827
9600	0.416404724	0.43927002	19.71169
9900	0.41582489	0.438148499	19.59197
10200	0.415977478	0.437919617	19.52865
10500	0.416191101	0.436767578	19.28949
10800	0.416946411	0.436637878	19.15758
11400	0.417259216	0.436355591	19.06159
12000	0.417610168	0.43586731	18.92284
12600	0.417625427	0.434242249	18.62657
13200	0.41809082	0.433959961	18.50867
13800	0.417869568	0.432937622	18.35542
14400	0.419021606	0.432739258	18.15413
15000	0.419303894	0.431999207	17.97967
15600	0.419670105	0.43132019	17.80422
16200	0.419754028	0.430450439	17.63477
16800	0.420532227	0.429885864	17.42087
17400	0.420341492	0.429641724	17.40408
18000	0.420852661	0.429161072	17.24371
19800	0.42111969	0.426673889	16.75527
21600	0.421546936	0.424789429	16.3529
23400	0.423164368	0.423439026	15.87631
25200	0.423934937	0.422676086	15.62761
27000	0.423980713	0.420440674	15.2165
28800	0.424209595	0.419303894	14.97792
30600	0.424804688	0.417984009	14.65363
32400	0.42515564	0.416679382	14.36714
34200	0.425888062	0.415512085	14.05075
36000	0.426429749	0.41431427	13.75621

Data Table 35: Molar Ratio of $DEBF_4$ to PPI-2 = 1:0.5

Time (sec)	Absorbance		Real-time Concentration of $DEBF_4$ ($\times 10^{-6}$ *M*)
	At 399 nm	At 419 nm	
0	0.361045837	0.411682129	22.66691
300	0.354995728	0.406013489	22.50966
600	0.352531433	0.403701782	22.44511
900	0.351753235	0.402168274	22.27932
1200	0.351020813	0.401550293	22.27264
1500	0.350944519	0.400917053	22.16899
1800	0.350112915	0.40096283	22.29667
2100	0.351066589	0.401245117	22.21084
2400	0.349578857	0.40019989	22.23527
2700	0.349586487	0.399780273	22.15824
3000	0.349220276	0.399452209	22.15145
3300	0.349517822	0.399276733	22.07697
3600	0.348815918	0.398872375	22.10457
3900	0.348869324	0.398681641	22.06239
4200	0.349021912	0.398345947	21.97973
4500	0.348716736	0.398208618	21.99869
4800	0.34967041	0.398147583	21.85073
5100	0.349487305	0.398834229	22.00128
5400	0.348503113	0.398086548	22.00727
5700	0.348388672	0.397735596	21.96019
6000	0.348907471	0.397758484	21.88985
6300	0.348442078	0.397285461	21.87106
6600	0.348815918	0.39730835	21.82153
6900	0.348373413	0.39704895	21.83812
7200	0.348419189	0.397216797	21.86192
7500	0.349372864	0.397781372	21.82717
7800	0.348449707	0.397079468	21.83269
8100	0.348930359	0.397338867	21.81062
8400	0.34815979	0.396766663	21.8177
8700	0.348564148	0.396781921	21.76241
9000	0.349235535	0.397499084	21.7958
9300	0.348587036	0.396850586	21.77155
9600	0.348953247	0.396713257	21.69412
9900	0.348426819	0.39654541	21.73932
10200	0.348846436	0.397140503	21.78677
10500	0.348129272	0.395744324	21.63707
10800	0.347946167	0.39604187	21.71721
11400	0.348175049	0.396286011	21.72853
12000	0.348434448	0.396339417	21.70095
12600	0.348381042	0.395889282	21.62716
13200	0.348960876	0.396339417	21.62537
13800	0.348762512	0.396064758	21.60415
14400	0.347259521	0.39415741	21.47476
15000	0.34828186	0.395141602	21.50609
15600	0.347999573	0.394989014	21.519
16200	0.347602844	0.39389801	21.37852
16800	0.347251892	0.393951416	21.43857
17400	0.347633362	0.394065857	21.40452
18000	0.347816467	0.393692017	21.31058
19800	0.346611023	0.392448425	21.25859
21600	0.347427368	0.393051147	21.25046
23400	0.34690094	0.392684937	21.25977
25200	0.347114563	0.391601563	21.03304
27000	0.347648621	0.391716003	20.97708
28800	0.347808838	0.391464233	20.90851
30600	0.348075867	0.391189575	20.82047
32400	0.348266602	0.391311646	20.81518
34200	0.348937988	0.391677856	20.78506
36000	0.348007202	0.390357971	20.67984
37800	0.349510193	0.391448975	20.66149
39600	0.349594116	0.391181946	20.60112
41400	0.349731445	0.390937805	20.53722
43200	0.349327087	0.391296387	20.66017

Data Table 36: Molar Ratio of $DEBF_4$ to PPI-2 = 1:0.25

Time (sec)	Absorbance		Real-time Concentration of $DEBF_4$ ($\times 10^{-6}$ *M*)
	At 399 nm	At 419 nm	
0	0.3565979	0.40826416	22.68694
300	0.353218079	0.404754639	22.53706
600	0.352119446	0.403320312	22.43523
900	0.350990295	0.402893066	22.52002
1200	0.351554871	0.402923584	22.44448
1500	0.350837708	0.403053284	22.57092
1800	0.351066589	0.402359009	22.41242
2100	0.351089478	0.402252197	22.3898
2400	0.351013184	0.402679443	22.47807
2700	0.350837708	0.402053833	22.39005
3000	0.350593567	0.402305603	22.47066
3300	0.350242615	0.401908875	22.44925
3600	0.351135254	0.401496887	22.24654
3900	0.350723267	0.402107239	22.41614
4200	0.350784302	0.402702332	22.51507
4500	0.350547791	0.401382446	22.31017
4800	0.350372314	0.401901245	22.42925
5100	0.350234985	0.401123047	22.30814
5400	0.350372314	0.401443481	22.34641
5700	0.350601196	0.400993347	22.23209
6000	0.349899292	0.400886536	22.31353
6300	0.350372314	0.401153564	22.29394
6600	0.350967407	0.402114868	22.38247
6900	0.350776672	0.401428223	22.2856
7200	0.350265503	0.400917053	22.26648
7500	0.350242615	0.400627136	22.2173
7800	0.349975586	0.401145935	22.34952
8100	0.351028442	0.40070343	22.11829
8400	0.350585938	0.401687622	22.35992
8700	0.350288391	0.400917053	22.26319
9000	0.350837708	0.40145874	22.28236
9300	0.350357056	0.400695801	22.21329
9600	0.350761414	0.400665283	22.14972
9900	0.350486755	0.401008606	22.25128
10200	0.35068512	0.4009552	22.21314
10500	0.350120544	0.400688171	22.24587
10800	0.35030365	0.401145935	22.30242
11400	0.350227356	0.40032959	22.16564
12000	0.350730896	0.400222778	22.07402
12600	0.350486755	0.40045166	22.15049
13200	0.351020813	0.400810242	22.13871
13800	0.35093689	0.401763916	22.32334
14400	0.351318359	0.400657654	22.06838
15000	0.351127625	0.401359558	22.22278
15600	0.350997925	0.400588989	22.10196
16200	0.352638245	0.402442932	22.20196
16800	0.350990295	0.400375366	22.06439
17400	0.352226257	0.400695801	21.94494
18000	0.351707458	0.400268555	21.9421
19800	0.35067749	0.40020752	22.07893
21600	0.351417542	0.4008255	22.08451
23400	0.353279114	0.403076172	22.22455
25200	0.35446167	0.403373718	22.10862
27000	0.35559082	0.403839111	22.03073
28800	0.357170105	0.40549469	22.10361
30600	0.357940674	0.406776428	22.22493
32400	0.359054565	0.408187866	22.32044
34200	0.360168457	0.408813477	22.27374
36000	0.360748291	0.409118652	22.24572
37800	0.360771179	0.409942627	22.39154
39600	0.36240387	0.411003113	22.34906
41400	0.360687256	0.409896851	22.39531
43200	0.361579895	0.409965515	22.27958

Appendix III – UV-vis Data for the Comparison of Catalytic Property between PPI-2 and Other Classic Primary Amines.

1. Data Table Index.

Data Table Index: Different Amines Comparison Studies

Amines	Initial pH Value	Data Table Number
PPI-2	8.2	Same as 33 in Appendix II
Ethyl Amine	8.2	37
Ethylene Diamine	8.2	38
None	8.2	39
PPI-2	7.0	40
Ethyl Amine	7.0	41
Ethylene Diamine	7.0	42
None	7.0	43

* Calculation of Real-time Concentration of $DEBF_4$ is the same as in Appendix II.

2. Absorbance Data Tables

Data Table 37: Ethyl Amine at pH=8.2

Time (sec)	Absorbance		Real-time Concentration of $DEBF_4$ ($\times 10^{-6}$ *M*)
	At 399 nm	At 419 nm	
0	0.320701599	0.370498657	21.00613
300	0.318710327	0.36920929	21.05868
600	0.318504333	0.369110107	21.07031
900	0.3177948	0.368293762	21.02444
1200	0.317054749	0.367797852	21.04094
1500	0.317001343	0.367630005	21.01824
1800	0.316940308	0.367408752	20.98696
2100	0.316162109	0.366744995	20.97856
2400	0.315963745	0.366882324	21.0319
2700	0.31603241	0.366317749	20.91987
3000	0.315818787	0.365821838	20.86079
3300	0.315132141	0.365859985	20.96628
3600	0.315429688	0.365867615	20.92494
3900	0.315246582	0.365104675	20.81316
4200	0.315002441	0.365318298	20.88687
4500	0.315063477	0.365341187	20.88225
4800	0.314659119	0.364822388	20.84641
5100	0.314857483	0.365493774	20.93944
5400	0.31464386	0.364936829	20.86931
5700	0.315032959	0.364967346	20.81898
6000	0.314849854	0.3646698	20.79142
6300	0.314712524	0.364555359	20.79042
6600	0.314483643	0.364082336	20.73768
6900	0.314041138	0.364479065	20.87301
7200	0.313659668	0.364143372	20.86702
7500	0.313980103	0.363937378	20.78374
7800	0.313835144	0.363731384	20.76727
8100	0.31362915	0.363700867	20.79132
8400	0.314254761	0.363571167	20.67804
8700	0.313697815	0.363868713	20.81184
9000	0.313560486	0.363769531	20.81361
9300	0.313102722	0.363487244	20.82824
9600	0.313346863	0.363998413	20.8857
9900	0.313606262	0.36277771	20.62755
10200	0.313407898	0.362991333	20.69469
10500	0.313713074	0.362831116	20.62188
10800	0.313163757	0.363304138	20.78634
11400	0.313285828	0.363197327	20.74949
12000	0.313186646	0.362617493	20.6588
12600	0.313369751	0.363227844	20.74296
13200	0.312950134	0.363067627	20.77421
13800	0.314071655	0.362594604	20.5276
14400	0.312843323	0.362289429	20.64872
15000	0.313011169	0.36264801	20.68951
15600	0.31337738	0.362434387	20.59828
16200	0.313713074	0.362472534	20.55699
16800	0.312843323	0.362510681	20.68876
17400	0.313446045	0.362266541	20.55804
18000	0.313171387	0.362861633	20.70517
19800	0.313407898	0.362457275	20.59804
21600	0.314048767	0.362335205	20.48394
23400	0.313995361	0.362327576	20.49023
25200	0.313789368	0.362991333	20.63992
27000	0.314117432	0.362625122	20.52655
28800	0.314239502	0.361961365	20.3889
30600	0.314598083	0.362380981	20.41336
32400	0.312858582	0.362464905	20.67828
34200	0.313995361	0.361976624	20.42671
36000	0.313728333	0.362304688	20.52442
37800	0.313705444	0.363121033	20.67544
39600	0.313941956	0.362876892	20.5973
41400	0.314338684	0.362136841	20.40642
43200	0.313819885	0.363258362	20.68386

Data Table 38: Ethylene Diamine at pH=8.2

Time (sec)	Absorbance		Real-time Concentration of $DEBF_4$ ($\times 10^{-6}$ *M*)
	At 399 nm	At 419 nm	
0	0.360679626	0.409469604	22.31909
300	0.349983215	0.398826599	21.9287
600	0.348686218	0.397499084	21.87467
900	0.347007751	0.394790649	21.6255
1200	0.344360352	0.393051147	21.69079
1500	0.345054626	0.393569946	21.685
1800	0.342948914	0.392311096	21.7595
2100	0.34261322	0.391288757	21.62268
2400	0.343437195	0.391494751	21.54166
2700	0.342605591	0.389671326	21.33107
3000	0.341300964	0.389862061	21.55289
3300	0.340644836	0.389144897	21.51731
3600	0.341186523	0.38874054	21.36636
3900	0.34122467	0.388305664	21.28219
4200	0.341331482	0.389175415	21.42425
4500	0.340766907	0.387756348	21.2485
4800	0.340248108	0.387748718	21.3216
5100	0.340156555	0.387779236	21.34027
5400	0.340965271	0.388237	21.307
5700	0.339736938	0.387054443	21.26935
6000	0.339622498	0.387275696	21.32582
6300	0.340293884	0.387405396	21.2529
6600	0.339530945	0.385871887	21.08491
6900	0.340293884	0.38583374	20.96848
7200	0.339569092	0.387046814	21.29206
7500	0.339447021	0.386985779	21.29854
7800	0.339523315	0.386306763	21.16471
8100	0.339614868	0.386352539	21.15985
8400	0.339874268	0.387023926	21.24411
8700	0.338699341	0.386428833	21.3051
9000	0.339492798	0.385940552	21.10282
9300	0.340103149	0.387153625	21.23472
9600	0.338829041	0.386016846	21.21192
9900	0.33820343	0.385627747	21.23132
10200	0.339057922	0.38596344	21.16939
10500	0.339309692	0.385910034	21.12358
10800	0.339179993	0.385726929	21.10907
11400	0.338928223	0.385894775	21.17559
12000	0.338569641	0.3854599	21.14837
12600	0.338630676	0.385231018	21.09819
13200	0.33883667	0.3853302	21.08656
13800	0.338577271	0.385360718	21.12933
14400	0.33846283	0.384864807	21.05601
15000	0.339385986	0.385688782	21.07259
15600	0.338996887	0.38470459	20.95034
16200	0.338317871	0.385017395	21.10444
16800	0.338500977	0.38469696	21.02016
17400	0.3387146	0.385070801	21.05714
18000	0.338623047	0.384246826	20.92117
19800	0.338752747	0.383796692	20.82109
21600	0.339355469	0.383590698	20.69728
23400	0.339927673	0.385391235	20.94097
25200	0.339302063	0.384147644	20.80574
27000	0.33972168	0.383651733	20.65575
28800	0.339393616	0.383209229	20.62277
30600	0.339378357	0.383918762	20.75337
32400	0.341018677	0.384307861	20.58828
34200	0.339729309	0.382980347	20.53316
36000	0.340034485	0.382865906	20.46863
37800	0.339256287	0.381866455	20.39949
39600	0.337188721	0.379600525	20.28626
41400	0.339706421	0.382148743	20.38595
43200	0.340141296	0.382858276	20.45192

Data Table 39: No Amine at pH=8.2

Time (sec)	Absorbance		Real-time Concentration of $DEBF_4$ ($\times 10^{-6}$ *M*)
	At 399 nm	At 419 nm	
0	0.333404541	0.381866455	21.23961
300	0.334373474	0.382141113	21.15021
600	0.333564758	0.381408691	21.13377
900	0.333580017	0.381546021	21.15643
1200	0.33316803	0.381248474	21.16173
1500	0.332214355	0.380981445	21.25033
1800	0.332344055	0.381996155	21.41534
2100	0.333221436	0.381271362	21.15821
2400	0.332221985	0.381080627	21.26718
2700	0.332008362	0.380569458	21.20534
3000	0.332420349	0.380531311	21.13929
3300	0.332321167	0.379905701	21.04032
3600	0.332122803	0.37940979	20.97905
3900	0.332084656	0.379364014	20.97624
4200	0.331809998	0.379997253	21.13027
4500	0.332077026	0.379470825	20.99667
4800	0.33152771	0.379684448	21.11419
5100	0.332214355	0.379302979	20.94658
5400	0.331802368	0.378845215	20.92288
5700	0.330978394	0.378662109	21.00804
6000	0.331176758	0.378181458	20.89258
6300	0.331062317	0.378753662	21.01256
6600	0.331016541	0.378578186	20.98738
6900	0.330307007	0.378311157	21.04092
7200	0.330726624	0.378219604	20.96411
7500	0.330322266	0.378669739	21.10362
7800	0.330917358	0.378105164	20.91602
8100	0.329971313	0.378036499	21.03941
8400	0.330429077	0.378196716	21.00269
8700	0.32988739	0.377548218	20.9631
9000	0.330711365	0.377685547	20.86965
9300	0.33001709	0.376968384	20.83955
9600	0.329750061	0.37714386	20.90964
9900	0.330001831	0.377288818	20.89972
10200	0.330574036	0.377609253	20.87556
10500	0.329498291	0.377746582	21.05486
10800	0.329795837	0.37714386	20.90307
11400	0.329086304	0.376655579	20.91657
12000	0.329467773	0.376594543	20.85076
12600	0.328964233	0.376586914	20.92167
13200	0.329216003	0.377075195	20.97388
13800	0.329086304	0.376647949	20.91519
14400	0.329360962	0.376739502	20.89232
15000	0.328804016	0.375968933	20.83283
15600	0.328659058	0.37638092	20.9282
16200	0.329475403	0.37587738	20.71988
16800	0.328552246	0.375831604	20.84413
17400	0.32875061	0.376075745	20.85983
18000	0.328720093	0.375839233	20.82141
19800	0.328765869	0.376045227	20.85212
21600	0.32875061	0.376121521	20.86812
23400	0.329490662	0.376014709	20.74254
25200	0.329414368	0.376312256	20.80734
27000	0.330238342	0.376502991	20.72356
28800	0.33039856	0.376312256	20.66604
30600	0.330612183	0.376876831	20.73754
32400	0.330703735	0.376235962	20.60842
34200	0.330734253	0.376876831	20.72002
36000	0.332015991	0.377670288	20.67959
37800	0.331878662	0.3777771	20.71864
39600	0.330833435	0.377128601	20.75134
41400	0.331535339	0.377799988	20.77207
43200	0.331413269	0.377334595	20.70537

Data Table 40: PPI-2 at pH=7.0

Time (sec)	Absorbance		Real-time Concentration of $DEBF_4$ ($\times 10^{-6}$ *M*)
	At 399 nm	At 419 nm	
0	0.314422607	0.364570618	20.83481
300	0.312606812	0.362800598	20.77518
600	0.311668396	0.361129761	20.60754
900	0.311103821	0.360153198	20.51186
1200	0.310928345	0.360015869	20.5122
1500	0.311004639	0.358421326	20.21269
1800	0.310974121	0.358100891	20.15908
2100	0.310829163	0.357658386	20.09981
2400	0.311424255	0.357795715	20.03923
2700	0.311134338	0.356704712	19.88342
3000	0.310951233	0.356132507	19.80615
3300	0.311294556	0.355949402	19.72373
3600	0.312026978	0.355171204	19.47774
3900	0.311462402	0.354942322	19.51738
4200	0.312255859	0.355102539	19.43246
4500	0.312324524	0.354347229	19.28591
4800	0.31275177	0.353851318	19.13483
5100	0.312599182	0.353744507	19.13741
5400	0.312538147	0.353096008	19.02881
5700	0.312400818	0.352577209	18.95464
6000	0.313575745	0.352600098	18.7901
6300	0.313819885	0.352241516	18.69016
6600	0.314231873	0.35219574	18.62273
6900	0.313774109	0.351707458	18.60008
7200	0.313865662	0.351150513	18.48615
7500	0.314544678	0.351104736	18.38038
7800	0.314674377	0.350616455	18.2734
8100	0.31439209	0.350975037	18.37882
8400	0.314331055	0.350128174	18.23432
8700	0.314910889	0.349884033	18.1069
9000	0.314804077	0.349517822	18.05596
9300	0.31552124	0.349205017	17.89639
9600	0.31477356	0.349464417	18.05067
9900	0.315673828	0.348258972	17.70328
10200	0.315429688	0.347839355	17.66239
10500	0.314582825	0.347709656	17.7605
10800	0.314369202	0.346542358	17.57993
11400	0.315589905	0.346611023	17.4171
12000	0.315193176	0.345657349	17.30147
12600	0.315757751	0.345962524	17.27564
13200	0.315788269	0.344703674	17.04345
13800	0.316047668	0.344360352	16.94408
14400	0.316581726	0.344482422	16.8895
15000	0.316947937	0.342895508	16.54974
15600	0.317047119	0.342643738	16.48994
16200	0.317008972	0.34299469	16.55892
16800	0.317520142	0.342208862	16.34333
17400	0.317550659	0.341300964	16.17464
18000	0.318435669	0.341567993	16.09591
19800	0.318099976	0.339523315	15.77408
21600	0.31892395	0.338226318	15.42107
23400	0.31993103	0.336746216	15.00863
25200	0.319908142	0.335891724	14.85728
27000	0.320213318	0.334793091	14.61465
28800	0.321060181	0.333938599	14.33843
30600	0.32144928	0.332565308	14.03405
32400	0.321899414	0.331710815	13.81479
34200	0.321968079	0.330200195	13.53156
36000	0.322692871	0.329750061	13.34604
37800	0.324417114	0.329452515	13.04465
39600	0.324295044	0.328964233	12.97381
41400	0.325141907	0.327537537	12.59404
43200	0.325843811	0.327392578	12.46703

Data Table 41: Ethyl Amine at pH=7.0

Time (sec)	Absorbance		Real-time Concentration of $DEBF_4$ ($\times 10^{-6}$ *M*)
	At 399 nm	At 419 nm	
0	0.329650879	0.38105011	21.63079
300	0.329452515	0.382194519	21.86637
600	0.328720093	0.381790161	21.89834
900	0.328804016	0.381340027	21.80483
1200	0.328239441	0.381217957	21.8638
1500	0.32711792	0.380111694	21.82461
1800	0.327049255	0.3801651	21.84414
2100	0.326698303	0.379478455	21.77026
2400	0.326660156	0.379272461	21.73846
2700	0.326118469	0.378890991	21.74719
3000	0.326911926	0.379264832	21.70093
3300	0.32610321	0.378540039	21.68587
3600	0.325531006	0.378059387	21.68104
3900	0.325759888	0.378936768	21.80696
4200	0.325195313	0.377754211	21.67401
4500	0.325538635	0.378387451	21.73931
4800	0.325210571	0.377593994	21.64282
5100	0.324768066	0.3777771	21.73949
5400	0.324539185	0.377403259	21.7047
5700	0.325027466	0.377624512	21.67463
6000	0.325469971	0.377700806	21.62491
6300	0.324531555	0.377578735	21.73755
6600	0.324516296	0.377532959	21.73145
6900	0.324829102	0.377304077	21.64512
7200	0.324539185	0.377296448	21.68537
7500	0.324440002	0.377288818	21.69822
7800	0.323600769	0.376235962	21.62818
8100	0.323738098	0.375930786	21.55323
8400	0.323707581	0.375549316	21.48858
8700	0.322990417	0.375534058	21.58878
9000	0.322616577	0.375984192	21.72391
9300	0.323104858	0.375144958	21.50194
9600	0.322715759	0.375732422	21.66411
9900	0.322944641	0.375946045	21.66991
10200	0.32258606	0.375160217	21.57918
10500	0.322860718	0.374771118	21.46933
10800	0.322227478	0.375190735	21.63618
11400	0.32220459	0.375610352	21.71541
12000	0.322753906	0.37512207	21.54818
12600	0.322555542	0.374588013	21.48001
13200	0.322525024	0.374916077	21.54376
13800	0.322799683	0.374832153	21.48914
14400	0.322463989	0.374267578	21.43517
15000	0.322189331	0.375053406	21.61681
15600	0.322090149	0.374687195	21.56478
16200	0.322731018	0.374145508	21.37474
16800	0.322158813	0.374153137	21.45827
17400	0.322021484	0.374488831	21.53874
18000	0.322280884	0.374885559	21.57329
19800	0.32232666	0.375961304	21.76139
21600	0.322059631	0.374671936	21.5664
23400	0.321731567	0.374229431	21.53342
25200	0.321807861	0.373298645	21.35402
27000	0.322151184	0.37436676	21.49802
28800	0.322311401	0.374450684	21.49021
30600	0.3227005	0.374198914	21.38879
32400	0.322166443	0.374008179	21.43094
34200	0.324264526	0.375190735	21.34373
36000	0.324951172	0.375976563	21.38736
37800	0.324966431	0.376335144	21.45006
39600	0.325271606	0.376281738	21.39658
41400	0.325256348	0.377182007	21.56169
43200	0.326164246	0.377037048	21.40512

Data Table 42: Ethylene Diamine at pH=7.0

Time (sec)	Absorbance		Real-time Concentration of $DEBF_4$ ($\times 10^{-6}$ *M*)
	At 399 nm	At 419 nm	
0	0.351470947	0.401748657	22.24391
300	0.337593079	0.388893127	21.90988
600	0.337463379	0.388153076	21.79457
900	0.334831238	0.385757446	21.73893
1200	0.333724976	0.384963989	21.75416
1500	0.333084106	0.383094788	21.50791
1800	0.332542419	0.383979797	21.74583
2100	0.332458496	0.383834839	21.73165
2400	0.331466675	0.382118225	21.56339
2700	0.331489563	0.382865906	21.69541
3000	0.331596375	0.381996155	21.52268
3300	0.331031799	0.382270813	21.65344
3600	0.331077576	0.381240845	21.46047
3900	0.330741882	0.381507874	21.55699
4200	0.331260681	0.381103516	21.40933
4500	0.331817627	0.381958008	21.48401
4800	0.330802917	0.381866455	21.61312
5100	0.330833435	0.381523132	21.54661
5400	0.33026886	0.380683899	21.47579
5700	0.330879211	0.381256104	21.49171
6000	0.330734253	0.381515503	21.55947
6300	0.329925537	0.380500793	21.49194
6600	0.329803467	0.3800354	21.42525
6900	0.330802917	0.379844666	21.24724
7200	0.330055237	0.37991333	21.36701
7500	0.329826355	0.379730225	21.36673
7800	0.329421997	0.379966736	21.46759
8100	0.330673218	0.380409241	21.36803
8400	0.330039978	0.379592896	21.31121
8700	0.331138611	0.379394531	21.11759
9000	0.329490662	0.379310608	21.33899
9300	0.330482483	0.379859924	21.29601
9600	0.330680847	0.379951477	21.2841
9900	0.33001709	0.379608154	21.31726
10200	0.329315186	0.378845215	21.27996
10500	0.329589844	0.379165649	21.29852
10800	0.33065033	0.379112244	21.1366
11400	0.329681396	0.379486084	21.34336
12000	0.329795837	0.379318237	21.29656
12600	0.330284119	0.379402161	21.24165
13200	0.329307556	0.378860474	21.28382
13800	0.330062866	0.379547119	21.29964
14400	0.329681396	0.379432678	21.3337
15000	0.33039856	0.378921509	21.13823
15600	0.32951355	0.37802887	21.10375
16200	0.330307007	0.378540039	21.08234
16800	0.329467773	0.378746033	21.24011
17400	0.329925537	0.378463745	21.1233
18000	0.329971313	0.377815247	20.99937
19800	0.329933167	0.378364563	21.10426
21600	0.330169678	0.3776474	20.94052
23400	0.329841614	0.378334045	21.11188
25200	0.329902649	0.377479553	20.94848
27000	0.330177307	0.377861023	20.97808
28800	0.330200195	0.377326965	20.87815
30600	0.330467224	0.377326965	20.83981
32400	0.330055237	0.377532959	20.93624
34200	0.330627441	0.376937866	20.7464
36000	0.330551147	0.377235413	20.8112
37800	0.330154419	0.376724243	20.77565
39600	0.330726624	0.37714386	20.76943
41400	0.331375122	0.37625885	20.51617
43200	0.330619812	0.375961304	20.57076

Data Table 43: No Amine at pH=7.0

Time (sec)	Absorbance		Real-time Concentration of $DEBF_4$ ($\times 10^{-6}$ *M*)
	At 399 nm	At 419 nm	
0	0.364997864	0.411689758	22.1009
300	0.37159729	0.418251038	22.34082
600	0.36971283	0.416610718	22.31453
900	0.367294312	0.413574219	22.11224
1200	0.36592865	0.413246155	22.24893
1500	0.364433289	0.41192627	22.22476
1800	0.363517761	0.410469055	22.09249
2100	0.361732483	0.409492493	22.17207
2400	0.360847473	0.408226013	22.06994
2700	0.359840393	0.407646179	22.10959
3000	0.359138489	0.406959534	22.0861
3300	0.358070374	0.405921936	22.05168
3600	0.357368469	0.405715942	22.11517
3900	0.35584259	0.404457092	22.10642
4200	0.356208801	0.404220581	22.01105
4500	0.350982666	0.398735046	21.76864
4800	0.350563049	0.398872375	21.85374
5100	0.350257874	0.398094177	21.75672
5400	0.350120544	0.397956848	21.75159
5700	0.349449158	0.397857666	21.83003
6000	0.349220276	0.397514343	21.80076
6300	0.349517822	0.397689819	21.78979
6600	0.351097107	0.399414063	21.87509
6900	0.350502014	0.398849487	21.85836
7200	0.350097656	0.398666382	21.88327
7500	0.349708557	0.398452759	21.90048
7800	0.349319458	0.397880554	21.85279
8100	0.349121094	0.397590637	21.8288
8400	0.347976685	0.396728516	21.83709
8700	0.348609924	0.395988464	21.61225
9000	0.347640991	0.396713257	21.88252
9300	0.346992493	0.395980835	21.84308
9600	0.347206116	0.395622253	21.74752
9900	0.347129822	0.394302368	21.51961
10200	0.346336365	0.395225525	21.80059
10500	0.346115112	0.394302368	21.66529
10800	0.345954895	0.393455505	21.53504
11400	0.34412384	0.39352417	21.81034
12000	0.343566895	0.39250946	21.70667
12600	0.343460083	0.392204285	21.66678
13200	0.343559265	0.391304016	21.48962
13800	0.343711853	0.390777588	21.37245
14400	0.342559814	0.391616821	21.68972
15000	0.342918396	0.390640259	21.46151
15600	0.342254639	0.391166687	21.65207
16200	0.342437744	0.391036987	21.60231
16800	0.342521667	0.390228271	21.44391
17400	0.342216492	0.390098572	21.46425
18000	0.341880798	0.389884949	21.47379
19800	0.340408325	0.389549255	21.62444
21600	0.340400696	0.389076233	21.53993
23400	0.340362549	0.388587952	21.45705
25200	0.33996582	0.387466431	21.31104
27000	0.339454651	0.387397766	21.372
28800	0.340080261	0.387435913	21.28909
30600	0.339363098	0.387832642	21.46385
32400	0.339447021	0.386566162	21.22261
34200	0.338928223	0.387145996	21.40202
36000	0.338417053	0.387428284	21.52649
37800	0.339439392	0.386856079	21.27617
39600	0.338874817	0.387626648	21.49667
41400	0.339019775	0.386528015	21.27704
43200	0.338523865	0.386985779	21.43108